Alma Mater Studiorum – Università di Bologna

DOTTORATO DI RICERCA IN

Scienze biotecnologiche, biocomputazionali, farmaceutiche e farmacologiche

Ciclo 34

Settore Concorsuale di afferenza: 05/G1 FARMACOLOGIA, FARMACOLOGIA CLINICA E FARMACOGNOSIA

Settore Scientifico disciplinare: BIO/14 FARMACOLOGIA

Preclinical studies of the combined effect of anti-MYCN PNA and Retinoic Acid as potential approach to treat *Neuroblastoma*

Presentata da: Dott.ssa Silvia Lampis

Coordinatore Dottorato:

Prof.ssa Maria Laura Bolognesi

Relatore:

Dott. Roberto Tonelli

Esame finale Anno 2022

Sommario

1. INTRODUCTION

1.1 NEUROBLASTOMA: AN ORPHAN DRUG CASE

1.1.1 Introducing rare disease and Neuroblastoma

A rare disease is "*a disease that occurs infrequently or rarely in the general population*". Legislations define a rare disease as a condition affecting fewer than 5 people in 10,000 in Europe, fewer than 200,000 people in the United States, and fewer than 50,000 people in Japan (1).

Despite the rarity of each rare disease, it is always surprising for the public to discover that, according to a well-accepted estimation, "about 30 million people have a rare disease in the 25 EU countries", which means that 6% to 8% of the total EU population are rare disease patients (2). Between 6,000 and 8,000 rare diseases have been identified, around 80% of which are thought to have a genetic origin, usually linked to genetic variants ranging from single base pair mutation to more complex structural variants, often presenting severe clinical manifestations(3)

The majority of rare diseases (50–75%) affect children, and many are represented by severe multisystem disorders. They are responsible for 35% of deaths in the first year of life (4); it is reported that one-third of children born with a rare disease has a life expectancy less than 5 years (2). However, less than 10% of rare disease patients are treated, reflecting a significant need for development of new medical treatments and the increment of studies to understand disease pathogenesis.

Therapeutic compounds for rare disease are known as orphan drugs or Orphan Medicinal Products (OMPs). These drugs are called "orphan" because, under normal market conditions, it is not cost-effective for the pharmaceutical industry to develop and market products intended for only a small number of patients suffering from rare conditions (2). For these reasons orphan drugs has been financially incentivized through US law via the Orphan Drug Act of 1983. The success of the original Orphan Drug Act in the USA led to its adoption in other key markets, most notably in Japan in 1993 and in the European Union in 2000 (1).

Among several specific and rare diseases occurring in the pediatric population, tumors like Neuroblastoma should be taken into great consideration.

Neuroblastoma (NB) was described in 1910 by James Homer Wright. He published a review of a series of cases of adrenal childhood tumors with neural fibrils and bundles of cells (*pseudorosettas*) resembled fetal adrenal morphology; he named those tumors neuroblastoma, as "blastoma" refers to a collection of immature, undifferentiated cells (5).

Today, NB ranks as the most common extracranial solid tumor in children, accounting for 7-10% of childhood malignancies and for 15% of cancer related mortality in patients less than 15 years old (6–11). The median age at the time of diagnosis is around 19 months, but diagnosis can occur in utero by fetal magnetic resonance imaging or, very rarely, in patients older than 19 years. Historically NB are more common in boys although the genetic and epigenetic bases of this phenomenon are not yet known(12). The incidence of NB in Black children is slightly lower than the incidence in White children. However, there are also racial differences in tumor biology, with African American patients more likely to have high-risk disease and fatal outcomes (13).

NB primary tumors derive from precursor cells of the peripheral (sympathetic) nervous system and can arise anywhere along the sympathetic chain, most frequently in the adrenal gland. The tumor may also develop from spinal cord of neck and pelvis and metastases are found in a majority of cases at diagnosis. Metastases in bone and bone marrow, with invasion of lymph nodes and liver are also frequently seen. Metastatic involvement of lung and brain is rare (Fig 1) (9–11,14).
Because of the tumor's origin, the disease is very remarkable for its broad of heterogeneous biological, morphological, genetic and clinical characteristics (15). Actually, despite current therapeutic advances and ongoing clinical trials, NB remains a complex medical challenge with an unpredictable clinical course: from the spontaneous regression and differentiation of the tumor, to the onset of metastases and the development of resistance to anti-cancer drug treatments (12).

Patients with NB are usually divided in risk groups by stage, age and biological factors as Shimada histopathology, DNA index, MYCN amplification. The low risk group has a survival rate of >90% with surgery alone or spontaneous regression; the intermediate risk group has a survival rate of >90% with surgery and chemotherapy; the high-risk group has survival rates of 30-40% despite multimodality therapy (chemotherapy, radiation therapy and stem cell transplantation) (14).

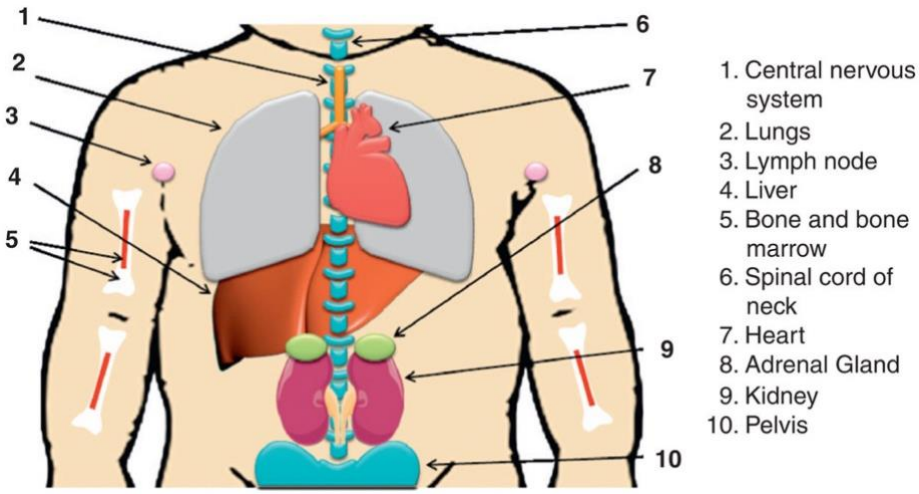

Figure 1: *NB Localization*

1.1.2 Neuroblastoma is a neural crest derived malignancy

NB is a developmental malignancy arising within the neuronal ganglia of the peripheral sympathetic nervous system. These neuronal structures derive from the ventero-lateral neural crest cells, which migrate away from the neural tube early during embryogenesis (12).

In vertebrates, normal trunk neural crest cells leave the dorsal aspect of the neural tube, migrate ventrally, close to the neural tube and begin to differentiate in response to local cues. The development, maintenance and differentiation of these progenitor cells require the activation of highly complex processes such as induction, speciation, delamination and differentiation. All these mechanisms are finely controlled by pathways involved in the tumorigenesis of NB and, indeed, it is known that inhibition of this maturation process may predispose early multipotent neural crest precursors to malignant transformation (Figure 2) (12) (16).

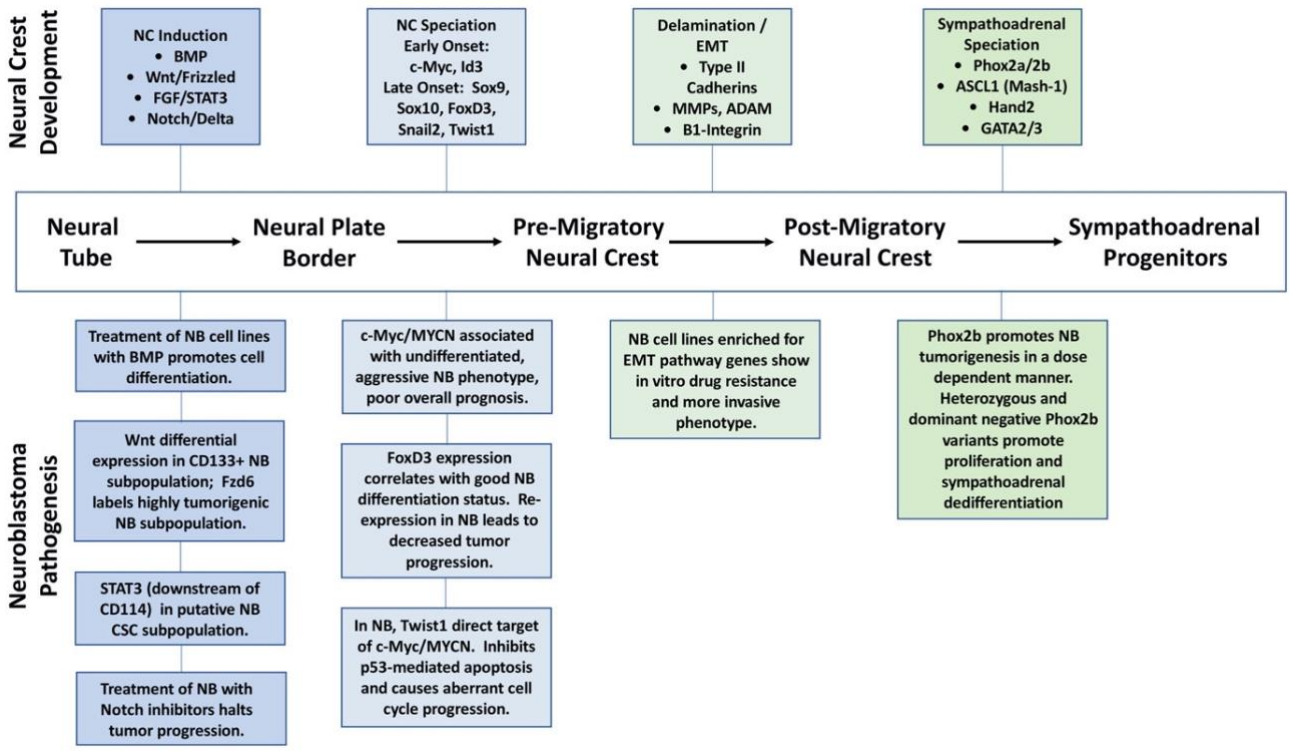

Figure 2: *Neural crest development and NB pathogenesis* (16)

Induction is mediated by interconnected signaling pathways of *bone morphogenic protein (BMP)*, *Wingless/Int (WNT)*, *Fibroblast growth factor (FGF)*, and to a lesser extent *Notch/Delta signaling*. This induction activates key transcription factors that specify the NPB and prime the NPB tissue for induction of genes that allow for NC speciation (16,17). BMP is a protein of the *transforming growth factor beta (TGFβ*) family that is secreted by neighboring non-neural ectoderm. Signaling through BMP receptors activates the Smad family of transcription factors and leads to transcription of genes involved in growth and differentiation. It is demonstrated that suppression of BMP signaling may represent a derangement *pathway* to maintain multipotency in NB (16).

Wnt is a secreted ligand that controls *β-catenin* signaling. Deregulation of Wnt signaling has been shown to stimulate proliferation and maintenance of CSC populations in many cancers including colorectal cancer, hepatocellular carcinoma, medulloblastoma, and some leukemias (18). However, studies in NB have shown conflicting evidence for the role of the Wnt pathway in tumorigenesis (16).

FGF is a secreted protein that binds and signals through receptor tyrosine kinases, also known as fibroblast growth factor receptors (FGFRs). Signaling through FGFR activates many

downstream pathways involved in proliferation and survival, including Ras/ERK and Akt/MTOR which converge in the activation of the transcription factor STAT3 (19).

STAT3 is an important transcription factor involved in the activation and regulation of genes related to proliferation, apoptosis, and tissue differentiation and plays an important role in many human cancers. An involvement of STAT3 in NB tumor biology was first identified when elevated levels of IL6 in the bone marrow and peripheral blood were linked to poor prognosis in high-risk patients. Odate *et al* demonstrated that treatment of NB cell lines NGP and IMR-32 in vitro with an antisense oligonucleotide (ASO) directed against STAT3, led to decreased cell proliferation. In vivo, treatment of xenograft tumors with the ASO greatly reduced re-implantation potential of NB tumors indicating the importance of STAT3 in NB tumor initiation (20).

Notch proteins are transmembrane signaling molecules that act as intracellular receptors for Delta/Jagged protein ligands. Upon binding Delta, the intracellular domain of Notch is cleaved, it translocates to the nucleus and binds associated transcription factors to activate transcription of target genes (21). Notch plays a critical role in embryological development including many pathways that maintain cells in a proliferative state with blocked differentiation. In neural systems, Notch1 is responsible for the maintenance of neural stem cells via regulation of cell cycle exit and prevention of neural differentiation. In NB, inhibition of Notch1 signaling within the human NB cell line SH-SY5Y, led to neuronal differentiation via a JNK-CRT mediated pathway. Correspondingly, treatment of NB xenograft mice with Notch inhibitors led to suppression of tumor progression (22).

Tomolonis and colleagues (16)are clear in explaining how the stimulation of the signaling pathways previously described results in the induction of the cells of the edges of the neural plate (NPB). These acquire the ability to differentiate to cells of the neural crest due to the activation of some transcription factors, finely regulated from the temporal point of view and which, for this reason, are defined as early and late. Once the activation of the NPB cells has taken place, they receive the commissioning of cells of the neural crest, which requires a second wave of expression of transcription factors, also temporally separated:

• *Early specifiers*: they are required for the promotion of proliferation, the suppression of neural differentiation and for the maintenance of these cells in a state of multipotency. The main factors involved are c-Myc and its downstream target Id3 (differentiation inhibitor 3). In particular c-Myc and related N-Myc are transcriptional regulators that are directly involved in the regulation of thousands of genes involved in the maintenance of pluripotency.

Amplification of MYCN leading to N-Myc protein overexpression is present in approximately 25% of high-risk NB representing one of the most critical prognostic factors. Myc-expressing tumors had unfavorable histology and poor 3-year event-free survival (46.5%) indicating the importance of both N-Myc and c-Myc in maintaining an undifferentiated state in NB (6).

• *Late specifiers*: they are responsible for the epithelial to mesenchymal transition, which allows the cells of the neural crest to assume a migratory phenotype and undergo delamination. Transcription factors involved in this program include Sox9, Sox10, FoxD3, Snail2 and Twist1 (16).

Neural crest delamination, also referred to as epithelial to mesenchymal transition (EMT), describes "a process by which these cells lose adhesion to neighboring neuroepithelial cells and acquire a migratory mesenchymal phenotype, allowing the cells to migrate away from the developing neural tube and colonize distant sites for further speciation and differentiation" (23). EMT is initiated by NC specifier genes Sox9/10, FoxD3, Snail2 and Twist1 to promote cell survival, loss of cell-to-cell adhesion, loss of cell-to-matrix adhesion, and digestion of extracellular matrix (16).

Upon the initiation of the EMT program junctions that are essential for epithelial integrity (tight junctions) are deconstructed and the junction proteins are relocalized and/or degraded. The dissolution of the tight junctions during EMT confers to cells a loss of apical and basal polarity resulting in reorganization of the cytoskeleton.

Changes to the integrin repertoire during EMT correlate with the increased expression of proteases, such as the matrix metalloproteinases MMP2, MMP9 and ADAM13 to digest matrix and allow for migration away from the neural tube.

It is known that the process of EMT has long been implicated in cancer, with loss of cell adhesion and upregulation of MMPs as a mechanism of invasion and metastasis. This happens because the process of EMT is very dynamic and while transitioning between the epithelial and mesenchymal phenotypes, cells can also attain a partial or hybrid epithelial/mesenchymal (E/M) phenotype. These mixed partial EMT states have been correlated to cell populations with increased aggressiveness and stemness as compared to strict epithelial and mesenchymal states. Jolly and colleagues noticed indeed that these cells have a much large repertoire of survival strategies in all stress conditions and are therefore better armed to seed metastases at distant organs and coordinate tumor relapse (24). In NB, EMT pathways have been associated with the development of drug resistance and correlate with lower overall survival (25).

Once they have undergone the EMT, the neural crest cells destined to become sympatho-adrenergic precursors, migrate ventrally to the neural tube and aggregate at the level of the dorsal aorta, to form the primary sympathetic ganglion. During migration, the cells of the crest receive signals from the somites, the neural tube and the notochord and this signaling determines the differentiation fate of the cells: catecholaminergic cells, chromaffin cells or sympathetic neurons (17).

A fundamental role in this phase of embryonic development is also played by the transcription factor Phox2b (paired-like homebox 2b), which plays a key role in neurogenesis, in particular in the differentiation of cellular progenitors that will give rise to the autonomic nervous system, allowing the activation of further specific transcription factors: MASH-1, Hand2 and GATA2 / 3 (16). In particular, MASH-1 is essential for the development of the sympathoadrenergic system and its absence causes the accumulation in the primary ganglion of the migrating cells from the neural crest , which fail complete differentiation and die through apoptosis. Hand2 and GATA 2 / 3 are instead activated by Phox2b and are required for the expression of markers of the sympathoadrenergic system (16). PHOX2B is a minimal residual disease (MRD) marker of poor prognosis in NB (26). Studies conducted on animal models and on human primary tumors have shown that the loss of heterozygosity or negative dominant mutations in the Phox2b gene lead to a block of cell differentiation and to a greater susceptibility to tumorigenesis; Phox2b therefore functions as a suppressor of tumorigenesis in a dose dependent manner and its partial loss represents a predisposition to the onset of NB (16).

1.1.3 Risk stratification

As anticipated one of the hallmarks of NB is its great clinical heterogeneity.

The staging of NB is of great importance for prognostic purposes: is very critical to appropriately risk-stratify patients to ensure that they will receive the optimal treatment regimen. Over the last several decades, numerous clinical and biologic factors have been incorporated into the risk classification system for to categorize NB patients as having low, intermediate, or high-risk disease (12) (27).

The *International Neuroblastoma Staging System (INSS)*, established in 1986 and revised in 1993, required the classification of tumors into different stages (1, 2A / 2B, 3, 4 and 4S) depending on the feasibility of surgery to remove the tumor at the time of diagnosis, based on the presence of metastases and the age of the patient. In this System children with early stage

1 and 2 have a better prognosis than those diagnosed with advanced stage 3 and 4 NB, who are highly metastatic. Children with less than one year of age and stage 4S are beyond this general vision: they actually have a higher probability of survival (27).
Although it has been used for more than 20 years, the INSS classification system is strongly influenced by the instrumental opportunities and techniques of pediatric surgery available to each country; it is therefore necessary to develop an approach independent from the surgical data. For these reasons, in 2009, the International Neuroblastoma Risk Group (INRG) task force developed an innovative staging system for NB (12)(28).

There are four INRG stages:

- **L1:** Localized tumor not involving vital structures as defined by the list of image-defined risk factors and confined to one body compartment
- **L2:** Locoregional tumor with presence of one or more image-defined risk factors
- **M:** Distant metastatic disease (except stage MS)
- **MS:** Metastatic disease in children younger than 18 months with metastases confined to skin, liver, and/or bone marrow

Since treatment decisions cannot be based solely on these staging criteria the INRG Task Force derived a new risk stratification including not only stage, but also tumor biology. The new risk stratification system was also created through the analysis of data collected on 8800 patients diagnosed between 1990 and 2002 in North America, Australia, Europe, and Japan. Based on predictive factors including INRG stage, age, histologic category, grade of differentiation, MYCN status, 11q aberration, and tumor cell ploidy, 17 cohorts were defined and were categorized as very low, low, intermediate, or high- risk (Table 1) (28).

INRG Stage	Age (months)	Histologic Category	Grade of Tumor Differentiation	*MYCN*	11q Aberration	Ploidy	Pretreatment Risk Group
L1/L2		GN maturing; GNB intermixed					A Very low
L1		Any, except GN maturing or GNB intermixed		NA			B Very low
				Amp			K High
L2	< 18	Any, except GN maturing or GNB intermixed		NA	No		D Low
					Yes		G Intermediate
	≥ 18	GNB nodular; neuroblastoma	Differentiating	NA	No		E Low
					Yes		H Intermediate
			Poorly differentiated or undifferentiated	NA			
				Amp			N High
M	< 18			NA		Hyperdiploid	F Low
	< 12			NA		Diploid	I Intermediate
	12 to < 18			NA		Diploid	J Intermediate
	< 18			Amp			O High
	≥ 18						P High
MS	< 18			NA	No		C Very low
					Yes		Q High
				Amp			R High

Table 1:. *International Neuroblastoma Risk Group (INRG) pre-treatment classification system* (27)

1.1.4 Current treatment regimens by risk group

Once the diagnosis of NB is established, the risk groups determined by the INRG staging system and the guidelines of the Children's Oncology Group are used to determine the optimal management strategy. The trend is to reduce therapeutic intensity in patients with low-risk; in contrast it is necessary to intensifying treatment in high-risk patients to improve survival (10,29). This treatment approach has resulted in improved outcome, although high-risk patients survival remains poor, emphasizing the need for more effective treatments (30).

1.1.4.1 Treatment of Low and Intermediate Risk Disease

Low risk group includes diseases at stages 1, 2, and 4S with favorable characteristics and without amplifications of MYCN(31). Low risk group patients at stages 1 or 2 are usually treated successfully, achieving complete tumor resection through surgery alone; in these subjects, exposure to chemotherapy is limited and reserved for only those who show residues that may cause spinal cord compression or respiratory impairment due to hepatic involvement

or relapses (30). Stage 4S NB usually regress spontaneously, or undergo differentiation without the need for treatment, so affected patients are exclusively kept under constant observation. The survival rate of patients of this group is greater than 95% (17). Intermediate risk group patients include stage 3 patients of any age with favorable features, stage 4 infants with favorable features, and 4S patients without MYCN amplification but unfavorable histology (31). Patients at intermediate risk usually receive moderate doses of multiagent chemotherapy in combination with surgical resection when possible. Radiation therapy is rarely indicated for these patients but should be considered for those with tumor progression or life-threatening complications from chemotherapy. Outcomes for patients at intermediate risk (event-free survival, 80%–95%) are very good (30).

1.1.4.2 Treatment of High- Risk Disease

Patients over 18 months, who have a metastatic lesion characterized by amplification of the MYCN oncogene, fall into the high-risk category. Consequently, NB at stages 2, 3 and 4, but also amplified 4S MYCN belong to this group (17). Current treatments for high-risk NB are very intensive multimodality therapy and can be divided into three phases: induction of remission, consolidation of remission and finally a post-consolidation (maintenance phase) focused on the eradication of minimal residual disease (10,32,33). The current treatment lasts approximately 18 months (33).

In general, during induction, patients receive 5 to 8 cycles (6 more frequently) of intensive chemotherapic agents like cisplatin, etoposide, doxorubicin, cyclophosphamide and vincristine. During induction therapy, stem cells are harvested in preparation for the consolidation phase (9,29,33). Surgical resection is done towards the end of induction chemotherapy, often after the 4th (typical), 5th, or 6th cycle. This timing is intended to maximize tumor shrinkage prior to surgery in order to achieve complete resection (29).

The goal of consolidation is to eliminate any remaining tumor, usually with myeloablative cytotoxic agents and stem cells rescue. External beam radiotherapy is provided once the patient has recovered from the transplantation and is associated with a high rate of local control (9). The standard amount of radiation administered is 21 Gy to the primary tumor bed, as well as radiation to end-induction sites of metastatic disease (33).

The last phase is the post consolidation therapy, that is developed to treat residual disease that remains despite intensive induction and consolidation treatment regimens. Since relapse is very frequent after autologous transplantation, biological therapy with the differentiating agent 13-

cis Retinoic Acid (isotretinoin) and immunotherapy has been added to current treatment regimens.

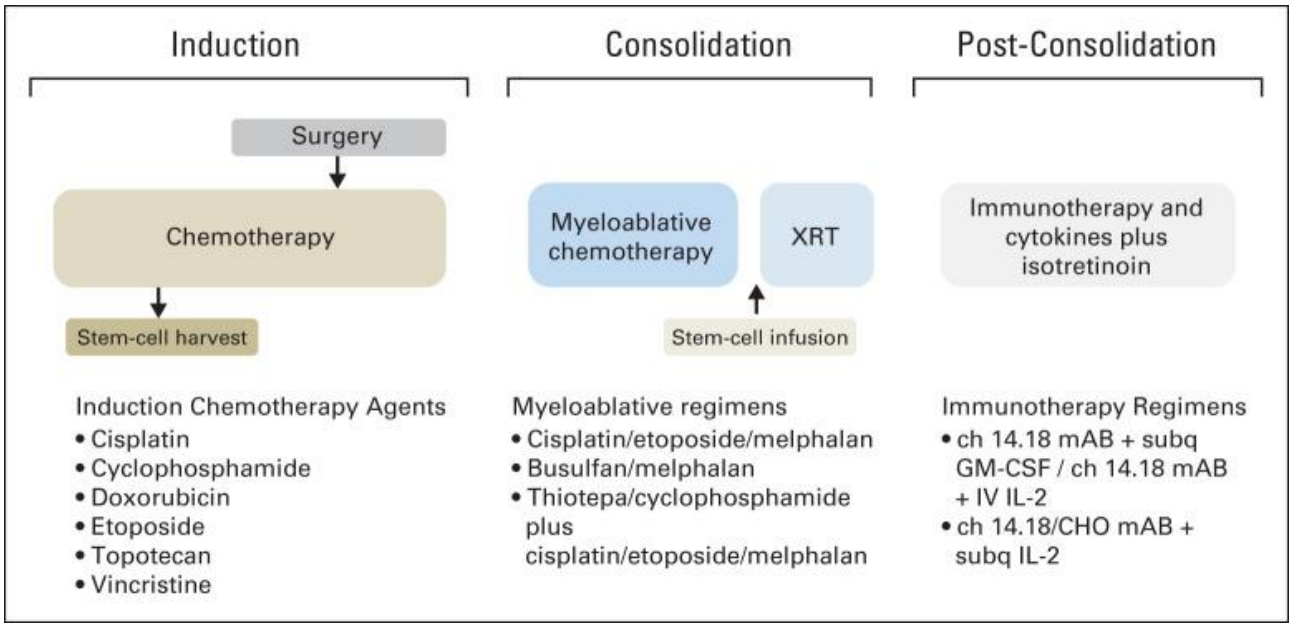

***Figure 3**: Current standard-of-care treatment strategy for high-risk neuroblastoma* (30).

1.2 TARGET IDENTIFICATION: MYCN

1.2.1 Overview of the genetic and genomics of Neuroblastoma

Briefly, NB originates from the incorrect regulation of cellular processes that take place during embryonic development; its characteristic clinical heterogeneity is due on one hand to the presence of a large number of transformation drivers, and on the other hand by the fact that the alteration of this complex process can take place at any level.
A large number of genetic alterations, including events of acquisition/loss of chromosomal material and epigenetic changes, affecting the development of the neural crest, have been identified and can lead to the formation of pre-neoplastic lesions or the tumor itself.

1.2.1.1. Familial Neuroblastoma

To date, only a few inherited mutations that predispose to NB were reported in a limited number of families, around 1-2% of all NB cases. In half of the familial NB cases three germline missense mutations have been identified in the tyrosine kinase domain of the protein encoded by the Anaplastic Lymphoma Kinase (ALK) and it was shown that they can lead to the tumor formation. Moreover, two germline missense mutations located in PHOX2B in a familial case and in a patient with NB were also reported, suggesting that this mutation can predispose to hereditary NB (34–37).

1.2.1.2 Sporadic Neuroblastoma

While in familial NB a small number of rare mutations lead to a high disease probability, for the 99% of sporadic NB, it is believed that several common germline variations, each with a low relative risk, act in concert and increase the likelihood of disease occurrence (36).
Genome-wide association studies (GWAS) revealed that there are at least a dozen significant polymorphic sites capable of influencing NB tumorigenesis. Some of these are found in specific genes: CASC15 (*Cancer Susceptibility 15*), BARD1 (*BRCA1-associated RING domain protein 1*), LMO1 *(LIM Domain Only 1)*, DUSP12 *(Dual Specificity Phosphatase 12)*, DDX4 *(DEAD-Box Helicase 4)*, IL31RA *(Interleukin 31 Receptor A),* HSD17B12 *(Hydroxysteroid 17-Beta Dehydrogenase 12)*, HACE1 *(HECT Domain And Ankyrin Repeat Containing E3 Ubiquitin Protein Ligase 1)*, LIN28B *(Lin-28 Homolog B),* NEFL *(Neurofilament Light)* and TP53 (*Tumor protein p53*)(35).

The genetic aberration most consistently associated with poor outcome in NB is the genomic amplification of the transcription factor MYCN on chromosome 2p24. The amplification of MYCN, that occurs in 20% of cases overall, rising to 50% in high-risk tumors, is strongly associated with advanced, aggressive tumors and frequent disease relapse (9,35,38,39). MYCN encodes the N-MYC protein, which is crucial for a correct neural development.

Deletion of the short arm of the chromosome 1 (1p) can be identified in around 35% of NB and correlates both with MYCN amplification and advanced stage disease. Instead, the allelic loss of 11q is present in around 40% of NB but does not correlate with MYCN amplification while remaining highly associated with high-risk disease. Also a gain of 1-3 additional 17q copies, often through unbalanced translocation, can correlate with a poor outcome in NB (9).

DNA index is also a prognostic marker for NB patients. The DNA content of NB falls into two broad categories: near-diploid or hyper-diploid. In general, less aggressive tumors have a defect in mitosis associated with whole chromosomes gain and losses. In contrast more malignant NB have a fundamental defect in genomic stability, resulting in chromosomal rearrangements, unbalanced translocations (like the loss of chromosome 1p material and the resulting 17q gain) and maintenance of a near diploid DNA content (9).

1.2.2 MYCN as oncogenic driver in Neuroblastoma

1.2.2.1 Discovery of MYCN and its structure

MYCN belongs to the MYC family proto-oncogenes, a set of transcription factors that control the expression of many target genes, which in turn regulate fundamental cellular processes including proliferation, cell growth, response to DNA damage, energy metabolism, apoptosis and differentiation (17,38,40,41).

In addition to MYCN, found in a human NB cell line in 1983 by Schwab and colleagues (42), the gene family also includes MYCC (a homolog of an avian retroviral gene v-myc) considered the founder of the family, and MYCL, found in small cell lung cancer (40,43–45). All three genes code for nuclear proteins that show subtle differences in the number of amino acids (aa) of which they are composed, but share a common structural organization, which consists of three main domains (Figure 4):

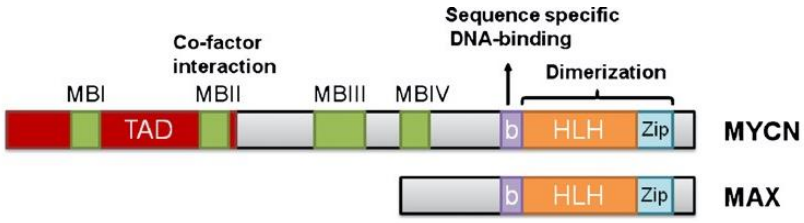

Figure 4: *Schematic representation of the structure of the MYCN protein and its partner protein Max. Important functional domains are depicted; MYC box (MB), transactivation domain (TAD), basic region (b), helix-loop-helix (HLH), and Leucin-zipper (Zip)* (38).

• *Domain of transcriptional activation* (TAD) in the N-terminal region;

• *MYC boxes I to IV*, which are interaction domains with protein co-factors;

• *Transcriptional regulatory domain* in the C-terminal region. The basic region is able to bind DNA, the bHLH-LZ domain is responsible for the physical interaction with is counterpart MAX (46).

1.2.2.2 Spatio-temporal expression pattern of MYC family

Despite the homology relationship between MYC genes and the redundancy of some of their functions, studies conducted at mRNA levels in developing mouse models have shown that the different members of the gene family are characterized by distinct expression patterns. These patterns depend on the stage of animal development and mainly on the kind of tissue considered (17,38,41).

In mice, expression level of both MYCN and MYCL transcripts is high in the early stages of embryogenesis, but are still restricted to particular areas and tissues; on the contrary, MYCC is expressed throughout the development period of the organism, without showing tissue or organ specificity (6,41). Furthermore, it was observed that MYCC and MYCN, but not MYCL, are required for organogenesis (41). In fact, the knockout of both genes causes embryonic lethality and the lack of expression of only one of the two, MYCN and MYCC, is incompatible with development the embryos die at day 11.5 and 10.5 respectively (6,38).

The Figure 5 shows clearly that the two genes possess a significantly different spatio-temporal expression pattern. MYCN levels are particularly high in forebrain, kidney and hindbrain of newborn mice but are practically absent in adult mice. MYCC, on the other hand, is found in a wide spectrum of tissues of newborn mice and is maintained in many, but not all, adult tissues (6,38,41).

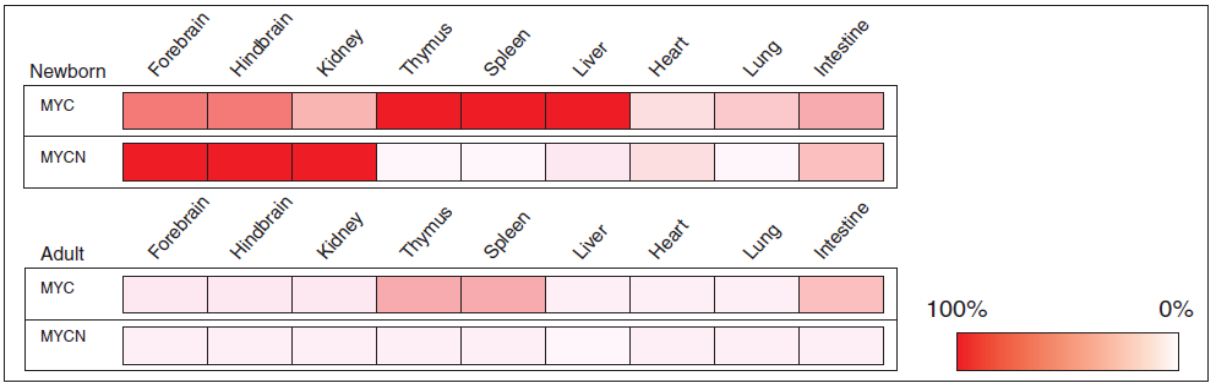

Figure 5: *Expression of MYC and MYCN at each tissue based on a relative percentage of the highest expression tissue (newborn forebrain for MYCN and newborn thymus for MYC), arbitrarily set to 100%* (6).

1.2.2.3 Transcriptional activity of MYCN

As transcription factors, Myc proteins are capable of activating and repressing gene transcription through direct binding to DNA and through the formation of protein-protein interactions.

The positive regulation of transcription by Myc proteins, as mentioned above, is generally associated with the heterodimerization with MAX consensus E-box sequences (CANNTG) (6). Through MYC boxes, Myc proteins can recruit multiple co-activation factors (Figure 6). These include p300 / CBP and TRRAP-containing complexes, as well as the histone acetyl transferases GCN5 and TIP60 (38).

In contrast, the transcription repression occurs when Myc proteins interact with the factors Miz-1, SP-1 and Smad (17,38). For example, with this latest function, MYCN can inhibit many negative cell cycle regulators and genes involved in cell adhesion (38).

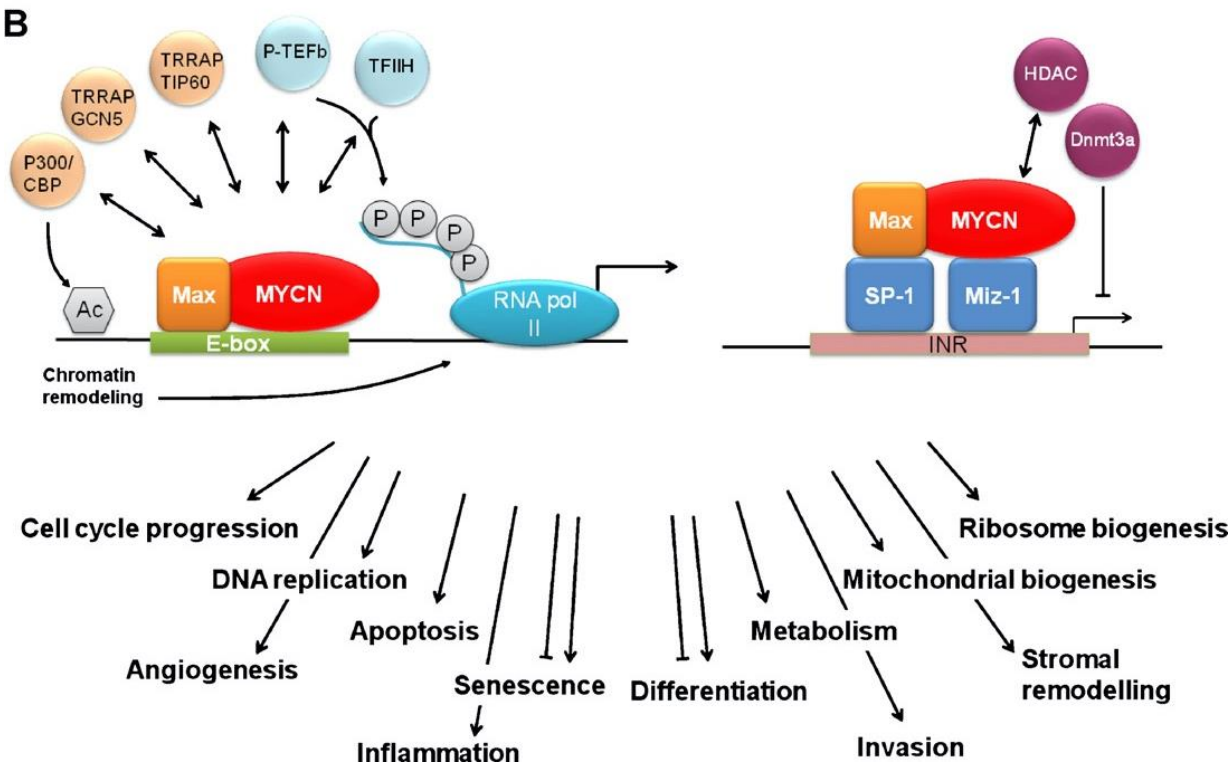

Figure 6: *MYCN influences a multitude of cellular processes through regulation of gene expression* (38).

Furthermore, MYCN is able to alter the expression profile of a cell not only directly, activating or repressing the transcription of a given gene pool, but also indirectly. In this regard, MYCN mediates the expression of multiple genes simultaneously through the activation of non-coding RNAs, such as miRNA and lncRNA, and has an effect on global methylation and acetylation, respectively markers of transcriptional repression and activation (6).

In general, MYCN plays many roles in NB tumorigenesis. He can activate transcription of genes involved in proliferation, metastasis, pluripotency, self-renewal and angiogenesis. In contrast he can suppress expression of genes involved in differentiation, cell cycle arrest, immune surveillance and genes that antagonize metastasis and angiogenesis (6).

1.2.2.3.1 MYCN and cell cycle

The main function in which MYCN is involved is the promotion of proliferation and cell cycle progression (6). Indeed, MYCN in normal embryonic expansion is involved in cell proliferation and cell growth and is crucial for embryonic development. The cell cycle is a strictly regulated process under the control of the CDK family of serine/threonine kinases (47).
Specifically, MYCN-amplified NB lose the ability to arrest in G1 phase in response to radiation or DNA damage. This phenomenon is usually due to the down-regulation of TP53INP1 and the up-regulation of CDK4 and SKP2, so that CDK2 can escape the inhibitory effect of p21 (6). MYCN is able to increase the expression levels of CHK1, an S-phase and G2/M checkpoint regulator, by implementing a system that allows amplified MYCN NBs to become refractory to chemotherapy. This is demonstrated by the fact that, in some tumors, the inhibition of CHK1 promotes the sensitization of cancer cells to chemotherapy (6).
In addition, MYCN is associated with changes in other cell cycle regulators such as the CDK inhibitor p27, E2 factor (E2F) and inhibitor of differentiation 2 (ID2). E2F is a transcription factor responsible of coordinating cell cycle progression and proliferation. Inhibition of MYCN can decrease E2F levels, resulting in inactivation of genes involved in G1 phase and DNA replication. ID2 is another helix-loop-helix transcription factor regulator of cell proliferation and tumor progression target of MYCN. MYCN-amplified cell lines show elevated levels of ID2 and this overexpression correlates with poor outcome in NB patients (6,47). Other target of MYCN that can drive proliferation are neuronal leucine rich repeat protein-1 (LRRN1), the transcription factor MYBL2 involved in drug resistance and minichromosome maintenance (MCM) genes that are responsible for DNA elongation and unwinding during the replication process (6).

1.2.2.3.2 MYCN has characteristics of self-renewal and pluripotency

As described previously NB arises from neural crest cells, which possess self-maintaining and multipotent characteristics. MYCN is likely involved in regulating both traits, playing a critical role in maintaining a stem-like state by blocking differentiation and activating self-renewal and pluripotency genes (6). Indeed, MYCN up-regulates the genes BMI1 and DLL3, required for the maintenance of stem cells, as well as increases the expression levels of some genes that ensure pluripotency, such as KLF2, KLF4, LIN28B and LIF (6,38).
Furthermore, NB with MYCN amplification tend to undergo symmetrical cell divisions, while those without MYCN amplification preferentially undergo asymmetric divisions (6). Finally, the exogenous expression of MYCN is able to promote the reprogramming of somatic cells that are induced to pluripotent stem cells. Neither MYCC nor MYCN are strictly necessary to obtain iPSCs, however their expression is crucial for the maintenance of pluripotency and self-maintenance of murine embryonic stem cells and iPSCs (38).

Regarding the involvement of MYCN in the differentiation is the following is known:
• Murine embryonic stem cells knockout for both MYC and MYCN show increased expression levels of endodermal and mesodermal differentiation markers (BMP6 and GATA6), lymphocyte differentiation activators (STAT1, EGR1 and ELK3), sensory organ development (DDL1, BMP4, GBX2, FGFR1), suggesting that MYC proteins repress the differentiation mechanism. CDKL5 and TG2 are among the differentiation proteins suppressed by MYCN (6).
• NB are favorable and susceptible to spontaneous regression or differentiation when TrkA is expressed. Commonly, in high-risk NB TrkA expression is low or absent, and these tumors do not undergo complete differentiation in response to NGF. On the contrary, TrkB and its ligands are highly expressed in unfavorable NB. MYCN silencing determines the increase in the expression levels of TrkA and TrkC and the occurrence of morphological changes attributable to cell differentiation (15).
• Down-regulation of MYCN is required for terminal differentiation in multiple lineages. In particular, the conditional deletion of mammalian N-Myc, that is highly expressed in neuronal progenitor cells, induces the premature differentiation of neuronal progenitor cells in the cerebral cortex and in neurospheres culture, arguing that N-Myc is critical for preventing the premature differentiation of neuronal precursor cells (48).

1.2.2.3.3 MYCN in Apoptosis and Cell Death

Like MYC, MYCN has both the ability to drive cell proliferation and growth, and can also promote apoptosis: this effect is strictly dependent on the state of certain apoptotic factors such as BCL2 and p53 (6).

TP53 mutations are rare in NB at the time of diagnosis, suggesting that MYCN is able to cooperate with suppressors of p53-mediated signaling: miRNA-380-5p, CUL7, BMI1, transcription factors H-Twist and MDM2. In contrast, mutation in TP53 and p53 pathway are common in NB at relapse, consistent with the idea that such mutation can arise after chemotherapy (6).

H-TWIST is an anti-apoptotic onco-protein the expression of which correlates strongly with MYCN levels and, indeed, is overexpressed in MYCN-amplified NB. By inhibiting TWIST expression, the apoptotic response of MYCN-amplified NB can be restored and this make the gene a therapeutic target for drug development (47)

MDM2 is a ubiquitin ligase E3, which promotes cell survival by adding ubiquitin monomers to p53 and directing it to degradation; in addition, this enzyme helps to improve the stability of MYCN mRNA by binding to AU-rich elements found in the 3 UTR of the transcript. MDM2 is a target of p53-mediated transcription and MYCN can stimulate the expression of both p53 and MDM2. The dual role of MYCN may partially explain the different sensitivity of NB to chemotherapy treatments: initially, an amplified MYCN tumor is sensitive to chemotherapy as the oncogene activates p53; however, if relapses occur, the tumors become resistant through the accumulation of mutations in p53 that are caused by the drug treatment itself (6).

NBs with MYCN amplification can also survive through the constitutive activation of signaling cascades that promote cell survival, such as that mediated by the tropomyosin receptor kinase B (TRKB). Interestingly, levels of TRKB are correlated with MYCN: the overexpression of TRKB in MYCN-amplified NB activates both autocrine and paracrine survival pathways and is therefore implicated in resistance. On the contrary MYCN down-regulates tropomyosin receptor kinase A (TRKA) which is a typical gene found in low-risk NB (6).

1.2.2.3.4 MYCN in metastasis

Metastases are detected in 50% of NB patients at the time of diagnosis, with frequent dissemination to the bone marrow 70%, bone 55%, lymph nodes 30%, liver 30% and brain 18%

(6,9,11). MYCN levels correlate with the metastasizing and invasive behavior of cells, as the expression of the oncogene affects adhesion, motility, cell invasion and the tendency of cells to degrade the extracellular matrix. MYCN indeed causes a decrease of the expression levels of integrins a1 and ß1, favoring the cells detachment from the extracellular matrix, favoring the processes of invasion and migration. MYCN also promotes the transcription of the focal adhesion factor FAK, an integrin-mediated signaling regulator, which generally promotes the increase of migration and metastasis of cancer cells (6). Furthermore, MYCN increases the activity of metalloproteinases (MMPs) that degrade the extracellular matrix (6).
Caspase-8 has a paradoxical role in both promoting and inhibiting metastasis in NB, depending on the cellular context. A significantly high expression of spontaneous metastasis was found in primary NB tumors without Caspase-8, when compared to tumor expressing the caspase; in TH-MYCN mouse model of NB the deletion of caspase-8 increases the incidence of metastasis specifically to bone marrow, probably by the up-regulation of genes involved in EMT. If the tumor becomes resistant to apoptosis caspase-8 acquires capacity to be prometastatic. In this setting caspase-8 associated with FAK promotes cell migration (6).

1.2.2.3.5 MYCN in angiogenesis

Tumor vascularity is correlated with an aggressive phenotype in NB characterized poor survival, increased dissemination and amplification of MYCN (6,9). As evidence that MYCN is involved in the angiogenesis process, NB with inducible MYCN expression have a decreased ability to release endothelial growth inhibitors, such as Activin A, leukemia inhibitory factor (LIF) and interleukin-6 (IL-6), into the conditioned medium. Furthermore, the mis-expression of MYCN has a positive effect on pro-angiogenic factors, including Angiogenin and vascular endothelial growth factor (VEGF) through the PI3K/mTOR pathway. For example, the PI3K/mTOR inhibitor NVP-BEZ235 suppresses growth in MYCN-amplified NB and disrupts angiogenesis by suppressing transcription and secretion of VEGF (6). To date, various pre-clinical studies of anti-angiogenic agents in NB models have met with varying degrees of success (9).

1.2.2.3.6 MYCN as immunosuppressive driver

Among the large network of intracellular pathways dysregulated by MYCN in NB, there is also the immune system pathway.
Since 2007, it is known that MYCN influences immune surveillance by modulating antigens expressed on tumor cells. MYCN is able to repress the monocyte chemoattractant protein 1/CC chemokine ligand 2 (MCP-1/CCL2) which is required for the chemoattraction of NK cells (49). NK cells have not been shown to be directly involved in the elimination of NB, however they can initiate an immune response by secreting pro-inflammatory cytokines, stimulating dendritic cell maturation and generating antigen-specific T cells that can target cancer cells (6).

A recent work of Raieli and colleagues investigated in details the relationship between MYCN and the immune system (50). The results of bioinformatic analysis showed that MYCN has a great role in dysregulating the immune network in NB and, actually, different immune pathways are enriched in MYCN correlated genes and in MYCN amplified NB. Among the most down-regulated pathways, those relating to the response to interferon gamma, phagocytosis and adaptive immunity were highlighted. In particular, MYCN anti-correlated with Th1 immunity while correlated with Th2, and these subsets are mutually exclusive enriched in NB. As expected, MYCN correlated with M2 macrophages and inversely correlated with M1 subset. In line with previous literature, Th1 and M1 subsets are associated to anti-tumor immunity while Th2/Th17 and M2 are hijacked by the cancer cells to sustain their growth. Moreover, the authors demonstrated that the MYCN effect on immune system can be considered an independent prognostic factor in NB. Targeting MYCN with an anti-MYCN antigene PNA was studied to verify if the specific inhibition of the gene can exert an effect on the immune suppression. The results showed that MYCN inhibition can restore the responsiveness of the immune system against NB. Indeed, the PNA caused a cascade of downregulation of negative immune checkpoints (CD276) and regulons implied (HMGA1) in the immune-suppression phenotype.

1.2.3 Targeting the “undruggable” MYCN

Considering the impact of MYCN in NB and its expression profile, N-Myc is a very promising target. Nevertheless, drug discovery approaches aimed to block the hetero-dimerization with

MAX or its binding with DNA, largely failed thus far, leading to consider N-Myc an undruggable target (51).

To date, all the strategies proposed to target the aberrant expression of MYCN through small molecules are indirect (6,15,41). Indeed, there are many complications in directly targeting MYCN, as its unstable fold, the absence of a binding pocket in the protein where small molecule inhibitors could attach or the risk of interfering with the highly homologous Myc, which is expressed in normal cells (41,51).

The possible strategies for indirectly targeting MYCN driven tumors include, as shown in Figure 7:

- blocking MYCN-dependent transcription with BET-bromodomain inhibitors;
- inhibiting HDACs;
- antagonizing proteins involved in stabilizing MYCN protein (PI3K/AKT);
- suppressing MDM2 (which stabilizes MYCN mRNA and disrupts p53-mediated apotosis);
- inducing differentiation.

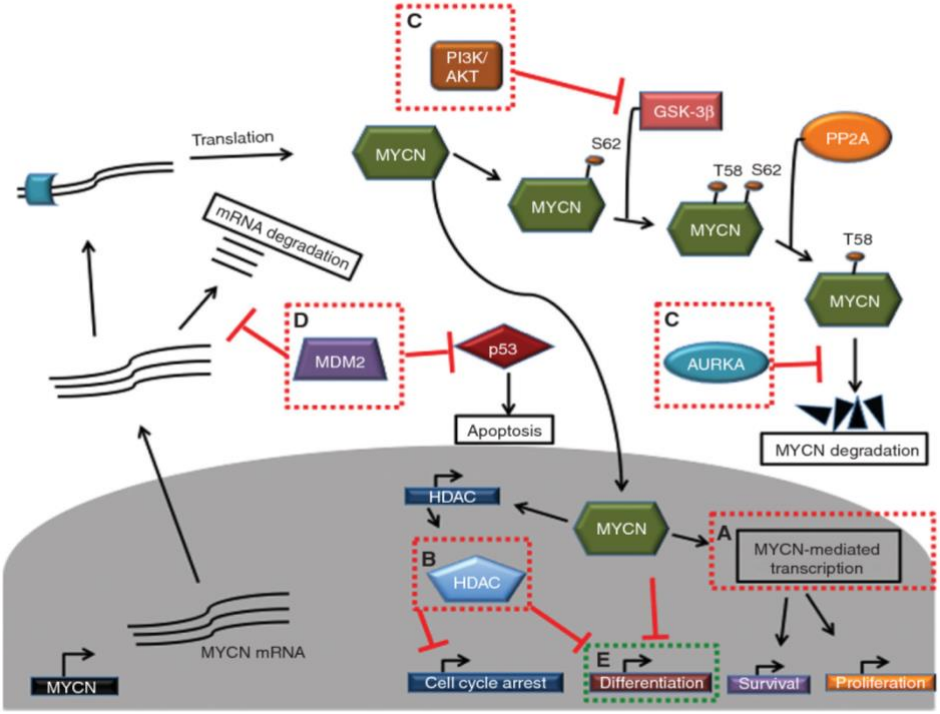

Figure 7: *Therapeutic strategies to target MYCN in neuroblastoma* (6).

1.2.3.1 BET Bromodomain inhibitors

A well accepted approach for indirect MYCN targeting is by inhibiting the BET (*bromodomain and extra-terminal domain*) family proteins (BRD2, BRD3 and BRD4) contain acetyl-lysine recognition motifs, or bromodomains, that bind acetylated lysine residue in histone tails usually associated with an open chromatin state and transcriptional activation (15).

Different reports have shown that the prototypic BET inhibitor JQ1 is capable to bind the bromodomain and disrupt BET recruitment to chromatin downregulating expression of MYCN in MYCN-dependent NB in vitro and in vivo (15,52).

OTX015 *(Oncoethix)* is a promising anti-tumor drug because it shows a potent inhibitory effect on the growth of either murine or human MYCN-driven NB. This synthetic inhibitor prevents the binding with BRD4, which is responsible for maintaing gene active transcription through super enhancers in their promoter region, just like MYCN (15,52).

TEN010 is up to now the only BET inhibitor in phase II clinical trials and the only one with a pediatric formulation (41).

1.2.3.2 HDACi

Since MYCN silences tumor suppressor genes by recruitment of DNA methyltransferase and elevated expression of HDACs (HDAC1, HDAC2 and HDAC5), HDAC inhibitors (HDACi) may be a viable route to target MYCN-amplified NB (6). The treatment of cells with HDACi inactivates MYCN super-enhancers by disrupting normal looping and depleting transcription factors that bind to the super-enhancers (53). It is demonstrated that, in vivo, various inhibitors are capable to reduce tumorigenesis (6).

1.2.3.3 Regulators of MYC Protein Stability: Aurora and PI3K/mTOR inhibitors

Degradation of MYCN is necessary for terminal differentiation of neuronal precursors (52).

MYCN is a short-lived protein (half-life of approximately 20 to 30 minutes) whose stability is regulated by different signaling pathways that target it for ubiquitin mediated degradation by the proteasome(53). The proteasomal degradation complex includes E3 ubiquitin ligases (FBXW7 and HUWE1), AURORA kinases and other undefined proteins (52).

A major signaling pathway affecting MYCN protein stability occurs upon activation of PI3K. Briefly PI3K activates AKT which phosphorylates glycogen synthase kinase 3β (GSK3 β) suppressing the activity of this kinase. This leads to a reduced phosphorylation at threonine 58

(T58) which is critical for targeting degradation by the proteasome (53). Moreover, mTORC1 down-regulates PP2A, which normally de-phosphorylates N-myc, decreasing ubiquitination and promoting its stabilization(54)(51).

There are more evidences supporting a role of the PI3K/AKT/mTOR pathway in the development and progression of NB. AKT is commonly activated in MYCN-dependent NB. Aberrant PI3K/AKT/mTOR pathway activity in NB correlates with poor outcome driving oncogenic stabilization of MYCN. Numerous inhibitors of both PI3K and mTOR have already been developed and some of them have just been tested in NB clinical trial(15,52,53).

Another strategy is targeting the serine/threonine kinases AURORA A (AURKA) and AURORA B (AURKB), crucial regulators of the cell cycle. AURORA A and N-MYC form a complex making the latter less sensible to degradable by the proteasome degradation. AURKA has earned much interest as target in NB because its mRNA expression has been described as a negative prognostic factor for the disease; it is frequently overexpressed and amplified in MYCN-dependent NB and cooperates with N-myc in promoting tumor proliferation and oncogenic activity. Moreover, it is demonstrated that AURKB is a direct transcriptional target of MYCN and its expression is correlated with poor outcome in patient. To date, many preclinical studies have been conducted with compounds targeting both kinases. In particular AURKA-inhibitors (as alisertib or CD532) have been used to destabilized N-MYC and induce rapid cell death in MYCN-dependent NB (15).

1.2.3.4 MDM2 inhibitors

Unlike adult cancers, NB is rarely associated to TP53 gene mutation. Despite this the p53 pathway is often impaired in childhood cancer and there is evidence that the pathway is inactivated in NB. The inactivation of the p53 pathway occurs mainly at the time of relapse and is related to chemoresistance. MDM2 acts as a negative regulator of p53 levels (15).

Down-regulation of MDM2 by inhibitors (like nutlin-3 or MI219) would have two possible effects in MYCN-amplified NB. Since MDM2 interacts with the 3'UTR of MYCN, the absence of MDM2 would destabilize mRNA and the expression of N-Myc protein. Moreover, decreased levels of MDM2 should stabilize p53 and increase the probability of a p53-dependent apoptosis (6). There are currently several ongoing clinical trials on this family of inhibitors (15).

1.2.3.5 Inducers of Differentiation: 13-cis Retinoic Acid

Since it is known that NB pathogenesis includes maturational arrest of neural crest precursor cells, intracellular targets for NB therapy have included proteins involved in induction and enactment of differentiation like the family of RA receptors, most commonly targeted with Retinoic Acid (RA).

Soon after the discovery of the MYCN gene, in 1985, Thiele and colleagues showed that RA treatment of NB cells caused a down-regulation of MYCN expression at the mRNA level, and this precede cell cycle arrest and implementation of a differentiation program (55).

Furthermore, knock-down of MYCN results in morphological and biochemical neuronal differentiation. RA treatment in vivo inhibited tumor growth rate and decreased tumor volume compared to control; smaller tumors were formed when the cells were pre-treated with RA before inoculation in mice (38).

All these data indicated that MYCN downregulation contributes partially to the biological effect of RA on NB cells and indeed this was the major motivation for the inclusion of 13-cis RA during the consolidation phase of treatment for high-risk NB patients (56).

However, although treatment with retinoid treatment is effective for some patients, about 50% of those who initially responded to RA therapy develops resistance. This resistance is largely due to MYCN: while retinoids reduce MYCN levels, the proto-oncogene prevents neuronal differentiation and this has been confirmed by the fact that aberrant signaling of MYCN alone is sufficient to induce NB in animal models (57).

1.3 LEAD IDENTIFICATION: ANTI-MYCN PNA

1.3.1 Introduction

Nucleic acids, such as DNA and RNA, are informational biopolymers formed by specific sequences of different monomers, which store the genetic information. These macromolecules are organized in double helices which constitute a repository system of all molecular and cellular functions for every known life form (58).

Over the years, thanks to the interest in the study and manipulation of DNA and the improvement of technologies, real structural analogues of DNA and RNA have been developed and synthesized; these new compounds are able to mimic their behavior and represent a new possible therapeutic frontier for the treatment of countless pathologies.

Among these, PNAs (Nucleic Peptide Acids) belong to the "third generation" of antisense oligonucleotides (AS-OD), a class that includes a large variety of modified nucleotides with improved properties such as target affinity, resistance to nucleases and pharmacokinetics (59).

Due to the strong, sequence-specific, and highly selective binding of PNA and its derivatives with DNA and RNA, PNA is an invaluable tool and has been widely employed in chemistry, biochemistry, medicine, nanotechnology, and many other fields (60).

1.3.2 PNA structure and properties

PNAs have been introduced in 1991 by Peter E. Nielsen and colleagues at the University of Copenhagen in an attempt to make a sequence-specific reagent capable of hybridizing with a DNA molecule. The idea was to develop an oligonucleotide with the ability of binding the major groove of the double helix through Hoogsteen bonds, without requiring the invasion of the double strand. In addition, they also strongly pursued the intent of identifying a molecule easy to synthesize (61).

Peptide nucleic acids (PNA) are synthetic analogues of DNA containing a peptide-like skeleton consisting of repeated units of N- (2-aminoethyl) -glycine, connected to pyrimidine (C and T) or purine (A and G) nucleobases through a methylene-carbonyl bond (Figure 8) (62).

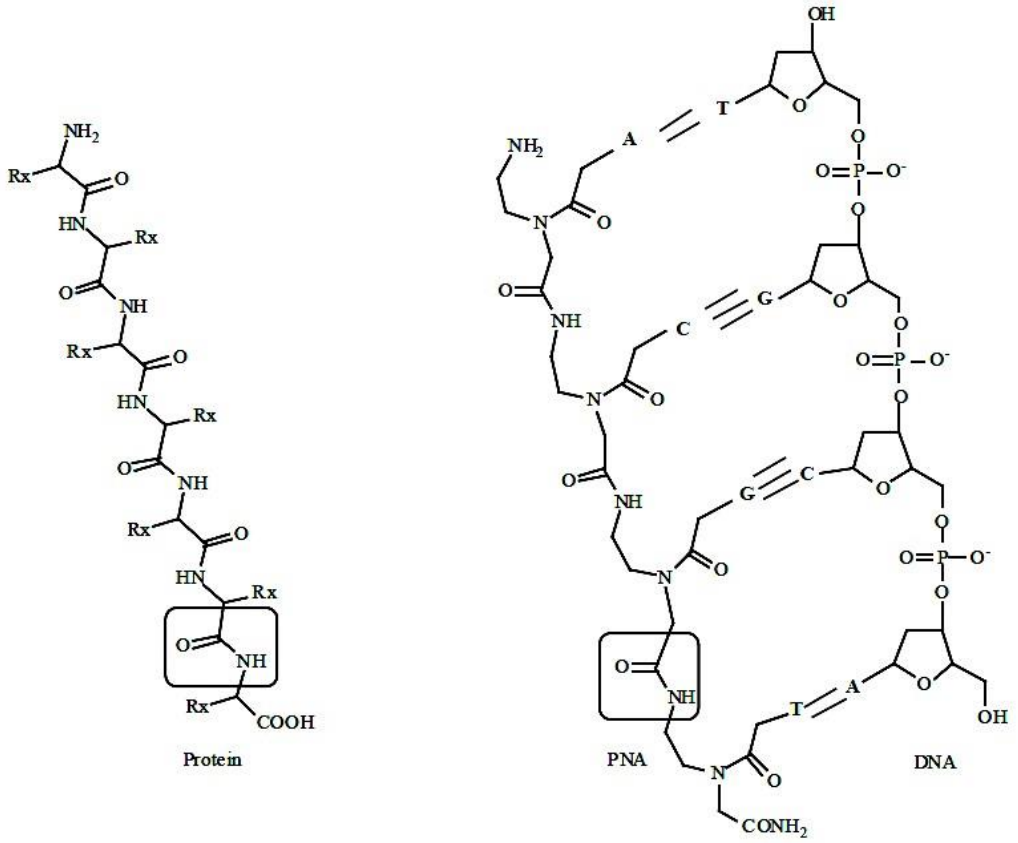

Figure 8*:Chemical structure of PNAcompared to DNA and protein (peptide), showing the different backbone linkages. R indicates a side chain α-amino acid while A, C, G, T are the different nucleobases (e.g. adenine (A), cytosine (C), guanine (G), thymine (T))* (63).

The decision to replace the deoxyribose-phosphodiester with a pseudopeptide skeleton had the scope to increase stability and affinity within the triple helix (Figure 8). However, although PNAs are characterized by a pseudo-peptide skeleton, the main chain is composed of N-(2-aminoethyl)-glycine units consisting of six atoms each, therefore the nitrogenous bases maintain between themselves the same distance present among sugar units in the canonical DNA. This allows them to base-pair other DNA, RNA or PNA strands by complementarity through Watson-Crick type hydrogen bonds (63).

These pseudo-peptides, which conventionally are represented as peptides (the N-terminus in the first position on the left and the C-terminus on the right), differ from nucleic acids since they can hybridize with complementary strands in both their parallel and antiparallel orientation, although the latter is preferred (64).

PNAs have unique chemical-physical characteristics: they are achiral and neutral. The achirality of the PNA skeleton allows to avoid all the problems related to the enantiomeric

purity of the synthetic product; the absence of electrostatic repulsion (due to the fact that the charges at the C and N terminus can be easily removed) determins a much stronger binding affinity between PNA and DNA strands than that between two negatively charged DNA strands; however, the neutral nature of PNAs negatively affects solubility (65). PNAs also show high resistance to enzymatic degradation by nucleases/proteases and a high chemical stability in a wide pH range, even within a strongly acidic environment.

1.3.3 Binding modalities: three-dimensional structures of hybrid PNA / DNA complexes

The original design of the PNA molecule involved a ligand able to recognize its target, the dsDNA, by forming a triple helix, through Hoogsteen bonds at the level of the major groove (63).

Surprisingly, Nielsen and co relized that the triple helix structure PNA · $(DNA)_2$ appeared only for some sequences, while the formation of the hybrid $(PNA)_2$ · DNA, which involves the displacement of the double helix, appeared to be favored. Subsequently, other types of PNA/DNA (RNA) complexes (as show in Figure 9) were synthesized and characterized through the use of different techniques, from computational biology to crystallography and spectroscopy.

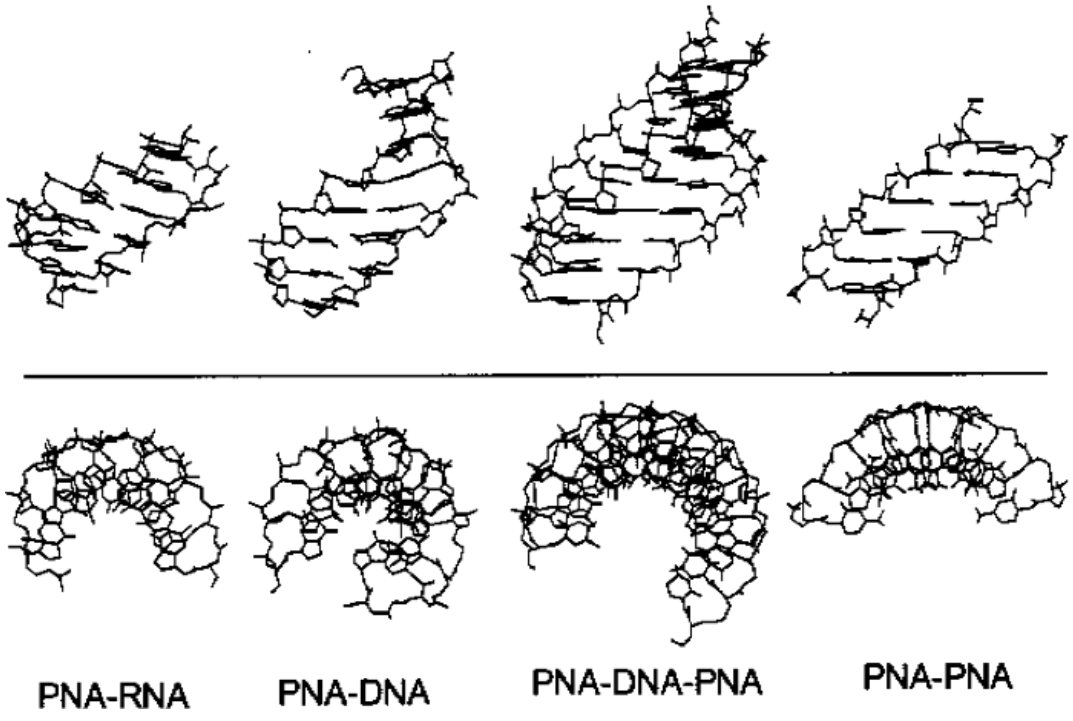

Figure 9 : *Structures of various PNA complexes (66)*

These structures clearly highlight that the PNA is able to adapt very well to its nucleic acid target: in fact, when the PNA interatcs with an RNA strand, the resulting PNA · RNA double helix assumes an A-form conformation, while the PNA · DNA double helix has a B-like conformation, like the DNA itself. On the other hand, the double helix PNA · PNA is very large (28 Å) with almost double the pitch (18 base pairs per revolution) of a A or B shaped helix. (66) The PNA interacts with its targets through the formation of various motifs, which strictly depend on how the analogue was designed, as show in Figure 10:

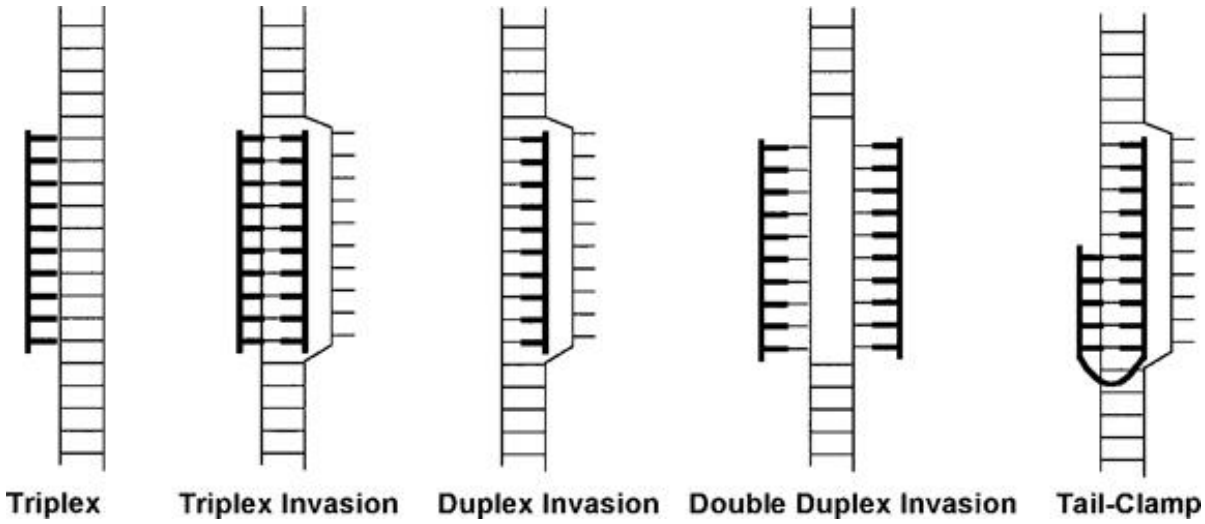

Figure 10: *PNA can bind double-stranded DNA in different modes: i) triplex ii) triplex invasion iii) duplex invasion iv) double-double invasion v) tail clamp. PNA are shown in bold.*

• *Triplex:* the PNA possesses a cytosines-rich sequence , therefore it interacts with the homopurine dsDNA in correspondence with the major groove, forming Hoogsteen-type bonds.
• *Triplex invasion*: PNA is characterized by a homo-pyrimidine sequence, so one strand of the molecule interacts with the homo-purine target ssDNA by Watson-Crick bonds in an antiparallel orientation, while a second PNA molecule binds the same DNA sequence, but in a parallel direction and with Hoogsteen-like ties.
• *Duplex invasion*: the PNA consists of a homo-purine sequence and invades the DNA double helix. Classical base pairs are formed between the PNA and the ssDNA target and lead to the dislocation of the non-complementary DNA strand, resulting in the formation of a structure called D-loop.
• *Double Duplex invasion:* these complexes arise from an attempt to carry out an extremely powerful double-strand invasion by creating double helices with both target DNA strands and not just one, hence the name. The realization of this complex, however, requires the use of two

PNAs which, as they are intended for two complementary portions of DNA, must also be complementary.

• *Tail clamp:* this structure is characterized by two homopyrimidine strands of PNA linked through a flexible linker which form a stable complex with a homopurine DNA target. This structure can be divided into a double helix region with the formation of canonical hydrogen bonds and a triple helix region with the formation of Hoogsteen and Watson Crick bonds.

1.3.4 Limitations of PNA: the challenge of the intracellular delivery

While PNAs hold tremendous therapeutic potential, they have been primarily studied using either cell-free systems or with artificial techniques for penetrating the cell membrane, such as electroporation, nucleofection, and microinjection. In terms of drug discovery, one of the major difficulties in using PNAs clinically, announced by Nielsen in 2003 (67), is intracellular delivery and bioavailability in vivo. Despite being neutral, PNAs are large hydrophilic molecules (> 2KDa) and this determines a limited cell permeability. In order to improve this limitation, a large variety of cellular transport systems have been developed and experimentally tested, with the aim to avoid or reduce the oligomers expulsion from the body without inducing any therapeutic effect. (68). These systems can be divided into two categories: those that use PNAs as they are and those that use modified PNAs or PNAs conjugated to suitable ligands. The first cell membrane model developed for the study of PNA uptake was obtained from liposomes, colloidal vesicles composed of a phospholipid layer (single or double) added with cholesterol, with sizes ranging from 50nm to 2.5um. PNA can be easily encapsulated in the internal aqueous compartment of a liposome in three steps: 1) the mixture of lipids is dried under vacuum to form a lipid film on the wall of the vial, then the film is hydrated and sonicated with the buffer; 2) PNA solution is added to the vial and liposomes undergo five freeze/thawing cycles; 3) liposomes are made stealth by adding DSPE-PEG2000 using the post-insertion method (69).

The properties of internalization can vary considerably in different cell types. PNA has been shown to enter some cells more effectively than others, suggesting the possibility that specific transport mechanisms exist. In particular, neuronal cells are able to internalize the PNA and, if injected, the PNAs can overcome the blood-brain barrier and trigger an antisense response (70). However, it has been shown that PNA has a rather slow efflux rate suggesting that its exit from the cell by passive diffusion occurs very slowly and sometimes it is not even detectable.

In general, therefore, the passive diffusion of PNA does not represent a reliable method for cellular delivery both in terms of timing and due to the high concentrations required, that could lead to a significant increase in toxicity and costs.

Another investigated strategy is to exploit lipophilic tails to penetrate the cell membrane. An example is the phosphonium cation, which easily permeates cellular lipid bilayers and allows PNA to enter the cytoplasm and subsequently the mitochondria of living cells, guided by plasma membrane and mitochondrion potentials (| 30-60 mV and | 150-180 mV negative inside, respectively) (67).

Currently, the most common approach to improve cytosolic delivery is the covalently conjugation of cell-penetrating peptides (CPPs) to PNA. This strategy originates from the discovery that some proteins, called Trojan peptides (such as the HIV virus TAT protein and the Drosophila Antennapedia transcription factor), possess specific amino acid sequences, that allow the recognition by appropriate receptors on the host membrane, and induce the consequent internalization of the compound, avoiding the process of endocytosis (71).

These observations broght to the idea of using CPPs, cationic polymers of different length (9-30 amino acids) and composition (lysine or arginine) that interact with the negatively charged glycoproteins present on the cell surface.

Nevertheless, the use of oligomers with an antigen strategy requires not only the achievement of the cytoplasm but also a subsequent nuclear internalization. From this perspective, the most successful mechanism relies on basic peptide motifs, characterized by the alternation of lysine and arginine interspersed with other amino acids, which reproduce the nuclear localization sequences (NLS). These sequences allow the entry into the nucleus through the recognition and processing of the NLS by the nuclear pores present on the nuclear membrane itself.

In conclusion, to date there is no vector peptide that can be universally used for the internalization of PNAs into cells and nucleus; the winning choice will be the result of the evaluation of several factors, such as the nature and size of the molecule to be transported, the target cell, the experimental conditions, as well as the target action site.

1.3.5 Applications of PNAs

The promising physico-chemical properties of PNAs and the absence of side effects, even at high concentrations, has always attracted chemists and biologists to the use of these molecules for the development of drugs aimed at specific targets (72).
It is in fact already used in many applications such as:

- Agent in Gene Based therapy:
- Probe for hybridization;
- Probe for PCR- clamping;
- Anti-miRNA agent.

1.3.5.1 PNAs as gene expression modifiers

Due to their high stability and ability to bind to both DNA and RNA targets with high specificity and affinity, PNAs can act on gene expression through two main mechanisms: antigene strategy and antisense strategy, as shown in Figure 11.

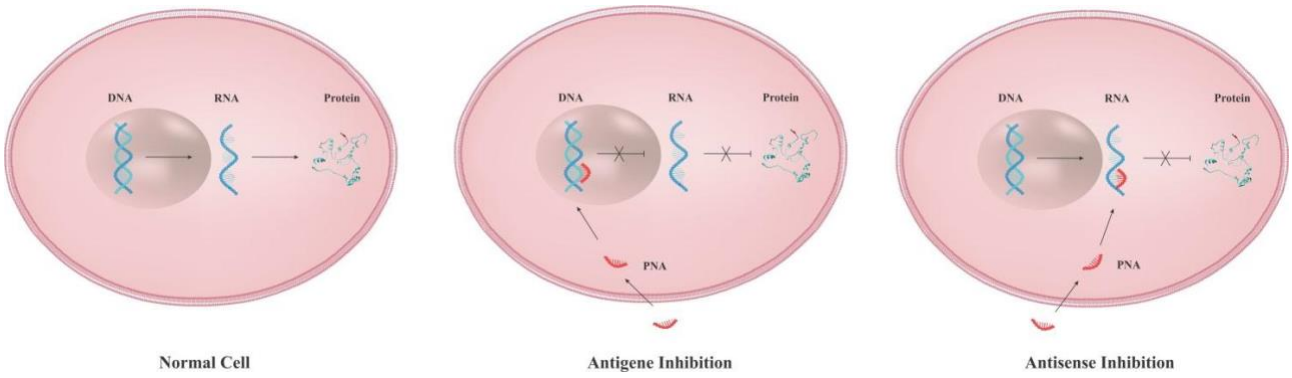

Figure 11: Schematic illustration of PNA-based strategy as antigene and antisense agents. Antigene PNA binds to a complementary sequence in DNA and inhibits transcriptional process, while antisense PNA hybridizes to a target sequence in mRNA and prevents translation process (62).

- *Anti-gene strategy:* PNA is designed to recognize and hybridize to the complementary sequence of a particular gene, interfering with its transcription and preventing the synthesis of the corresponding mRNA.

In the anti-gene mechanism, PNAs forming stable PNA_2/DNA triple helices lead to transcription blockade through various pathways, including the formation of structures that prevent the unwinding of the DNA double helix (required for the attack of the different transcription pre-initiation factors and subsequent recruitment of RNA polymerase) or the blocking of the RNA polymerase itself during the elongation process, which leads to the formation of truncated mRNAs. The use of PNAs as antigenic agents is however limited to polypurine genomic regions and with an invasiveness of the double helix limited by non-physiological saline concentrations. However, the addition of positively charged lysine residues or non-natural bases such as pseudocysteines are adopted to increase the PNA/DNA hybridization rate and the stability of the complex(65),

- *Anti-sense strategy:* PNA is designed to recognize and hybridize to complementary sequences of a particular mRNA, interfering with its translation and preventing the synthesis of the corresponding protein.

Many of the antisense systems developed base their effect on the degradation of the messenger RNA (mRNA)-oligonucleotide hybrid through the recruitment of the H ribonuclease system (RNase H) or the RNA-induced silencing complex (RISC). Instead, several studies have shown how PNAs act through a mechanism of steric interference, by hindering the transcriptional process at the cytoplasmic level, preventing ribosomal attachment or inhibiting the elongation of the translated strand thanks to the mRNA accessibility and its strong hybridization with PNA. In particular, it was discovered that PNAs forming double helixes have the ability to hybridize to the 5 ' of the mRNA or to the translation start codon (AUG region) preventing the recruitment of the ribosome. Triple helix-forming homopyrimidine PNAs, on the other hand, have been seen to block the elongation process leading to filament deletions (62).

In conclusion, compared to the antisense strategy, the anti-gene approach has the advantage of being able to modulate gene expression upstream of the messenger RNA formation, and to act directly on the DNA double helix,pointing out the possibility of using PNAs to control the dynamics of tumor gene expression. An example confirming this assumption is the experiment conducted by Tonelli and co. in which dose-dependent inhibition of MYCN gene expression was achieved in human rhabdomyosarcoma cell lines using an agPNA directed against the MYCN gene (74). Noteworthy, the anti-gene PNA can be used at much lower concentrations and shows a stronger and prolonged inhibitory effect in the time.

Table 4. Some recent antisense and antigene applications of PNA.

Application	Description	(Ref)
regulating var gene activation	Antisense long noncoding RNAs regulate var gene activation in the malaria parasite Plasmodium falciparum	(97)
Exon Skipping Enhancement	peptide conjugates of phosphorodiamidate morpholino oligonucleotide showed enhanced activity in an exon skipping assay in Duchene's muscular dystrophy using skeletal mouse mdx cells	(102)
Regulation of gene expression	PNAs can inhibit miR-509-3p, Cystic Fibrosis Transmembrane Regulator and disease-gene of Cystic Fibrosis	(95, 103)
Silencing of the B-cell lymphoma 2 (Bcl-2) protein expressions	Antisense PNA by conjugation to Fluorescent Mesoporous Silica Nanoparticles. PNA conjugated mesoporous silica nanoparticle was endocytosed by HeLa cancer cells and released PNA into cancer cells inducing effective silencing of the B-cell lymphoma 2 (Bcl-2) protein expression.	
Antimicrobial peptide PNAs	Species-selective PNA antibacterials can selectively inhibit growth of *B. subtilis*, *E. coli*, *K. pnuemoniae* and *S. enterica serovar Typhimurium* in axenic or mixed culture.	(104)
PNA functionalized cationic nanocomplex for in vivo mRNA detection	The early diagnosis of acute lung injury was enabled by electrostatic complexation of a radio labelled antisense PNA-YR9. oligodeoxynucleotide (ODN) hybrid and a cationic nanoparticle (cSCK). The nanocomplex efficiently entered RAW264.7 cells and efficiently detect iNOS mRNA in vitro and in vivo.	(105)
Antibacterial Antisense PNA	Peptide–PNA conjugates targeted to the translation initiation region of the acpP and ftsZ gene of P. aeruginosa (PA01) can completely inhibit P. aeruginosa strains LESB58, PA14 and PA01 at 1–2 mM concentrations.	(106)
Cellular inhibition of miR-122	Efficient miR-122 inhibition was obtained with cationic PNAs at sub-micromolar concentrations. PNA anti-miRs were able to sustain miR-122 inhibitory effects.	(107)
PNA-based artificial nucleases	Artificial nucleases composed of a PEG–PNA–PEG domain conjugated to HGG·Cu and DETA as well-known cleavage sites act as potential antisense and anti-miRNA agents.	(108)
Local and Systemic Dystrophin Splice Correction	Long-term splice correction of the *DMD* gene in *mdx* mice was obtained by intramuscular PNA delivery and effective splice correction in aged *mdx* mice.	(109)
Efficient inhibition of miR-155 function in vivo	MiR-155 inhibition by PNA in primary B cells was achieved in the absence of any transfection agent. Interestingly, PNA also induced additional changes in gene expression.	(110)

***Table 2**: Summarization of recent publications in PNA in antisense and antigene therapy (72).*

2. AIM OF THE RESEARCH

Neuroblastoma (NB) is an enigmatic, multifaceted tumor that predominantly affect children under 5 years of age. NB develops mainly in the adrenal medulla and in the sympathetic ganglia so, it can be viewed as resulting from a failure of neural crest differentiation. The malignancy is characterized by substantial genetical, morphological and clinical heterogeneity. Despite advances in multimodal-therapy the survival rates of high-risk neuroblastoma patients are still disappointingly low and so the treatment of High-risk neuroblastoma remains a significant challenge.

MYCN gene is an oncologic driver in NB actually his amplification occours in approximely 22% of neuroblastomas. MYCN-amplification (MNA) correlates with high-risk disease, rapid progression and poor prognosis. Many of the pro-tumorigenic functions of MYCN are attributed to its ability to regulate global gene expression programs including proliferation, cell growth, response to DNA damage, energy metabolism, apoptosis and differentiation. Since many evidences suggests a causal role of MYCN in NB and because it is a tumor specific gene and not expressed in normal tissue, MYCN is an attractive therapeutic target. However MYCN is considered “undruggable” and, to date, the attempts to directly and specifically target MYCN using traditional small molecules have failed.

In 2019 our group described how the anti-MYCN antigene Peptide Nucleic Acid (agPNA) developed by Biogenera Spa was able to overcome this limitation by inhibiting MYCN expression and its related tumorigenic alterations in NB cell line and specially in MNA-NB. Nevertheless, is known that a drug combination strategy, with lower doses, can have several clinical advantages including fewer adverse events and better patient outcomes.

The aim of this PhD project takes a step forward from agPNA (BGA002) by aiming at the possibility of combining the BGA002 with 13-cis Retinoic Acid (13-cis RA). 13-cis RA is an anti-proliferative and pro-differentiative agent used in the post-consolidation phase of NB therapy. However, many patients who initially respond to therapy with this biological compound acquired resistance that is thought to be due to the aberrant expression of MYCN. Since RA is less toxic than traditional chemotherapy and is able to induce differentiation in malignant cells, different studies propose the use of RA in combination with other treatments. Taken together I decided to evaluate whether BGA002 and 13-cis RA could act synergistically

by restoring sensitivity to RA in resistant NBs (*in vitro and in vivo*) trying to analyze the molecular mechanisms underlying their pharmacological interaction.

3. MATERIALS AND METHODS

3.1 *IN VITRO*

3.1.1 Cell-lines

Neuroblastoma cell lines are cultured in RPMI-1640 (Lonza, Verviers, Belgio) and supplemented with 10% Fetal Bovine serum (FBS) (GIBCO-Invitrogen, Carlsbad, CA, USA) and 2mM of L-Glutamine (Euroclone, Milano, Italia). All cell lines are incubated at 37°C in a 5% CO_2 atmosphere. Culture medium is renewed as needed depending on cell line. Adherent cells, are detached with PBS/EDTA1x solution (NaCl 137 mM, KCl 2.55 mM, Na2HPO4 8.1 mM, KH2PO4 1.4 mM [PBS], EDTA 2 mM) and splitted, when confluence is reached.

All cell lines used with most relevant genetic features are reported in Table 3.

Cell Line	MYCN	p53	Source
KELLY	Amplified	Not mutated	DSMZ
IMR32	Amplified	Not mutated	Kindly provided by professor Della Valle G
LAN-5	Amplified	Not mutated	DSMZ
CHP-134	Amplified	Not mutated	DSMZ
SiMa	Amplified	Not mutated	DSMZ
MHH-NB11	Amplified	Not mutated	DSMZ
GI-LI-N	Amplified	Not mutated	Kindly gifted from Institute Gaslini, Genova
SMS-KAN	Amplified	Not mutated	Kindly gifted from Institute Gaslini, Genova
NGP	Amplified	Not mutated	DSMZ
LS	Amplified	Not mutated	DSMZ
NMB	Amplified	Mutated	DSMZ
SK-N-BE(2)-C	Amplified	Mutated	Kindly provided by professor Della Valle G
LAN-1	Amplified	Mutated	DSMZ
SK-N-F1	Not amplified	Mutated	ECACC
LAN-6	Not amplified	Not mutated	DSMZ
NBL-S	Not amplified	Not mutated	DSMZ
SH-SY5Y	Not amplified	Not mutated	Kindly gifted of professor Spampinato SM

Table 3: *List of cell lines used in this study.*

3.1.2 Cell-lines treatment for viability and RT qPCR.

NB cells are removed from flask and counted using a Burker's chamber. Cells are centrifuged and culture medium is replaced with OPTIMEM withouth FBS. Cells concentration is adjusted up to 5 x 10^4 cells/well for 24 well or 5 x 10^3 cells/well for 96 well flat-bottom plate, then cells are plated for treatment. PNA anti-MYCN (BGA002) is provided as powder by the chemistry department of Biogenera Spa (73–75) and resuspended in NaCl 0.9%. 13-cis Retinoic acid (13 cis-RA) (Sigma Aldrich) and is resuspended in absolute Ethanol (VWR-International, France). BGA002 or 13 cis-RA are administered as single or in combination from concentration of 0.6 μM to 10 μM. FBS is added to medium up to 4% six hours after treatment.

3.1.3 Cell viability assay

Viability is evaluated using CellTiter-Glo Viability Assay ® kit (Promega). Cells are treated as previously described for 72 hours, then kit reagent is added and luminescence is recorded using Infinite F200 instrument (Tecan). The percentage of the effect is calculated on the basis of mean luminescence of the control and the results are graphed using Graphpad software.The combination index (CI), is calculated from growth inhibition curves, using CompuSyn software.

$$\text{D-Luciferine} + \text{ATP} + O_2 \xrightarrow[Mg^{2+}]{\text{D-Luciferase}} \text{AMP} + \text{PPi} + \text{Oxyluciferin} + CO_2 + \text{Light}$$

Figure 12: *The cell is the source of the ATP in the luciferase reaction so, the luminescence produced is proportional to the number of viable cells.*

3.1.4 Quantitative real-time PCR

After 12 hours of treatment, cell lines were lysed and stored at 20° C. Then the RNA was extracted using the RNAspin Mini RNA isolation Kit (GEHealthcare, Little Chalfont, Buckinghamshire, England) according to the manufacturer's instructions.

Each sample of RNA was quantified with the NanoDrop Spectrophotometer ND-100 (Nanodrop Tecnologies, Wilmington, DE, USA) then 100 ng of RNA are retrotranscribed to

single-stranded cDNA using the High Capacity cDNA Reverse Transcription Kit (Applied Biosystem). According to instructions, after preparing the Reverse Transcription Master Mix, RNA is added and the reactions is loaded into a thermal cycler as follow: 25° for 10' , 37° for 120' and 85° for 5'.

The cDNA obtained was used to perform Real Time PCR. 10 ng of each cDNA sample are loaded in duplicates then real Time PCR is performed using CFX Connect (Bio-Rad, Hercules, CA, USA) and iTaq Universal SYBR Green Supermix (Bio-Rad, Hercules, CA, USA). Primers sequences are indicated in the Table 4. PCR is performed as follow: 95° for 3', 95° for 5'' and 55° for 15'' (repeated for 39 cycles), and melting as follows: 95° for 10'', 65° for 5'' and 59 cycles of 10'' of increment of 0.6° per cycle up to 95° .
Crossing points (Cp) from each sample were calculated using the second derivative maximum method, and the expression level was quantified by comparison with the housekeeping gene identified in BIRC4.

Primer	Sense	Antisense
MYCN I	ACCCGGAGACACCCGCGCAGAATC	GTAGAAGCAGGGCTGTAGCGAGTC
BIRC4	ACAAGGAGCAGCTTGCAAGA	AGCATGTTGTTCCCAAGGGT
CRABP1	CCACTGCACGCAAACTCTTC	GCCTGCATCCCTTCCTGAAA
CRABP2	GGCAACTGGAAAATCATCCG	GGTGGTGGAGGTTTTGATGTAG
SLC7A5	CTCTTCCTGATCGCCGTCTC	GACCACCTGCATGAGCTTCT
SLC1A5	ACCATATCTCCTTGATCCTGGC	TACGGTCCACGTAATTTTGGAG
IGF1R	GAAGGAGTTGCCAAGGGTGT	GCTTGGAGGTGCTAGGACTG
SLC38A5	AAATCTGAGCTCCCCCTGGT	GTGTTTCATGAGGGCGAGGG
AKT1	GCACAAACGAGGGGAGTACA	AAGGTGCGTTCGATGACAGT
AKT1S1	TGAGCCCACAGAGACAGAGA	CGGGGTCTGACTCACAGAAG
AKT2	TGATGGAGTATGCCAACGGG	GTCCTCCAGCACCTTGATGT
MLST8	TGGCAGCTGTCAATAGCACC	TCTTGATGCTCAGCTCCGTC
RPTOR	GGTGCTGTTAAGCCAAGTGC	TAGGGGAAGATGCCGACAGA
ADORA1	CTTCTTTGTGTGGGTGCTGC	GGTAAGGATGCTGGGCTTGT
EIF4EBP1	ACCTGTGACCAAAACACCCC	GGTAGTGCTCCACACGATGG
LARP1	GGTGGCACTCGAACCCATTT	CACTCGGTGGAAGGAAGCAA
LYK5	TGAAGGCCCTCGACTACATCC	GGAAAATCGTGGACCACTCGC
SKP2	GAGCCCGACAGTGAGAACA	GGAGGCACAGACAGGAAAA
TFDP1	AGCCAACGGAGAACTCAAGG	GCAGACCAAGGTGAGGAGTC
NRP2	GGGATCCTCTCCCTGACCTT	GGGTCCAGCCATTGTCATCA
ACACA	CAGAGGGAACATCCCTACGC	AAGAGACCATTCCGCCCATC
FASN	AGCAGTTCACGGACATGGAG	ATGGTACTTGGCCTTGGGTG
TP53	GCCCTATGAGCCGCCTGAG	CCAGGACAGGCACAAACACG

E2F1	GCATCCAGCTCATTGCCAAG	CAGGGTCTGCAATGCTACGA
CDK2	TGGTACCGAGCTCCTGAAATCCT	CGGAAGAGCTGGTCAATCTCAGAA
ELMO1	CATTGTTCTTCAGGGGGACGA	CAGGGAGCTAGGCTTGGTTG
ODC1	GGCTTTCCTGGATCTGAGGAT	ACATAGTATCTGCCGGGCTCA
TKT	TCAAAAAGGAGCACCCGGAC	GAGCCGCAGAGGTTGATGTT
DNMT1	GAGGAGGGCTACCTGGCTAAAG	GGGGCTAGGTGAAGGTTCAG
HMGA1	AACCACCACAACTCCAGGAAG	TTCCTTCCTGGAGTTGTGGTG
MMP2	TGATGGCATCGCTCAGATCC	GGCCTCGTATACCGCATCAA
NRCAM	CAGGCGATGACAACAATAGCC	ATCACGCGGAAGGAGTAGTTCA

Table 4: *List of primers used in this study.*

3.1.5. Synergy calculation

The combination index plot was calculated for each cell line using all the biological replicates (the procedure was the same for MYCN mRNA inhibition or for cell growth inhibition). Data were inserted in CompuSyn according to the guidelines (74). The combination index (CI) and fractional inhibition (FA) are obtained from the compiled report. As described in the original pubblication, the combination index equation defines the synergism (CI < 1), additive effect (CI = 1) and antagonism (CI > 1) (75).

3.1.6 Western blot analysis

After treatment for 24h, cells were lysed in RIPA lysis buffer (containing 20 mM Tris-HCl (pH 7.5), 150 mM NaCl, 1 mM Na2EDTA, 1 mM EGTA 1% NP-40, 1% sodium deoxycholate, 2.5 mM sodium pyrophosphate, 1 mM,b-glycerophosphate 1 mM, Na_3VO_4, 0.1% SDS) supplemented with Protease and Phosphatase Inhibitor Cocktail (Thermo Fisher Scientific Inc., Rockford, IL). After sonication, cells were centrifugated at 15,000× g, 4 °C, for 20 min and protein fractions were collected. A total of 30 μg of proteins were separated by SDS–PAGE using Criterion TGX polyacrylamide gels (Bio-Rad, Hercules, CA, USA) and blotted onto a nitrocellulose membrane (Bio-Rad, Hercules, CA, USA). Proteins were detected using the Amersham ECL Prime Western Blotting Detection Reagent (GEHealthcare, Little Chalfont, Buckinghamshire, England), the ChemiDoc-It2 Imaging System and the Vision Works LS Software for the analysis (UVP, LLC, Upland, CA, USA). Bands were revealed by the Amersham ECL detection system.

The expression of specific proteins was assessed by using the following antibodies: anti-N-

MYC 1:800, anti-Phospho-Akt (Ser473) (#4060) 1:1000, anti-Akt (#9272) 1:1000, anti-Phospho-p70 S6 Kinase (Thr389) (#9206) 1:1000, anti-p70 S6 Kinase (#9202) 1:1000, anti-Phospho-S6 Ribosomal Protein (Ser235/236) (#4858) 1:1000, anti-S6 Ribosomal Protein (#2217) 1:1000, anti-Phospho-4E-BP1 (Thr37/46) (#2855) 1:1000, anti-4E-BP1 (#9452) 1:1000, anti-GAPDH (#5174) 1:1000. All these antibodies, except N-MYC, were from Cell Signaling Technology, Danvers, MA, USA. N-MYC was from Santa Cruz Biotechnology (sc-53993)

3.1.7 Apoptosis analysis

Kelly, LAN-5 and SK-N-BE(2)-C cell lines were treated as described above. Cells are detached using trypsin/EDTA, pelleted by centrifugation, resuspended and washed twice with PBS buffer additioned with 4% FBS. Cells were stained with Annexin V / FLUOS Staining Kit (Roche, Mannheim, Germany) according to the manufacturer's instructions. Cell samples were analyzed by the CytoFLEX flow cytometer (Beckman Coulter) using 488nm excitation, 515nm filter for fluorescein and 600nm filter for PI detection. Results are analyzed with FlowJo software (Tree Star).

3.1.8 Confocal microscope analysis

Kelly and LAN-5 neuroblastoma cell lines are seeded 30.000 cell/cm2 24 hours before treatment in Lab-Tek Chambered Coverglass (Thermofisher: 155411 16/PK) using OPTIMEM at 4% FBS. Culture medium is changed with fresh OPTIMEM and cell are treated with BGA002, 13-cis RA, or both at concentration of 2.5 μM each. After 6 hours FBS is added up to 4%. Cells are treated for 48 hours. For staining, culture medium is removed and cells are incubated with Lysosome staining kit (Green Fluorescence) (Abnova: KA4111) and 25nM of MitoTracker™ Deep Red FM (Thermofisher: M22426), at 37°C for 45 minutes. After the incubation staining solution is removed and cell are washed twice with filtered NaCl 0.9% for about 2 minutes. Fresh culture medium is added at last.

Image are acquired using confocal microscope Nikon Eclipse Ti2-E, in oil immersion with 100x objective. Z-stacks are acquired using 0.2 μm Z-step. Image are analyzed using NIS-Element viewer.

Image analysis is performed with Fiji. For mitochondrial footprint evaluation, Z-stack ROIs are

defined for each single cells, and image are processed using MiNA approach (76). Mitochondrial areas are measured using Fiji measure tool. Mitochondrial volumes are measured as sum of mitochondrial area multiplied for Z-step (0.2 μm).

3.1.9 Transmission electron microscopy

Kelly and LAN-5 cells are seeded at the density of 20.000 cells/cm^2 in 6-well culture plates. 24 hours after seeding, cells are treated with different compounds (NaCl 0.9%; BGA002 2.5 μM ; 13cis-RA 2.5 μM ; Combination) in low FBS culture medium; after 6 hours FBS is added up to 4% and treatment proceed for up to 48 hours in an incubator at 37°C with 5% CO2. Before fixing, cells are treated with chloroquine 60 μM overnight.

At the end of experiments,cells are fixed in 2.5% buffered glutaraldehyde directly in 6-well culture plates for 20 minutes at room temperature, detached with scraper, collected in tubes, pelleted and kept at +4°C overnight. After washing in phosphate buffer, the cells are post-fixed in 1% buffered osmium tetroxide for 1 hour at +4°C, washed and dehydrated through graded ethanol followed by embedding in Araldite resin. Then, samples are sectioned with ultramicrotome and the obtained ultrathin sections are collected on grids and counterstained with uranyl acetate and lead citrate before the ultrastructural observation in a Philips CM100 (FEI Company, ThermoFisher, Waltham, MA, USA) Transmission Electron Microscope. Digital images are obtained using an Olympus camera.

3.1.10 Morphological analysis of differentiation

Kelly, LAN5, SK-N-BE(2)-C, SH-SY5Y are seeded in Optimem (4% FBS) in 6 wells plate (Thermo-scientific). After 24 hours cells are treated with BGA002 (1.25 μM), 13cis-RA (1.25 μM) and BGA002 + 13cis-RA (1.25 μM) and the treatment is repeated every 48 hours. Photos are taken every 48 hours with the Eclipse TE2000-S (Nikon). Cells are maintained in cultutre for 18 days,changing medium every 48 hours. After 12 hours, 9 and 18 days cells are lysed and RNA is extracted as described above. I measure the extension of the neurites with Simple Neurite Tracer, using ImageJ software.

3.1.11 Wound healing assay.

Kelly, LAN5, SK-N-BE(2)-C, LAN-1, SH-SY5Y cell-lines are seeded in Optimem (4 % FBS) to reach confluence after 24 hours in 12 wells plate. TET-21N are cultured with or without tetracycline for at least 72 hours as described above. The day after seeding, scratch is mechanically done in the middle of each well using a 200µL tip. Treatment with BGA002 (at 1.25 and 2.5 µM), 13cis-RA (at 1.25 and 2.5 µM) and BGA002 + 13cis-RA (at 1.25 and 2.5 µM) is performed immediatly after the scratch.

Cells are maintained in culture up to 72 hours and photos were taken every 24 hours (0, 24, 48, 72h after scratch) using the microscope Eclipse TE2000-S (Nikon). At the end, cells were lysed and RNA extracted as described above. Images were analysed at different time-points using Wound Healing Tool on ImageJ (IJ 1.46r, NIH), the gap area were calculated in respect to day 0.

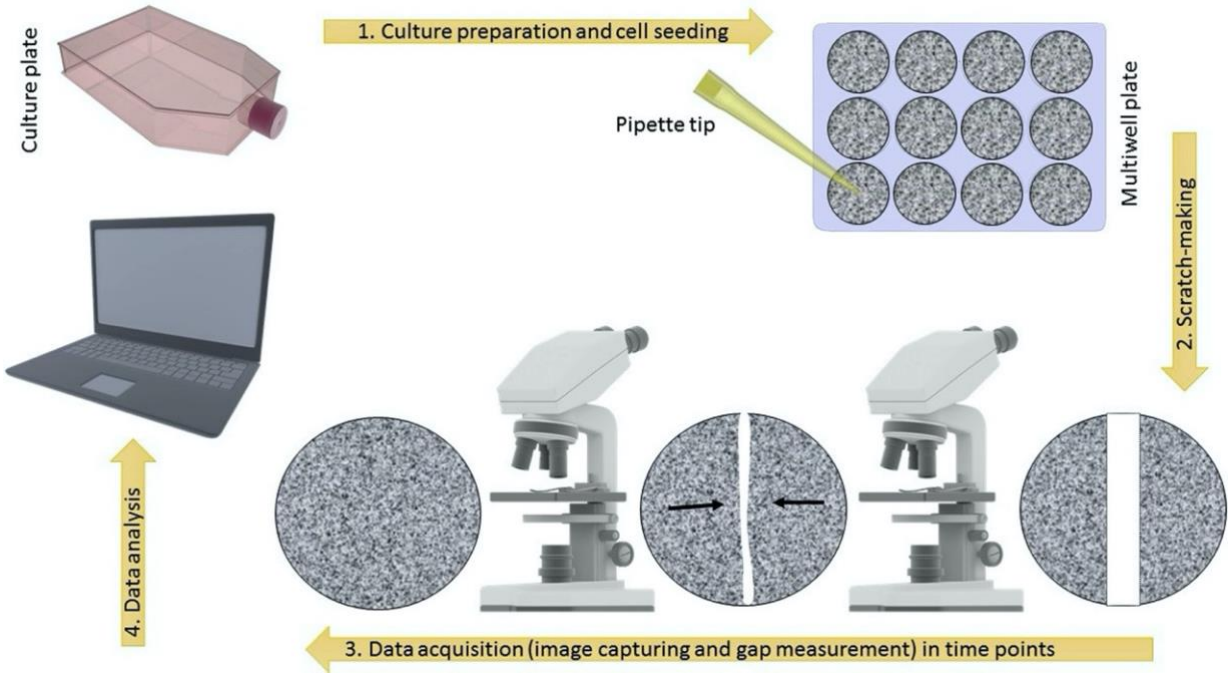

***Figure 13**: Graphical abstract summarizing the workflow of the in vitro wound healing assay* (77).

3.1.12 Lysosome area measurement

Kelly and LAN-5 neuroblastoma cell lines are seeded 30.000 cells/cm^2 24 hours before treatment in Lab-Tek Chambered Coverglass (Thermofisher: 155411 16/PK) using OPTIMEM at 4% FBS. Culture medium is changed with fresh OPTIMEM and cell are treated with BGA002, 13-cis RA, or both at concentration of 2.5µM each. After 6 hours, FBS is added up to 4%. Cells are treated for 48 hours.For staining, culture medium is removed and cells are incubated with Lysosome staining kit (Green Fluorescence) (Abnova: KA4111) and 25nM of MitoTracker™ Deep Red FM (Thermofisher: M22426), at 37°C for 45 minutes. After the incubation, staining solution is removed and cells are washed twice with filtered NaCl 0.9% for about 2 minutes. Fresh culture medium is added at last.

Image are acquired using confocal microscope Nikon Eclipse Ti2-E, in oil immersion with 100x objective. Z-stacks are acquired using 200nm interplane distance.

Lysosome are elaborated using Fiji plugin on ImageJ software. Z-stack containing lysosome are selected using Image>Stack>Tool>Slice Keeper, once selected all images are binarized using Process>Binary>Make Binary, Yen method. Lysosome are then analyzed using Analyze>Analyze Particles, size lower value is set to 0.1 µm^2. Mitochondria are qualitatively analyzed using NIS-Element viewer.

3.2 IN VIVO

3.2.1 Neuroblastoma Luminescent cells

Phoenix-Ampho cells are transfected with Lipofectamine 2000 (Invitrogen) and plasmid pMMP-Luc-neo (kindly provided by Professor Andrew Kung, Harvard Medical School, Boston, MA). The viral particles are collected at 48 and 72 hours after transfection. The CHP-134 cell line are inoculated with the viral particles and polybrene (hexadimethrine bromide, Sigma). The cells are subjected to selection for 15 days with 1 mg/mL of G418 (Calbiochem). The best clones are selected and their luminescence is measured. The resulting cell line is stored as CHP-134 Luc.

3.2.2 Xenograft ectopic Neuroblastoma Mouse Model

All experiments involving animal model are performed under approved ministerial protocol 564/2018-PR.

Xenograft ectotopic mouse model are generated from both male and female *Mus Musculus* NOD / SCID CB.17 5 weeks old. Animal are purchased from ENVIGO and are maintained in filtered cages, in standard condition (20-24 ° C temperature, relative humidity 50-60%), with light/darkness cycle of 14-10 hours. Feed and water are sterile and provided *ad libitum* litter is sterile as well. After moving, animal are housed for settle down, at least one week before proceeding with the xenograft. When proper cell number is reached $10x10^6$ cells per animal are resuspended in 100 µl of PBS. Animals are sedated with gas anesthesia and cells are implanted under the skin in the posterior- right region on the back. The cell suspension is inoculated using 0.3 ml insulin syringe with 30 G needle a. The growth of the tumor is evaluated by luminescence acquired by the UviTec Imaging System (Uvitec). Treatment is performed after the tumor reached the predefined starting point in the bioluminescent acquisition.

Treatment is performed daily for 28 days with vehicle, BGA002 (10 mg/kg/day), 13cis-RA (10 mg/kg/day), or both. Vehicle and BGA002 are administered with subcutaneous injection, 13cis-RA is administered with intraperitoneal injection. Animal are monitored until they reached the endpoint (10 mm of tumor linear diameter and a total tumor volume of 523 mm^3) or until they reached 60 days after the treatment start. Tumor size and volume are measure using electronic caliper. After reached the endpoint mice are sacrificed. Tumors are removed, measured, weighed, and fixed in 4% formalin.

3.2.3 Immunohistochemistry

After fixation tumor are washed under running water and kept in 70% ethanol solution. For slice preparation tumors are dehydrated, embedded in paraffin, and cut into 4-mm sections. Paraffin removal was accomplished by incubating histologic slides in toluene followed by incubation in ethanol. The slides were incubated in 2% H_2O_2/methanol for inhibition of endogenous peroxidase activity. Hydration was performed by serial incubation with 96% ethanol, 70% ethanol, and distilled water. For the histological analysis the slides were stained with hematoxylin, dehydrated, and mounted. For the immunochemistry analysis, after hydration, antigen retrieval was performed by heat processing in 1 mmol/L EDTA, pH 8, both for N-Myc antibody and ki-67 antibody. The slides were blocked with 10% BSA in PBS, stained with the N-Myc (OP13, Calbio- chem), Ki-67 (MIB1, Dako) antibodies and subsequently treated with secondary antibody (peroxidase conjugated anti-mouse, Dako). The peroxidase coloration reaction was performed using the Dako DAB Kit. The slides were stained

with hematoxylin, dehydrated, and mounted. Images were acquired with the Leitz Diaplan microscope.

3.2.4 Histology image processing and immune-histochemistry quantification

For each condition around 200 images were acquired. The following pre-processing steps were conducted on the whole image and in batch. Image were processed using Fiji (78,79) to enhance separation between diaminobenzidine (DAB) and hematoxylin (HE). Briefly, we removed the background, color correct the image to improve red and blue separation and to increase overall image contrast (the same modifications are applied to each image under analysis). Processed images were analyzed on python. Each image was randomly divided in 20 images of 512 x 512 pixels. The separation of the immunohistochemical (IHC) diaminobenzidine (DAB) staining from the hematoxylin (HE) counterstaining was conducted with the method described in literature (80). The analysis was conducted on the separate channel images. Briefly, we used Otsu threshold, removed small object, eroded and filled the gap to select the stained cells and then we segmented the cell using watershed segmentation. The analysis were done using the scikit-image library in python (81). After segmentation, the number of individual cells were counted. We calculated the ratio for each image between the number of DAB-stained cells (DABn) and the number HE-stained cells (HEn) for each image:

$$ratio = \frac{DAB_n}{HE_n}$$

The following libraries from Python (version 3.7) was used for the analysis: Scikit-image, Pandas, Numpy, imageio, scipy.

4. RESULTS

4.1 BGA002 in combination with 13-cis RA cooperates to inhibit MYCN activity in NB

4.1.1 BGA002 in combination with RA downregulates MYCN expression and affects cell viability in NB

We have previously shown that the anti-MYCN PNA BGA002, was capable of specifically inhibiting the expression of MYCN oncogene in NB cell-lines. The specific inhibition caused by BGA002 resulted in apoptosis induction and potent cell-growth inhibition both in MNA and non-MNA NB (82).

Previous studies showed that treatment with 13-Cis RA (RA) induces differentiation and cell cycle arrest after the down-regulation of MYCN expression at mRNA level (55). However, since many patients developed a resistance after the treatment, probably dependent on MYCN expression, it is clear that single-agent therapy could limit the therapeutic results, whereas combination of different strategies may improve the outcome.

Here, I investigated how the combined treatment of BGA002 and RA (BGA002-RA) affects MYCN expression in a broad panel of NB cell lines: among the 17 cell-lines tested, 10 are MNA, 3 are MNA p-53 mutated, 3 are non-MNA and 1 is non-MNA p-53 mutated.

First of all, I evaluated the specific inhibition of MYCN mRNA expression after 12 hours of treatment at 2.5µM. Interestingly, treatment with RA alone achieved a poor inhibition of the target, while treatment with BGA002 alone showed a massive reduction in all the NB cell line and the MYCN inhibition was strengthened by the use of BGA002-RA combination (Fig 14A). This result is also confirmed at different doses and it shows a dose-dependent trend (Fig. 14B).

Then I tested cell viability inhibition after treatment in the same NB cell lines panel with increasing doses (from 0.3 µM to 10 µM of 13-cis Retinoic Acid, BGA002, BGA002 + 13-cis Retinoic Acid) for 72 hours. As shown in Figure 15 both molecules lead to a reduction in cell viability, but in a distinct way: RA alone had a limited effect, BGA002 strongly inhibited cell viability in a dose-dependent manner (especially in the MNA cell-lines) and the combined treatment further enhanced the inhibition level.

I further analyzed viability data comparing GI_{50} value of all cell lines tested, using Wilcoxon matched pair test: BGA002 showed low GI_{50} values both alone and in combination with RA.

In particular, BGA002-RA combination showed lower GI50 value also compared with BGA002 single treatment. Instead RA alone had much less efficacy and interestingly it performed better in non-MNA cell lines, that commonly do not develop resistance. (Fig 15C)

4.1.2 BGA002 in combination with RA shows synergic effect in NB

To understand if combination properly enhances single agent approach, I evaluated the consistency of combination effect in both MYCN mRNA and cell viability data using the software CompuSyn. I perform FA-CI analysis, as reported in Figure 16 A and B respectively for mRNA and viability. Although the distribution of data for each cell line appeared very different, the majority showed a polarization in the lower area of the representation (CI < 1) where combination of BGA002 and RA resulted in synergic effect.

4.1.3 BGA002 in combination with RA blocks N-Myc protein expression in NB

Western Blot analysis was performed to evaluate N-Myc protein inhibition after treatment (Fig 17). Following the trend of previous results, RA alone was unable to reduce protein expression, while the combined treatment led to a stronger N-Myc decrease respect of BGA002 alone only in MNA and p53 wild type cell lines. In fact SK-N-BE(2)-c showed less responsive protein reduction after compound administration both alone or in combination, probably due to p53 mutation.

4.1.5 BGA002-RA induces apoptosis in NB cell-lines

Drug treatment showed high cell growth inhibition, so I investigate in details the mechanism behind cells death. To do this, AnnexinV-Fluorescein-PI assay was performed for apoptosis evaluation. Following the trend of previous results, RA failed to induce apoptosis in the NB cell lines, while BGA002 alone induced apoptosis and the treatment in combination with RA reinforced this effect, in MNA-NB Kelly cells but not in MNA-NB LAN-5 cells (Figure 18).
These results are consistent with data shown in our previous article (82) in which *MYCN* inhibition by BGA002 led to mitochondrial damage, with ultrastructural damage and reduction in the mitochondrial connection pattern, followed by apoptosis in MNA-NB cells (Kelly).

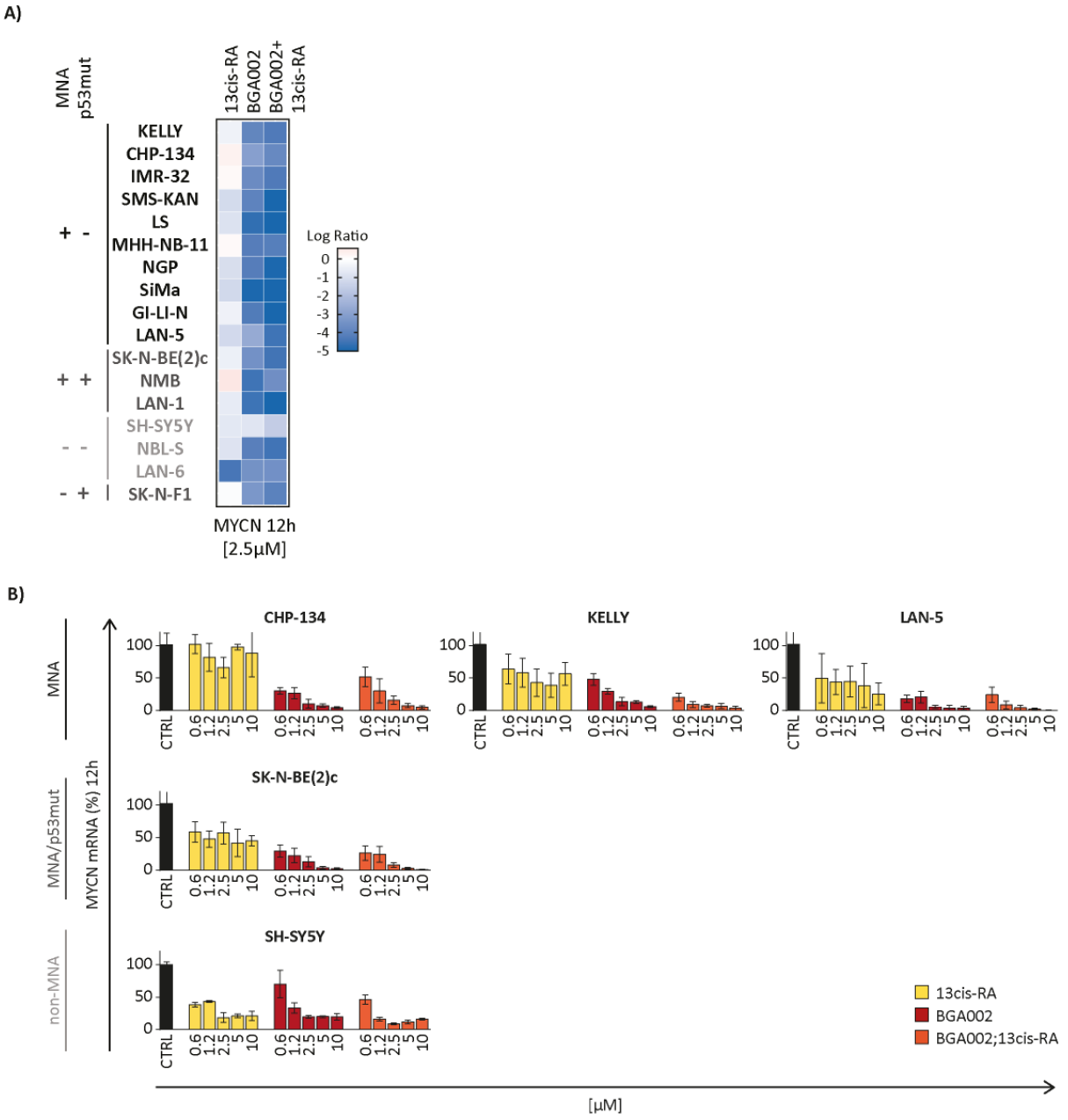

Figure 14: A) *Heatmap represents in vitro efficacy for cell viability inhibition after 72 hours of treatment at different doses. The color scale represents the percentage of inhibition normalized over the control (n = 3 experiments).* ***B)*** *NB cell-lines treated with increasing doses (13-cis Retinoic Acid, BGA002, BGA002 + 13-cis Retinoic Acid) for 12 hours. The MYCN mRNA expression was evaluated through RT-PCR (n = 3 biological replicates). Columns represent the mean percentage of MYCN mRNA normalized over the control, the whiskers represent the standard deviation. NB cell-lines are ordered according to their MYCN amplification and p53 mutation status.*

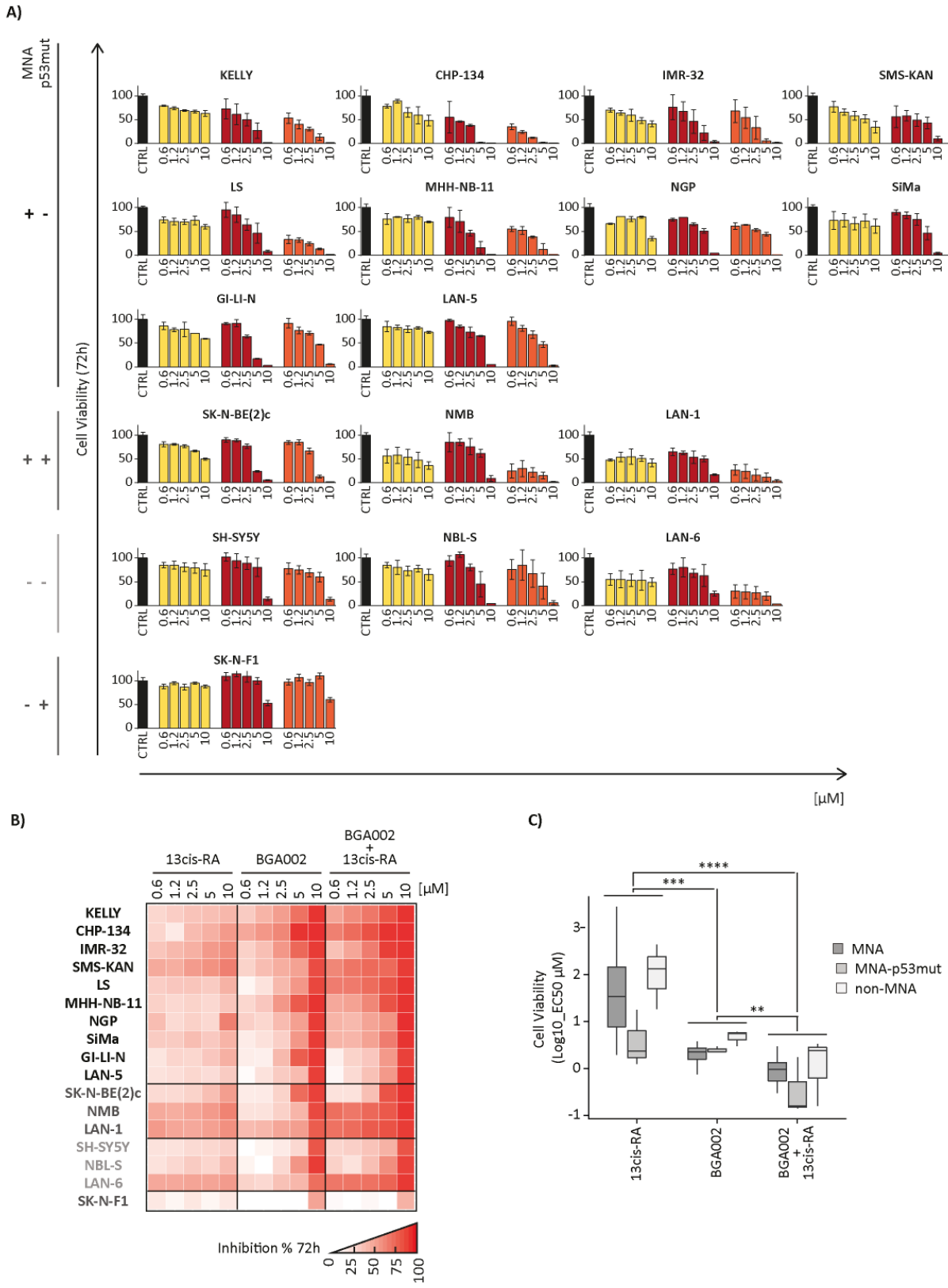

Figure 15: A) *NB cell-lines treated with increasing doses (13-cis Retinoic Acid, BGA002, BGA002 + 13-cis Retinoic Acid) for 72 hours. The cell viability was evaluated through luminescence assay (n = 3 biological replicates). NB cell-lines are ordered according to their MYCN amplification and p53 mutation status.* ***B)*** *Heatmap represents in vitro efficacy for cell viability inhibition after 72 hours of treatment at different doses. The colour scale represents the percentage of inhibition normalized over the control (n = 3 experiments).* ***C)*** *Viability decrement GI_{50} grouped for MYCN amplification status and/or p53 mutation*

*status. Each dot represents a singular experiment (n = 3 for each cell line). In the box plot the median is indicated as middle lane, the box limits represent the first and third quartiles, whiskers represent sample within the 1.5 interquartile ranges. Wilcoxon matched-pair test; **, p< 0.01; ***, p< 0.001; ****, p< 0.0001.*

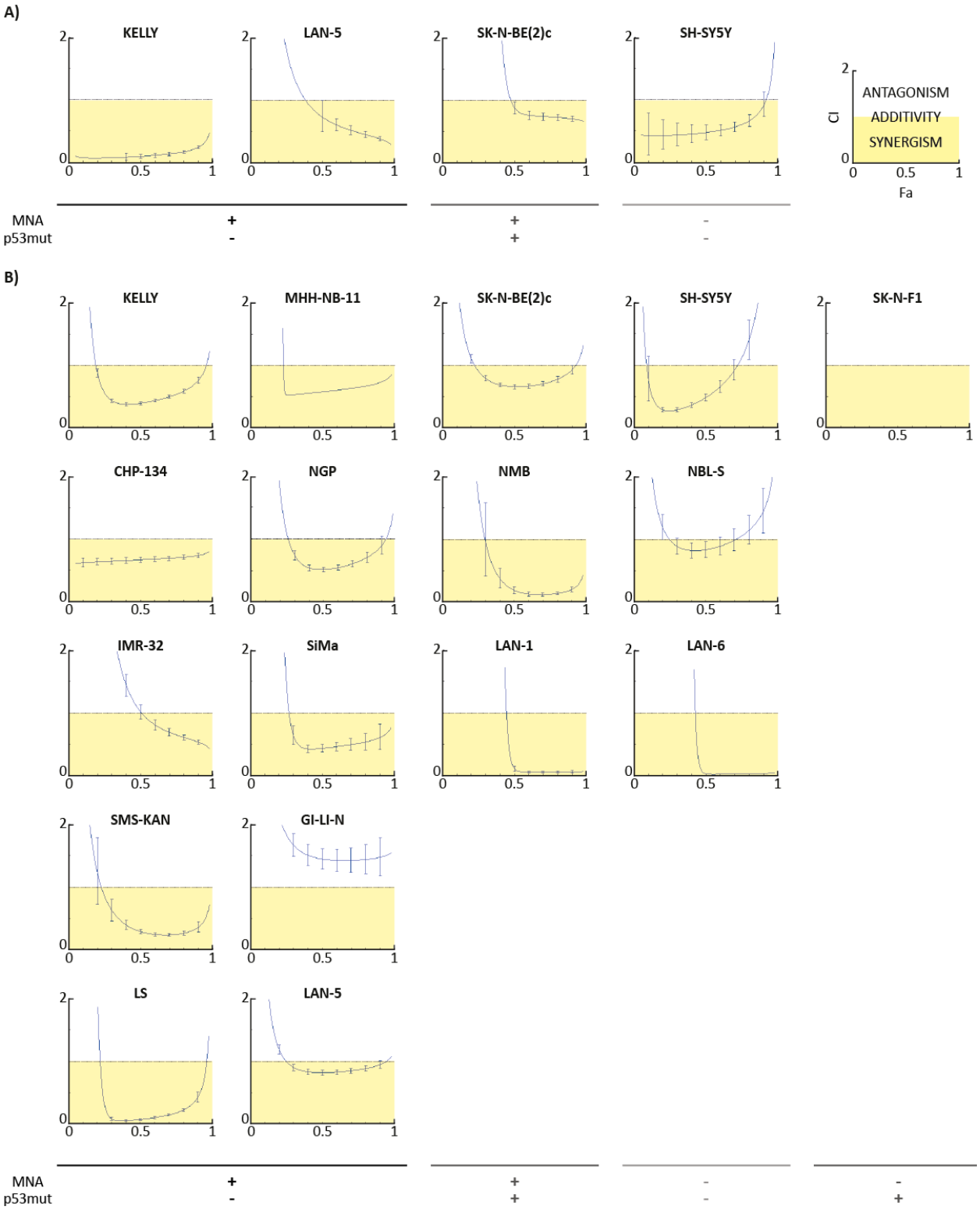

***Figure 16**: FA-CI plot (combination index and fractional inhibition) for A: MCYN mRNA in NB cell lines; B: cell viability decrease.*

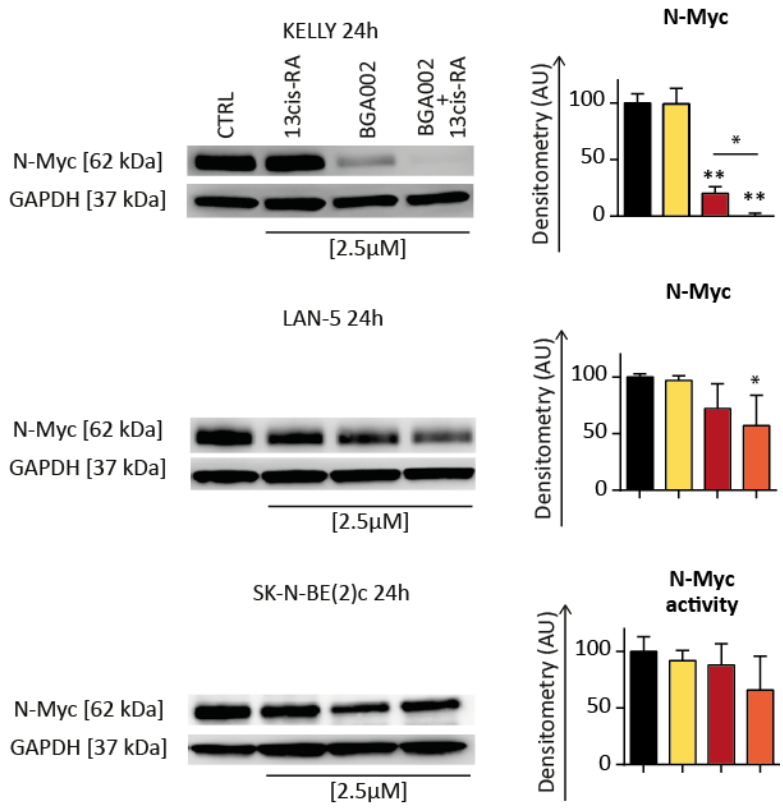

Figure 17 : Representative western blot analysis for MNA cell-lines Kelly *and* LAN-5 after 48 hours of treatment (n = 3 experiments for cell line). Left, representative staining for N-Myc (top) and associated GAPDH staining (down). N-Myc quantification normalized over the GAPDH is presented on the right; the bar represents the mean of 3 experiments, the whiskers represent the standard deviation; (n=3 experiments, *data were analyzed with a two-tailed Student's t Test* **** *p-value ≤ 0.0001*, *** *p-value ≤ 0.001*, ** *p-value ≤ 0.01* *p-value ≤ 0.05, were not indicated p-value >0.05).*

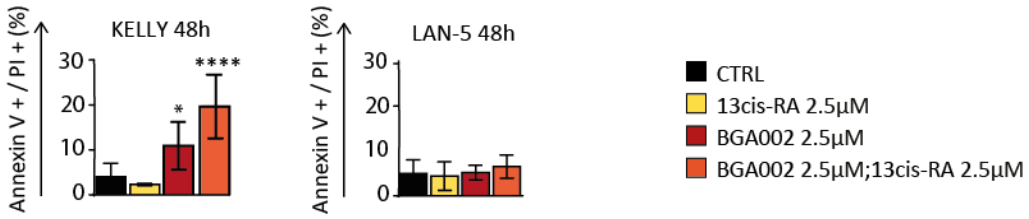

***Figure 18**: Apoptosis measurement after 48 hours of treatment for Kelly, LAN-5 and SK-N-BE(2)c cell lines (n = 3 experiments for each cell line). Bar-plots represent the percentage of cells stained by* Annexin V+/PI+, *bars represent mean, whiskers the standard deviation; (n=3 experiments, data were analyzed with a two-tailed Student's t Test **** p-value ≤ 0.0001 *p-value ≤ 0.05, were not indicated p-value >0.05).*

4.1.5 BGA002-RA leads to a consistent mitochondrial damage in NB

To evaluate mitochondrial condition after treatment I assessed with Pasquinelli group electronic microscope ultra-structural analysis Treatment with BGA002-RA strengthened the BGA002-induced mitochondria alteration in Kelly cells, while RA alone had no activity. Analysis also showed that BGA002-RA led to a consistent appearance of macrovacuoles as major apoptosis morphological feature. In contrast we found a lower apoptotic effect and less pronounced apoptotic features in LAN-5cell line. Interestingly we noticed that in MNA-NB cells (LAN-5) with lower apoptosis effect, after BGA002-RA treatment, mitochondria were similar to the untreated cells (Fig 19A).

Moreover, confocal image analysis showed a dramatic signal in mitochondria volume in Kelly cells while we did not find the same damage extent in LAN-5 cells (Fig 19B). We further investigated mitochondrial alteration analyzing mitochondrial distribution by footprint evaluation in single cells. As seen in previous results, Kelly showed a high reduction in mitochondrial distribution after combination treatment compared to controls while LAN-5, showed normal morphological structures (19C).

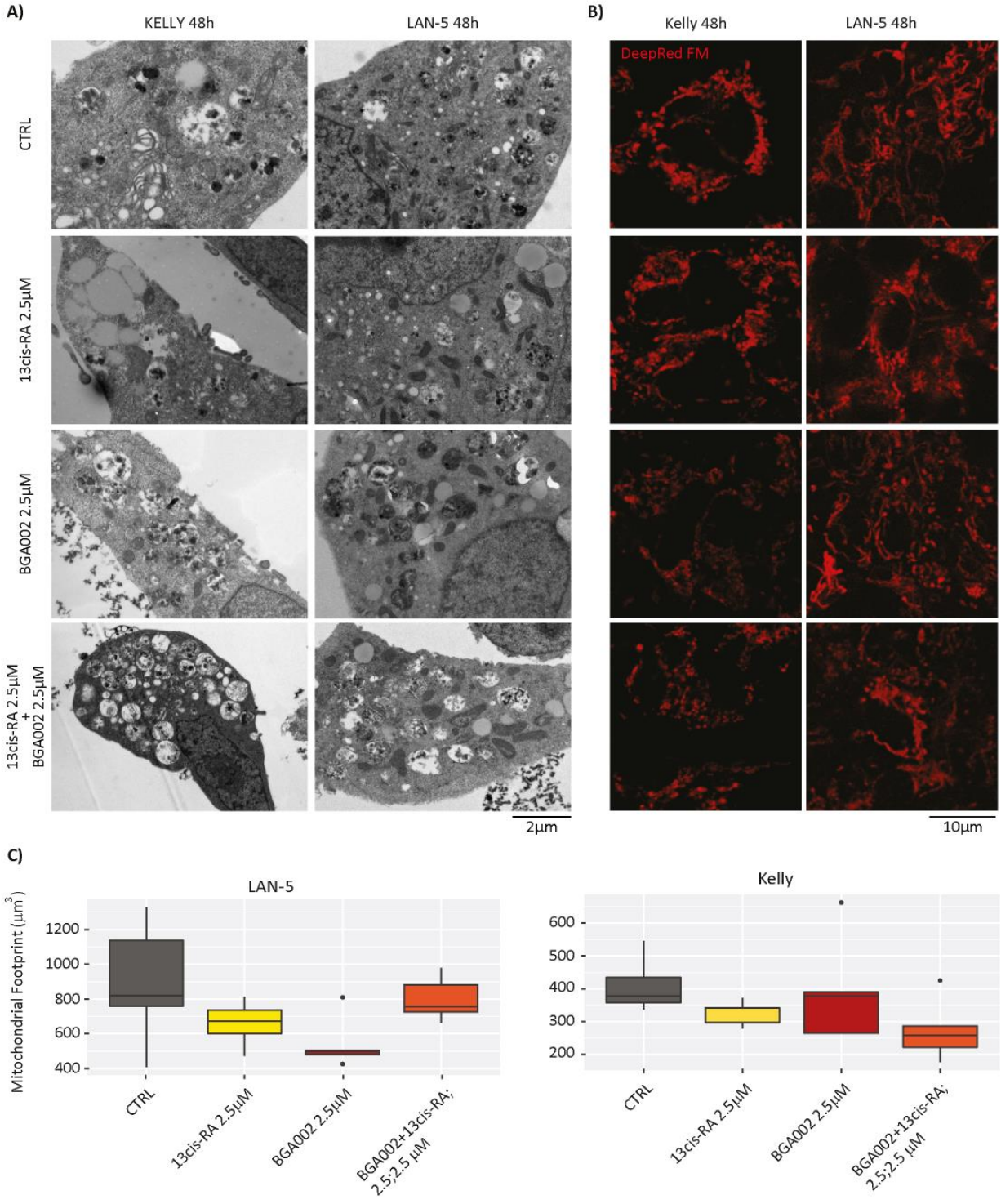

Figure 19: A) *Transmission electromicrographs of MNA-NB treated for 48 hours. Kelly (left) and LAN-5 (right) representative images for each condition are presented in figure (n = 2 biological experiments for cell line).* ***B)*** *Confocal microscopy of NB cell lines MNA Kelly (left) and LAN-5 (right) treated for 48 hours. Cell line were fixed and stained Mitotracker. (n = 2 biological experiments for cell line).* ***C)*** *Representation of the analysis conducted on confocal images. Mitochondria volume quantification for MYCN in amplified cell-lines LAN-5 and Kelly after 48 hours treatment. Each dot represents the volume measurement for a single mitochondrion, the middle line represent the median while the box limits indicate the first and the third quartiles and whiskers specify samples comprised 1.5 times the interquartile range. the graph represents the results of the pooled quantification of 5 cells (randomly selected).*

4.2 BGA002 in combination with 13-cis RA induces differentiation in MNA-NB cells

Undifferentiated NBs are considered high-risk and show poor survival. Since retinoic acid pathway and MYCN gene regulation are both involved in neuron differentiation, I tested if BGA002-RA can lead to MNA differentiation.

We used SHSY-5Y treated with 10 μM of 13-cis RA as positive control for differentiation. After 9 days of treatment the cells appeared more elongated and spindle-shaped, showing neurite like structures ($p< 0.0001$) (Fig. 20A-B).

Since the MNA-NB cell line LAN-5 did not undergo apoptosis I tested if these cells could differentiate. I treated LAN-5 with BGA002 and/or RA for nine days and I acquired optical microscope images at different times points (1-3-5-7-9 days). Images analysis shows that after 9 days of treatment, the molecules are able to produce evident morphological changes, with some differences (Fig. 20C) RA alone induces single cell growth with the development of many but shorter neuritis than either BGA002 or BGA002-RA treated samples. Where PNA has been used, cluster growth is visible. Compared to single molecules, the combination appears to produce significantly longer neurites (Fig. 20D).

Considering these results I also tested differentiation with lower concentration of BGA002 and RA (1,25 μM) in MNA-NB cell lines (LAN-5, SK-N-BE(2)-c and Kelly) for nine days.

Microscopy acquisition (data not showed) showed that while RA alone induced differentiation in SH-SY5Y, the same treatment did not induce differentiation in MNA-NB cell-lines, that are indeed RA resistant. In contrast, BGA002 did increase the neurite length in the same cell line, and this effect was strengthened by the combination with RA. As expected, the Kelly cell line, that showed good levels of apoptosis, failed to undergo differentiation (Fig. 21A).

In addition, in order to measure the differences between the four conditions, our bioinformatic group trained a convolutional neuron network (CNN) to calculate the Euclidean distance between CTRL and other conditions. This complementary approach confirmed that BGA002 and BGA002-RA treated MNA-cells were different from the untreated cells, while RA treated cells did not show any difference (Fig. 21B).

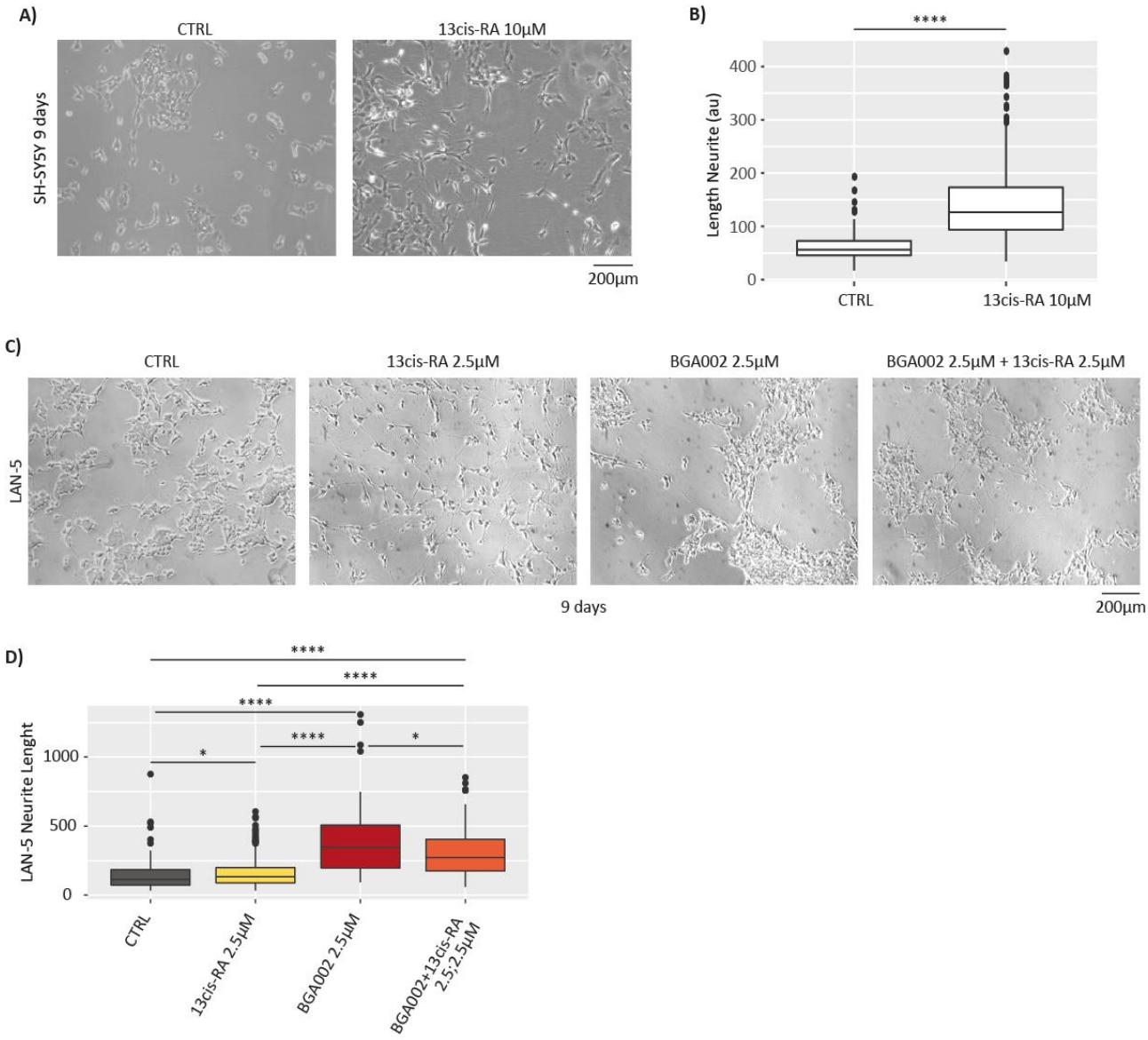

Figure 20: A) *Optical microscope image of SH-5YSY treated for 9 days (with CTRL (medium alone) or with retinoic acid). Cell images were acquired at the 9th day. Representative image of 1 of 2 biological replicates.* ***B)*** *Box-plots represent the length of neurite in SH-5YSY after 9 days of treatment (with CTRL (medium alone) or with retinoic acid). Each dot represents the measurement for a single neurite, the middle line is representing the median while the box limits indicate the first and the third quartiles and whiskers specify samples comprised 1.5 times the interquartile range. Statistic: Wilcoxon matched-pair test *P ≤ 0.05, **P ≤ 0.01, ***P ≤ 0.001, ****P ≤ 0.0001.* ***C)*** *Optical microscopy image for LAN-5 cell-line treated for 9 days (from left to right, untreated, 2.5 µM RA, 2.5 µM BGA002, 2.5 µM BGA002+RA). Two biological replicates for experiment.* ***D)****,Box-plots represent the length of neurite in MNA-NB cell-line LAN-5after 9 days of treatment (CTRL: medium alone, RA: retinoic acid 2.5 µM, BGA002: BGA002 2.5 µM, BGA002 + RA: BGA002 2.5 µM and retinoic acid 2.5 µM). All the analyses have been conducted using the same parameters as reported at point B.*

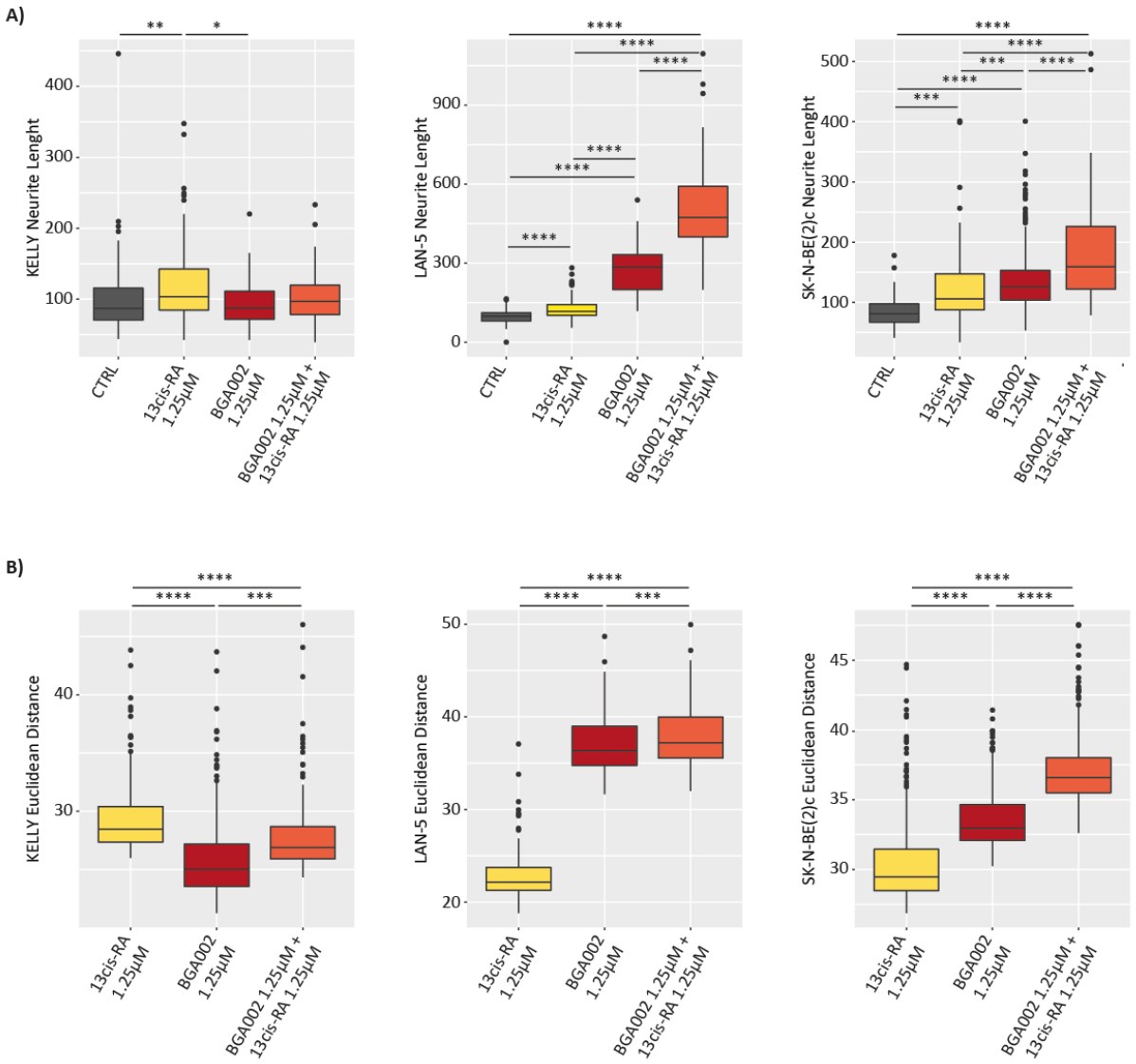

Figure 21: A) *Box-plots represent the length of neurite in MNA-NB cell line (Kelly, LAN-5, SK-N-BE(2)-C) after 9 days of treatment (CTRL: medium alone, RA: retinoic acid 1.25 µM, BGA002: BGA002 1.25 µM, BGA002 + RA: BGA002 1.25 µM and retinoic acid 1.25 µM). Each dot represents the measurement for a single neurite, the middle line is representing the median while the box limits indicate the first and the third quartiles and whiskers specify samples comprised 1.5 times the interquartile range. The graph represents the results of two pooled experiments. Statistic: Wilcoxon matched-pair test.* ***B)*** *Box-plots represent the Euclidean distance in MNA-NB cell-line (Kelly, LAN-5, SK-N-BE(2)-C) after 9 days of treatment. The Euclidean distance is calculated between the CTRL (medium control) and each treatment condition (RA: retinoic acid 1.25 µM, BGA002: BGA002 1.25 µM, BGA002 + RA: BGA002 1.25 µM and retinoic acid 1.25 µM). All the analyses have been conducted using the same parameters as reported at point A.*

Finally, since MYCN inhibits differentiation and treatment with RA should induce differentiation following the lowering of oncogene levels, I hypothesized that the samples in which the greatest cell differentiation was recorded were those showing the greatest inhibition of MYCN. The RT-PCR of the treated cells showed a reduction of MYCN mRNA levels after 12 hours and 9 days of treatment (Fig. 22A-B). Remarkably, the evaluation of the differentiated phenotype of BGA002-RA treated LAN-5 cells and SK-N-BE(2)-c performed after other additional 9 days without treatment showed a persistence of the differentiation status. Indeed the MYCN inhibition induced by BGA002 persisted after additional 9 days without treatment in LAN-5 cells and SK-N-BE(2)-c while, after rest, cells treated with RA alone restored an high expression of MYCN (Fig. 22C).

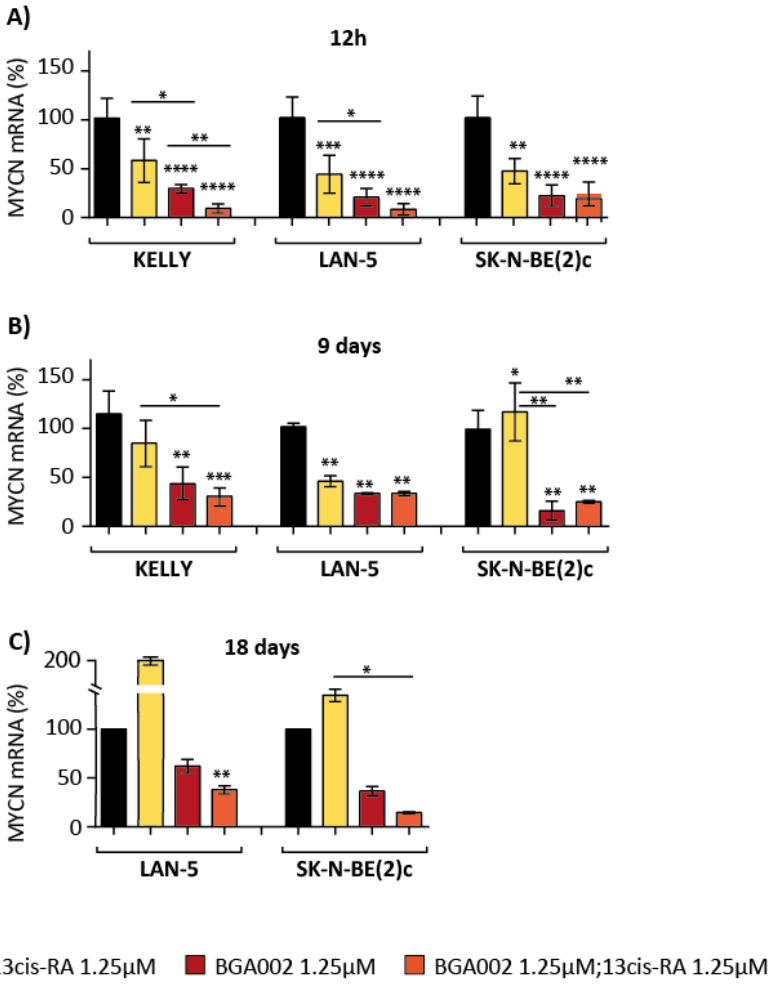

Figure 22: A-B-C) *MYCN mRNA expression normalized over the control (n = 3 experiments for cell-line). The bar represents the mean, the whisker the standard deviation.* ***A)*** *MYCN mRNA expression in Kelly, LAN-5 and SK-N-BE(2)-C after 12 hours of treatment.* ***B)*** *MYCN mRNA expression in LAN-5 and SK-N-BE(2)-C after 9 days post treatment* ***C)*** *MYCN mRNA expression in LAN-5 and SK-N-BE(2)-C after 18 days post treatment. (n=3 experiments, data were analyzed with a two-tailed Student's t Test **** p-value ≤ 0.0001, *** p-value ≤ 0.001, ** p-value ≤ 0.01, *p-value ≤ 0.05, were not indicated p-value >0.05).*

4.3 BGA002 in combination with 13-cis RA inhibits migration capacity in MNA-NB cells

4.3.1 BGA002-RA affects cellular migration capacity over time

As described above MYCN expression levels correlate with a metastatic behavior leading to decreasing adhesion and increasing motility, invasion and matrix degradation (6,83,84).
By decreasing the expression levels of integrins and increasing those of metalloproteinases and focal adhesion factor FAK, MYCN contributes to migration and metastasis phenomena. It is therefore likely to hypothesize that the inhibition of the oncogene by BGA002-RA can lead to a reduction in the ability of cancer cells to migrate.
So, I investigated how BGA002-RA affected the invasion and migration through Wound Healing Assay in various MNA-NB. I observed a modest effect after RA treatment with two different concentrations (1.25 and 2.5 µM) and only at late time points (48 or 72 hours) (Fig. 23A-B).
Instead, I found inhibition of migration capacity after treatment with BGA002 (2.5 µM) already at the earliest time point (24 hours), that increased at later time points (Fig. 23C). Moreover, the combined treatment with BGA002-RA further increased the impact on the migration inhibition. Specifically, I observed an inhibitory effect at the earliest time-point which increased during time, with the inhibition being observable also at lower doses (0.6 and 1.25 µM)
These data are not supported by statistical analysis.

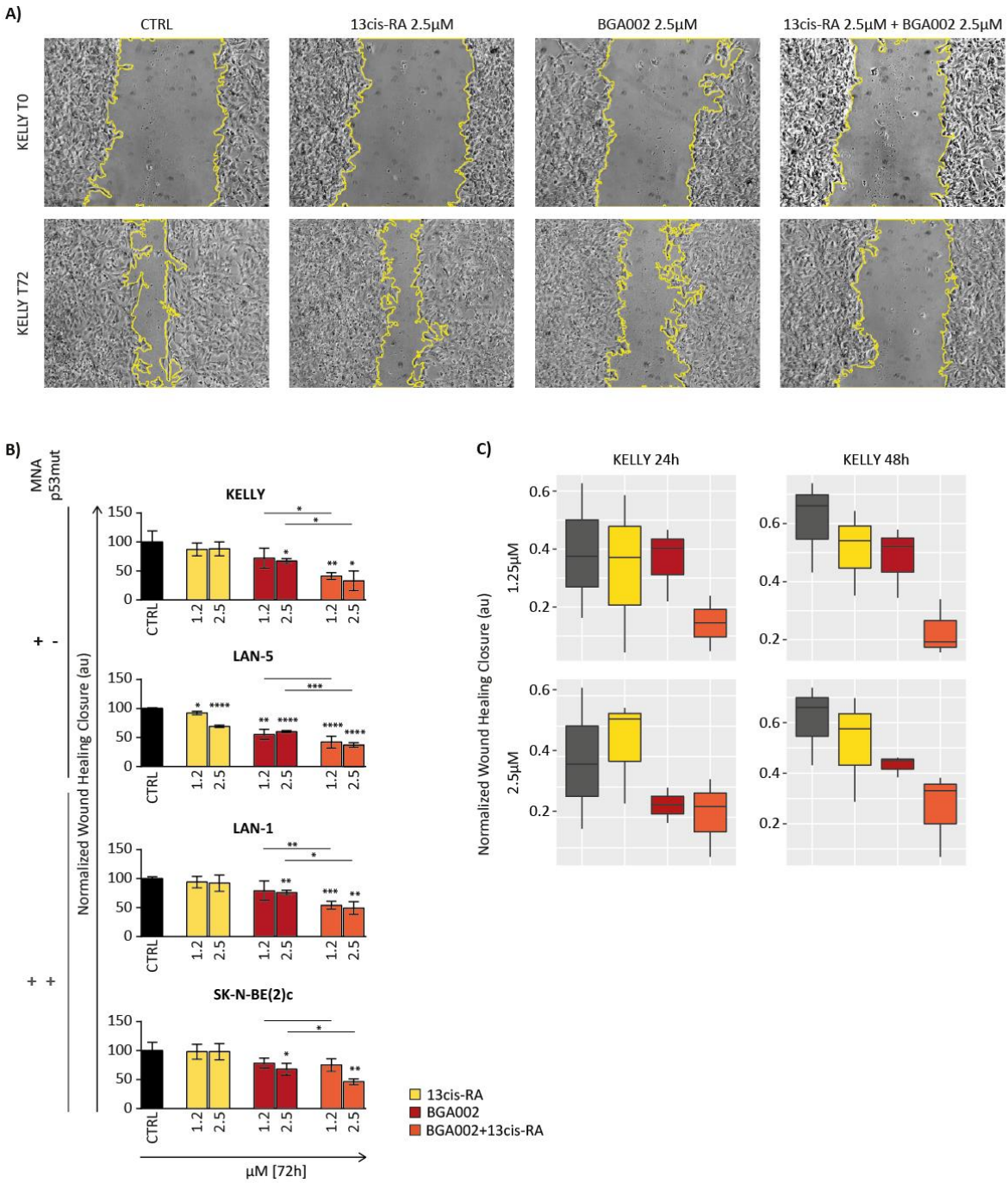

Figure 23: A) *Optical microscopy image of Kelly cell line treated at time zero (above line) or after 72 hours (below line). Exemplative images of 1 out of 3 experiments. Scratched zone is highlighted by yellow boundaries.* ***B)*** *Bar-plot representing the Wound healing Assay closure normalized over the control after 72 hours for 4 different MNA-NB cell lines (n=3 different biological replicates). Middle line represents the mean, the whiskers represent the standard deviation. Data were analyzed with a two-tailed Student's t Test **** p-value ≤ 0.0001, *** p-value ≤ 0.001, ** p-value ≤ 0.01, *p-value ≤ 0.05, were not indicated p-value >0.05.* ***C)*** *Bar plot representing the wound healing closure normalized over the control after 24 and 48 hours for Kelly (n = 3 different biological replicates). Middle line, the mean; whisker, the standard deviation.*

4.3.2 BGA002-RA down-regulates the expression of genes involved in migration in NB

At molecular level, after Wound Healing Assay, I investigated if genes involved in migration were downregulated following MYCN inhibition. BGA002, but even more BGA002-RA treatments, downregulate genes involved in the migration in MNA-and MNA p53mutated lines of NB, while I did not find a substantial effect after RA treatment alone (Fig. 24).

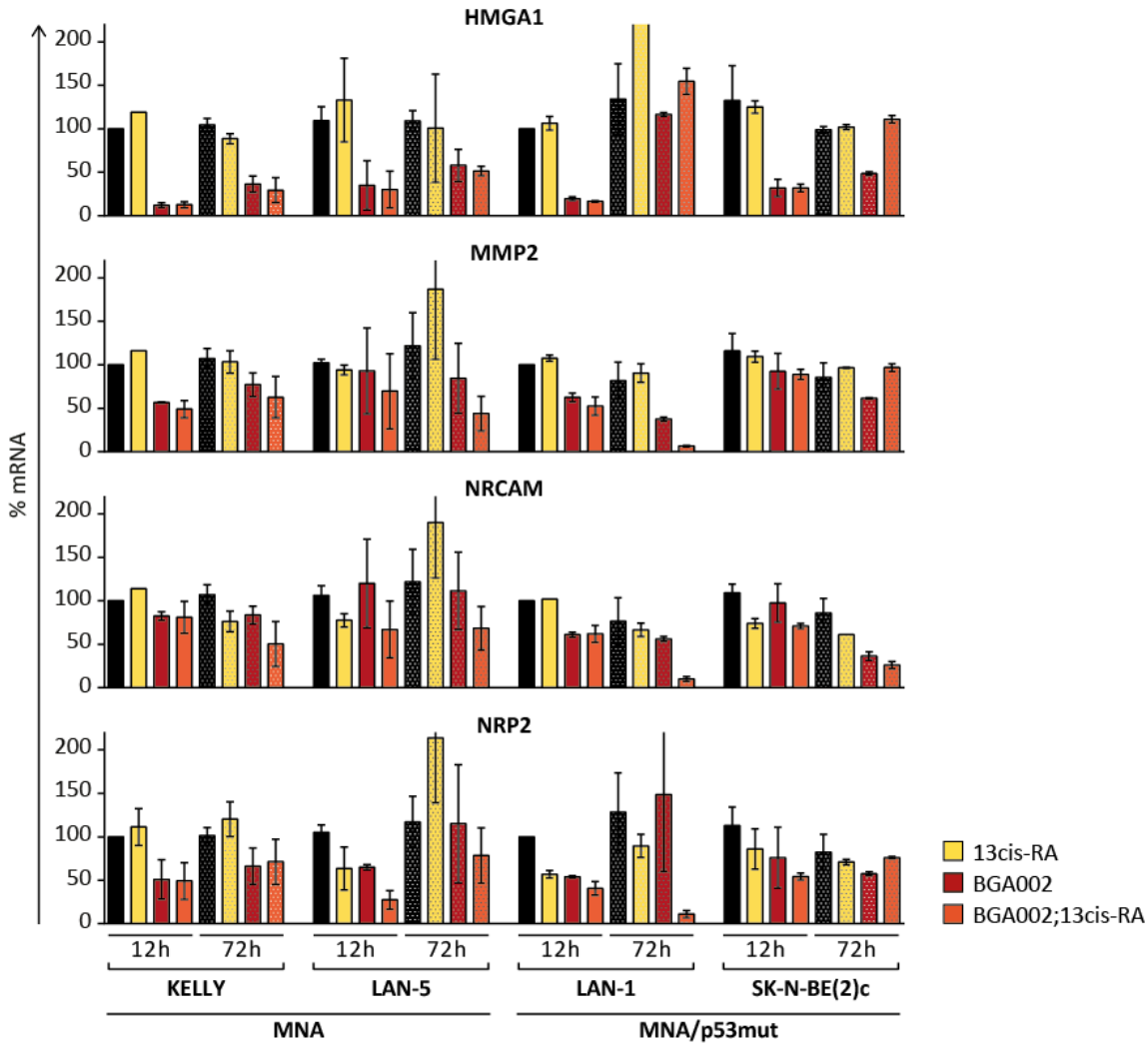

***Figure 24**: mRNA expression normalized over the control (n = 3 experiment for cell line). The bar represents the mean, the whisker the standard deviation. From top to down, mRNA expression for High Mobility Group AT-Hook 1 (HMGA1), Matrix Metallopeptidase 2 (MMP2), Neuronal Cell Adhesion Molecule (NRCAM) and Neuropilin 2 (NRP2). From left to right, Kelly, LAN-5, LAN-1 and SK-N-BE(2)-c after 12 and 72 hours of treatment (CTRL: medium alone, RA: retinoic acid 1.25 µM, BGA002: BGA002 1.25 µM, BGA002 + RA: BGA002 1.25 µM and retinoic acid 1.25 µM each). Cell lines are ordered according to their MYCN amplification and p53 mutation status.*

4.4 BGA002 in combination with 13-cis RA leads to mTOR complex inhibition in NB cells

The data in the literature highlight that MYCN amplification lead to activation of many downstream pathways including mTOR, that is a master regulator of cell growth and metabolism.

Several studies have shown how inhibition of the PI3K/mTOR pathway can inhibit the growth of NB cells while other studies report that N-Myc could regulate mTor pathway in NB. Indeed, since inhibition of mTOR pathway destabilized MYCN, mTOR pathway inhibitors could be a potential therapy for MNA-NB.

To date, it has been proposed the use of mTOR pathway inhibitors for NB therapy but these inhibitors are not specific for cancer cells, leading to many side effects. In contrast BGA002 is very specific so I hypothesized that MYCN targeting by BGA002 can inhibit mTOR pathway only in cancer cells. Therefore, I tested if BGA002-RA can inhibit the mTOR pathway in MNA-NB.

I found that BGA002 and BGA002-RA strongly inhibited the expression of many genes involved in the mTOR pathway (either up and down-stream), while RA alone failed in down-regulating their expression (Fig 25B).

In addition, with Martelli group I evaluated the mTOR pathway activity through protein phosphorylation. The results showed reduction in AKT, p70S6K and 4E-BP1 phosphorylation after treatment with BGA002 that was strengthened by BGA002-RA, demonstrating an mTOR pathway inhibition in MNA-NB (Fig 26 A-B).

The *in vitro* analysis was supported also by bioinformatic data. We found that NB displays the *highest* level of mRNA expression of genes involved in the mTOR pathway and small cell lung cancer (SCLC) ranked second; this observation is very interesting because these two highly aggressive tumors both derive from peripheral nervous system cells. Moreover, NB cell-lines presented high expression for different genes of the mTOR pathway and a higher expression was found in MNA versus non-MNA patients. Remarkably, these genes are also significantly predictive for the overall survival and were highly correlated with *MYCN* expression (Fig 25A). Lastly, we noticed that NB patients with high mTOR pathway activity showed a significantly worse survival (data not shown).

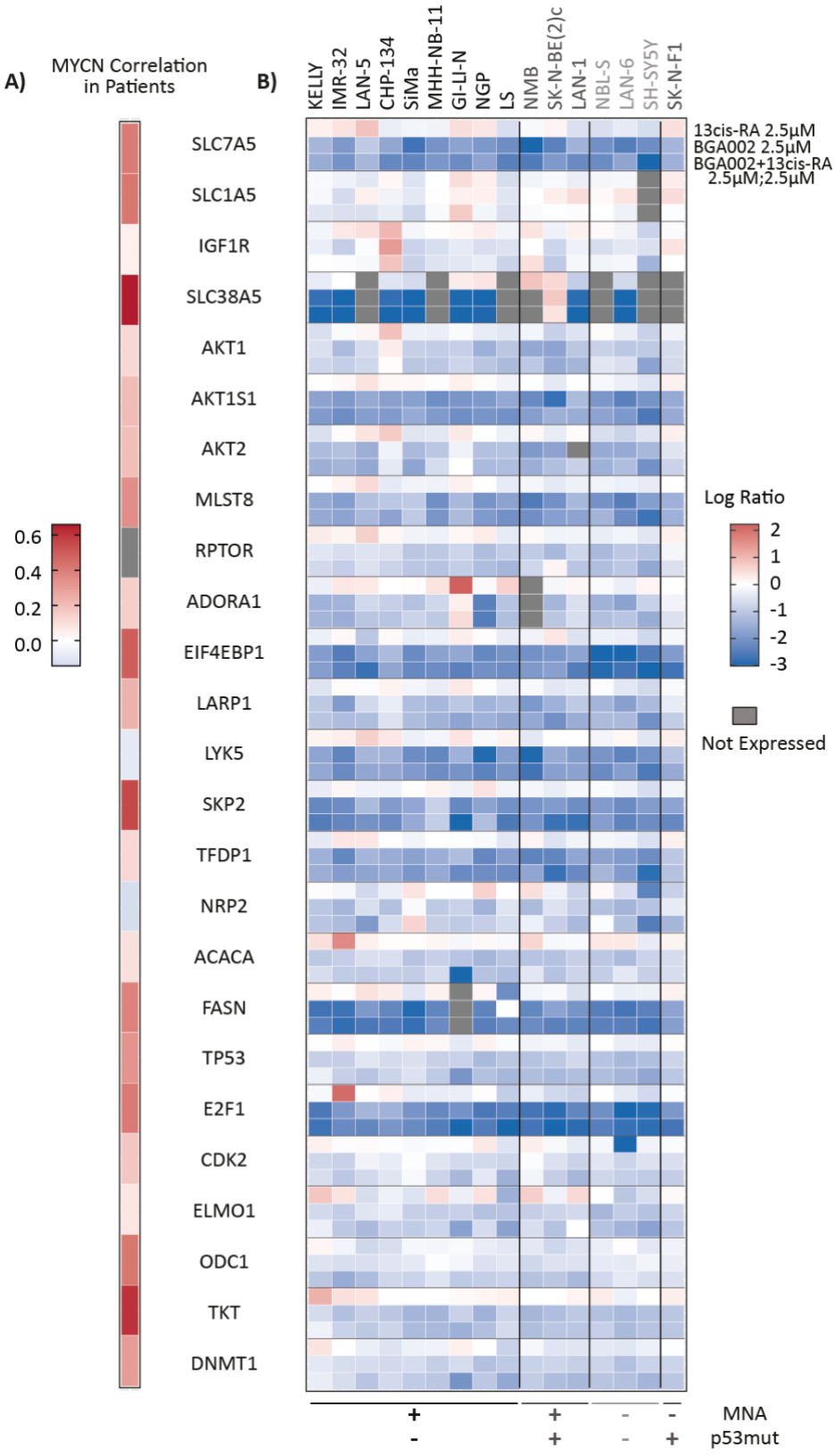

Figure 25: A-B) *gene name listed in the middle are referring to both panels. A) Heatmap representing Pearson correlation coefficient for mTOR pathway genes.* ***B)*** *Heatmap of the gene expression variation after 12 hours treatment in NB cell-lines. Columns represent cell lines (grouped according MYCN amplification and p53 mutation status), rows represent genes belonging to mTOR pathway, color scale represents log2 fold change over the control (untreated). Grey color indicates not expressed genes.*

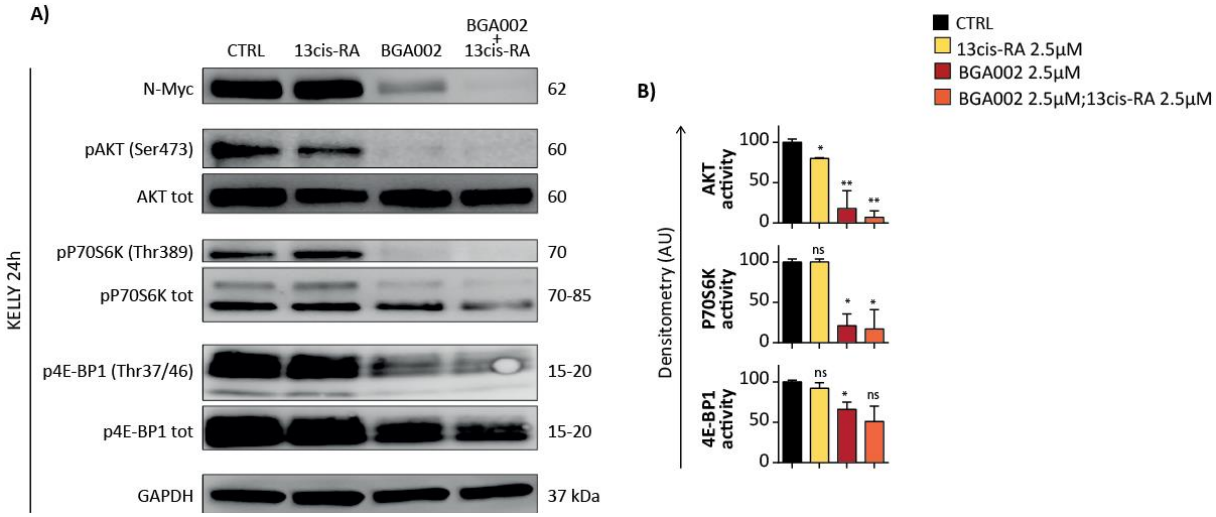

Figure 26: A) *mTOR pathway activity measured through Western Blot in Kelly cell-line after 24 hours of treatment (representative image of 1 out 2 biological replicates) B) mTOR pathway activity quantification, normalized over the control (n = 2 experiments. Data were analyzed with a two-tailed Student't Test **p-value ≤ 0.001 * p-value ≤ 0.05, were not indicated p-value >0.05).*

4.5 BGA002 in combination with 13-cis RA leads to autophagy reactivation in NB

It is known that mTORC1 complex plays an important role in metabolic control and suppresses autophagy (85). Since I found mTOR pathway downregulation after BGA002-RA treatment I evaluated if this event may result in autophagy reactivation. Here I noticed an increase of lysosomes after the treatment in Kelly MNA cell-line after 48 hours (Fig 27A-B).

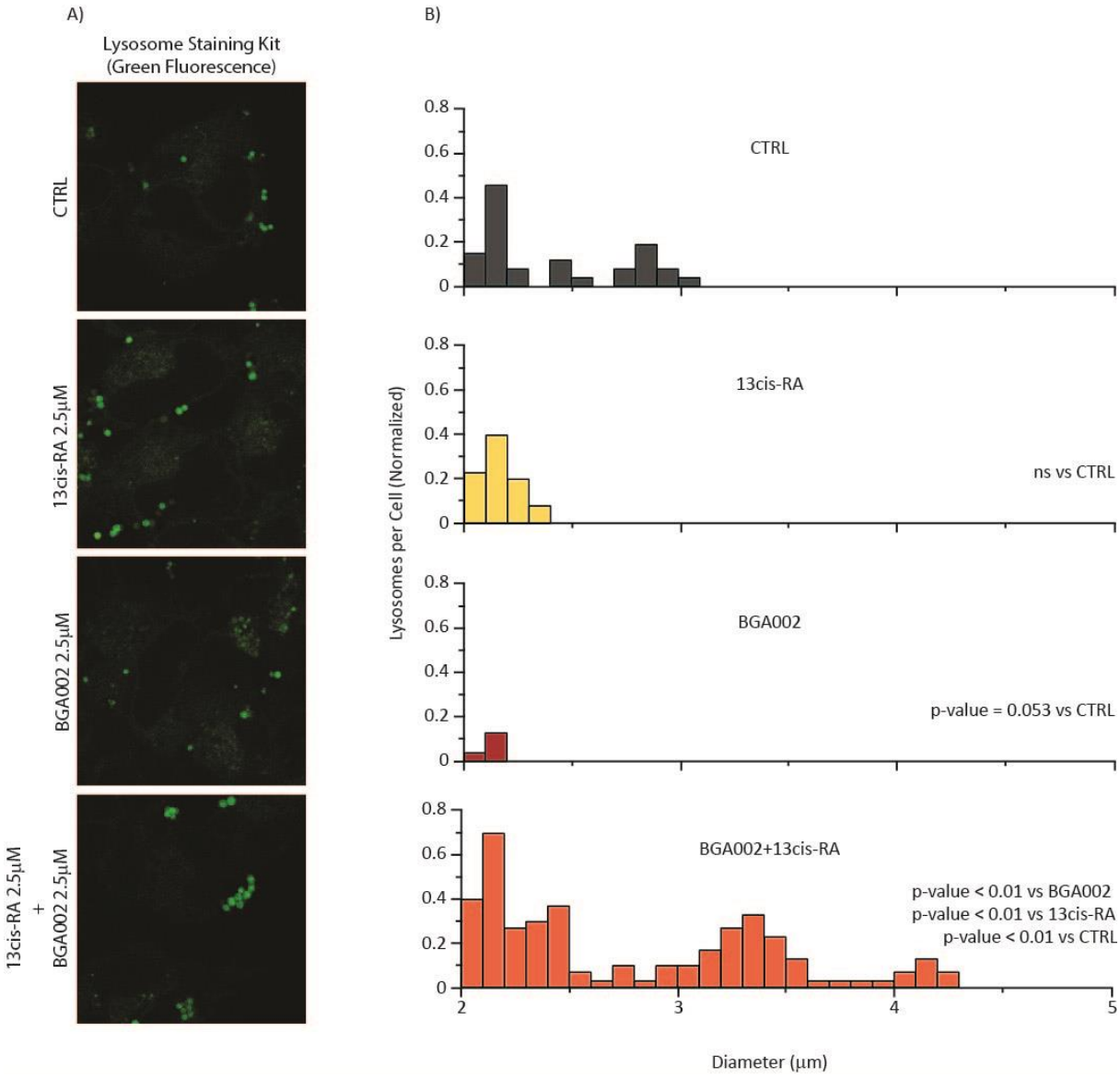

Figure 27: A) *Neuroblastoma cell lines MNA Kelly treated for 48 hours (CTRL: medium alone, RA: retinoic acid 2.5 µM, BGA002: BGA002 2.5 µM, BGA002 + RA: BGA002 2.5 µM and retinoic acid 2.5 µM). Cell lines were fixed and stained with lysosome staining kit. Representative experiment (n = 2 biological replicates).* ***B)*** *Stacked bar-plot, vertical axis representing the number of lysosomes per cell after 24 hours of treatment in Kelly MNA-NB cell line, horizontal axis the diameter range of the lysosomes. Color represents treatment (control, 13-cis RA, BGA002, BGA002+RA). Data were analyzed with a two-tailed Student's t test.*

4.6 BGA002 in combination with 13-cis RA reduces N-Myc and improves survival in a MNA-NB mouse model

We previously showed that BGA002 has an *in vivo* anti-tumor effect in MNA-NB xenograft mouse model (82). Here, I evaluated the anti-tumor activity of BGA002-RA in comparison with vehicle, BGA002 or RA alone in an MNA-NB xenograft mouse model (CHP-134-Luc cells). BGA002 or RA treatment alone already showed an increased survival ratio compared to the vehicle, but the combined treatment BGA002-RA showed a higher increase ($p < 0.05$)(Fig. 28A).

In addition, BGA002-RA treatment reduced the tumor growth during the treatment in comparison to the vehicle (data not shown). To further analyze BGA002 activity *in vivo* I performed histological analysis of mice tumor after they reached end-point. The tumor vascularization was highly present in the vehicle and still present in RA treated mice, while it was not present in BGA002 and BGA002-RA treated mice (Fig. 29A). Moreover, immunohistochemistry analysis showed that N-Myc protein expression in RA treated tumors was similar to the vehicle, while BGA002 treatment and BGA002-RA were capable to reduce N-Myc protein (Fig. 29A).In addition, I found that the trend of results observed for the N-Myc protein staining in tumors was very similar to Ki-67 staining, a marker of cells proliferation.

This observation was confirmed by the quantitative analysis: N-Myc protein expression was similar in vehicle and RA, while BGA002 treatment was already capable of reducing N-Myc protein, and BGA002-RA treatment consistently strengthen this effect ($p < 0.0001$) (Fig. 29B).

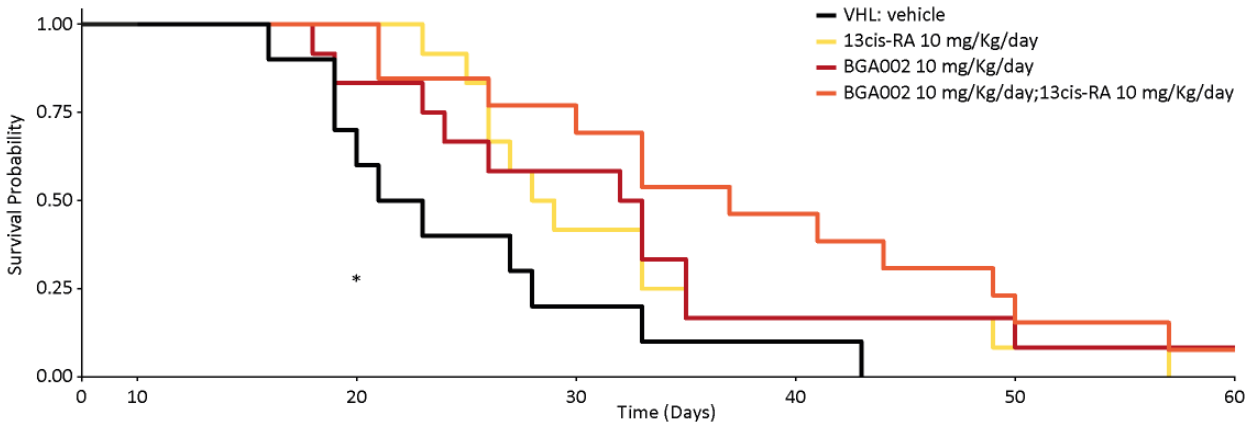

Figure 28: *Kaplan-Meyer plot for the probability of event-free survival over time for CHP-134-luc xenograft mice treated with: vehicle (black line, n =10), 13-cis RA 10 mg/kg/day (yellow line, n =12), BGA002 10 mg/kg/day (red line, n =12), 13-cis RA and BGA002 10 mg/kg/day each (orange line, n =13). In the middle of the plot the associate p- value (log-rank test). *, p < 0.05.*

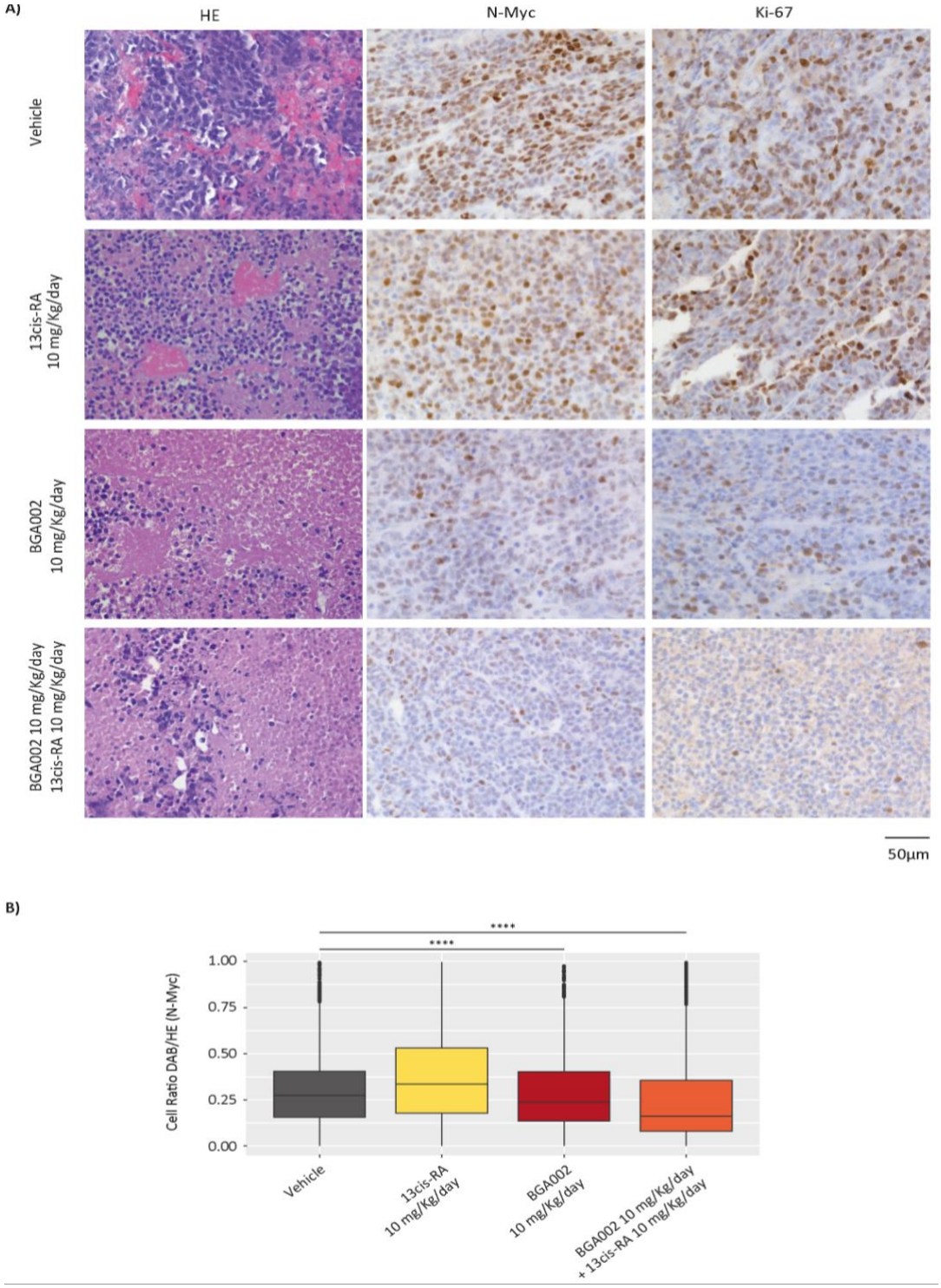

Figure 29: A)*Immuno-histochemistry analysis of neuroblastoma mice untreated (first row), treated with 13-cis RA 10 mg/kg/day (second row), treated with BGA002 10 mg/kg/day (third row), 13-cis RA and BGA002 10 mg/kg/day (forth row). First column shows staining with hematoxylin and eosin (H&E), second column N-Myc antibody, third column Ki-67 staining.* ***B)*** *Box-plots represent the ratio of DAB stained/ HE stained cells for vehicle, BGA002 (10 mg/kg/day), retinoic acid (10 mg/kg/day), BGA002 and retinoic acid (10 mg/kg/day each). Each dot represents the ratio calculated in one image. the middle line represents the median while the box limits indicate the first and the third quartiles and whiskers specify samples comprised 1.5 times the interquartile range. Statistic: Wilcoxon matched-pair test. *$p \leq 0.05$, **$p \leq 0.01$, ***$p \leq 0.001$, ****$p \leq 0.0001$.*

5. DISCUSSION

PNAs belong to a third generation of nucleic acid-based-gene-specific drugs and offer greater clinical potential than conventional oligonucleotides, due to its resistance to degradation and stronger binding abilities with targets. The anti-MYCN agPNA (BGA002) object of this study is a compound of great pharmacological interest and indeed has obtained the ORPHAN DRUG Designation for the treatment of Neuroblastoma (NB) from EMA and FDA.
The aim of this PhD project was to evaluate the use of BGA002 in combination with the 13-cis Retinoic Acid as therapeutic approach for the treatment of NB. In particular the aim of this study was to characterize both molecular and phenotypic changes that occur in cells after the administration of drugs' combination in vitro and in vivo. Different therapeutic approaches have been developed to treat NB but, high-risk cases MYCN-dependent, still remain critical (12). This is the reason that led me to think that targeting the oncogene with BGA002 could be the winning strategy. Considering the results of BGA002 as a single agent (82) I decided to couple the PNA with the 13-cis RA, a drug well known as differentiating agent that has showed an impressive clinical efficacy in NB. Despite its usefulness in high-risk NB for controlling minimal residues disease therapy, approximately 50% of neuroblastoma patients develops intrinsic or acquired resistance to RA treatment. In particular this occurs in patients with amplification of MYCN (MNA-NB) which is therefore responsible of resistance and subsequent relapses (57).

As described previously 13–cis RA could be a strong inhibitor of neuroblastoma proliferation (86)at high concentration (up to 50 µM). The use of RA in combination with BGA002 was able to inhibit MYCN expression and as well cell viability, at significant lower doses of both drugs (about 4-8 fold lower), in both MNA- and non-MNA-NB cell lines. BGA002-RA was also able to reinforce significantly the reduction of N-Myc protein amount and increase apoptosis at the same low dosage. This is particularly significant considering that 13-cis RA side effects occur in NB patients (87). Surprisingly, in MNA/p53mut neuroblastoma cell lines which are, on average, more resistant to 13-cis RA as well as other chemotherapy compound (88) BGA002 further increase the pharmacological activity—as indicated by a lower EC_{50} values. Starting from these premises I wanted to investigate the molecular mechanisms responsible of the growth inhibition.

I noticed that BGA002 at the low dose of 2,5µM induces apoptosis and BGA002-RA strengthens apoptosis in some MNA-NB. This data is consistent with our previous study in

which we showed that MYCN inhibition by BGA002 lead to the reactivation of mitophagy and cell death via mitochondria damage (82). Indeed, here I found a mitochondria alteration following BGA002-RA administration, which is associated with apoptosis in the Kelly MNA-NB cell-line.

Furthermore, I focused on cell differentiation, a pathway in which RA is well known to act and in which, at least during embryonic development, MYCN is involved as an inhibitor. NB pathogenesis has been also associated to failure of differentiation and, especially in MNA-NB, to persistence of cancer cells in undifferentiated embryonal-like state (16,38). Interestingly, here I found that BGA002-RA at very low doses was able to induce differentiation in some MNA-NB cells. While untreated or RA-treated MNA-NB cell lines failed to undergo differentiation, BGA002 treated MNA-NB cells were capable to induce neurite length increase, and I found a stronger significant effect after BGA002-RA combined treatment. In particular, MNA-NB cell line LAN-5 undergo differentiation but not apoptosis, while Kelly cells did the opposite. Thus, I demonstrated that blocking MYCN through BGA002 treatment (data confirmed by RT-PCR) reverted the differentiation resistance to RA in MNA-NB cells. Finally, I performed the analysis 9 days after the end of treatment (18 days total) and I noticed that the effect persists over time at both the molecular and phenotypic level in MNA-NB cells. In contrast, cells treated with RA alone start again to express levels of the oncogene similar or higher than control cells. Furthermore, here our bioinformatic group used a new complementary approach to quantify NB differentiation that is based on convolutional neural network. This innovative method is highly scalable and can be used to monitor differentiation in NB cell-lines with different drug combinations. Indeed, a similar approach can be used to monitor changes in cellular morphology in high-throughput screening.

Another pathway in which MYCN is well known to be involved is the migration (83). In literature is well described that cancer cells with an undifferentiated and mesenchymal phenotype are more prone to metastasize and indeed high-risk NB is characterized by metastasis in different target sites of the body (6,9,10,14). Using the Wound Healing Assay technique, it was possible to study the variation in the displacement capacity of the cells as a function of the drug treatment tested. Our results remarkably showed that the inhibition of MYCN expression affects the migratory phenomenon, decreasing the ability of cells to move. Cell lines treated with BGA002 alone appeared a BGA002 treatment causes a slower migration than RA

treatment, but when the two molecules were used together the effect was enhanced and stable over time

Early studies showed mTOR pathway activation in two third of NB patients, with AKT and mTOR phosphorylation in primary NB, and this activation is correlated with reduced event free and overall survival (89). The AKT-mTOR pathway regulates various cellular processes and the activation of the mTOR kinase leads to an increase in cell metabolism and glycogen synthesis, blocking apoptosis and increasing protein synthesis and cell proliferation (90). The data in the literature highlight the correlation between the overexpression of MYCN in cancer cells and the activation of mTOR, a transcription factor responsible for controlling many effectors. Several studies have shown how inhibition of this pathway, in particular of mTOR, can inhibit the growth of NB cells and, indirectly, down-regulates the expression of MYCN (52,91).

However, inhibitors of mTOR, such as rapamycin or its analogues (rapalogs), or other key molecules of the same pathway, are not very selective towards cancer cells; if they are not adequately addressed, they have an effect on all cells, without distinction, and can lead to toxicity, making clinical application very challenging. In contrast, BGA002 is very specific (82).

We evaluated genes involved at both upstream and downstream mTOR pathway, that we found correlated to MYCN in NB patients. In particular SLC7A5 (*Solute carrier family 7 member 5)*, known as LAT1, and ADORA1 *(Adenosine A1 receptor)* act upstream of the PI3K-AKT-mTOR pathway. Genes such as AKT2 *(AKT Serine/Threonine Kinase 2)* and MLST8 (*MTOR Associated Protein, LST8 Homolog)* are directly involved in mTOR activation, while EIF4EBP1 *(Eukaryotic Translation Initiation Factor 4E Binding Protein 1)*, SKP2 *(S-Phase Kinase Associated Protein 2*) and FASN *(Fatty Acid Syntase)* are mTOR targets and are involved in protein translation, cell cycle progression and metabolism respectively. Remarkably, we found that all of them were strongly inhibited following treatment with BGA002 and the combination of BGA002 with RA, while RA alone failed in down-regulation. Moreover, we showed an overall reduction in the pathway activity of mTOR also by WB analysis. In this context is relevant the reduced phosphorylation of the 473Serin of AKT. It is well known that Akt phosphorylation, which denotes activation of the PI3K / Akt / mTOR pathway, occurs in several primary tumor samples and this is associated with reduced overall survival and poor EFS (Event Free Survival) (92). Among the various mTORC1 targets, kinase S6K and 4EBP and stand out. p70 S6 kinase is a mitogen activated Ser/Thr protein that phosphorylates the S6 protein of the 40S ribosomal subunit and is involved in translational

control. Less significant but still present is the reduction of the phosphorylation of the translation repressor protein 4E-BP1*(Eukaryotic initiation factor 4E-binding protein 1)* while, 4e-BP1 phosphorylation is practically insensitive to rapamycin (85).

Because MYCN has a very restricted pattern of expression in normal cells and can be considered a cancer-specific target, I hypothesized that the specific MYCN targeting by BGA002 can result in the inhibition of mTOR pathway only in cancer cells, leaving it unaffected in healthy cells.

Since mTORC1 complex plays an important role in metabolic control and suppresses autophagy (85), I have assumed that the mTOR pathway downregulation after BGA002-RA treatment should result in autophagy reactivation.

Indeed, I observed a great reactivation of autophagy documented by an increase of macrovacuoles in Kelly (MNA-NB) after treatment with BGA002-RA. The increase of macrovacuoles with the largest diameters is relevant because they are those responsible in the phenomenon of autophagy (93).

Autophagic cell-death (ACD), also known as type 2 cell death, is a process of cell elimination that can occur in normal cells (fibroblasts or thymocytes), but not in most cancer cells (94).

Furthermore it is reported that the ATRA (all-trans retinoic Acid), during differentiation in APL (Acute promyelocytic leukemia) cells, promotes the accumulation of autophagosomes and the activation of autophagy with increased expression levels of several autophagy-regulatory proteins as well as down-regulation of pathways that repress autophagy (mTOR) (95).

Our results, support and verified the hypothesis that the reduction of MYCN by BGA002 restores the RA-mediated autophagy also in NB cells, leading to autophagic cell death.

Previously our group showed that BGA002 has an in vivo anti-tumor effect in MNA-NB xenograft mouse model (82). Here, I evaluated the anti-tumor capacity of systemic treatment of BGA002-RA in comparison with the vehicle (0.9% NaCl), or BGA002 or RA alone in an MNA-NB xenograft mouse model using CHP-134 cells. Considering our result we decide to use a dose lower than therapeutically relevant 50mg/kg so that we can reach a dose at least 10 times lower than LD50 for ip administration (96)For in vivo studies the therapeutic dose was determined starting from a careful study of the literature for RA and from efficacy/toxicity experiments previously carried out for BGA002. Actually at 10mg/kg/day is a tolerable dose for each one alone and for RA in combination with other small-molecules (97). The animals, treated for 4 weeks and then sacrificed when reached end-point, were used to build a Kaplan-

Meyer plot for the probability of event-free survival over time. The treatment with BGA002 alone was more potent to reduce tumor growth and to increase the survival than RA alone. The combination of both agents has a greater capacity in increasing EFS than either treatment alone. Moreover is important underline how the enhanced therapeutic efficacy associated with BGA002-RA was not accompanied by systematic toxicity.

Then was performed histologic and immunohistochemistry analysis. Here the most impressive discovery was that BGA and BGA002-RA treatment lead to the elimination of tumor vascularization while this was highly present in the vehicle and still present in RA treated mice. Probably the reduction of vascularization was caused by the reduction of N-Myc. This is consistent with the literature that agrees that hat tumor angiogenesis can be induced by cellular oncogenes and in particular by MYCN. It was already known twenty years ago that enhanced expression of the N-myc oncogene in human neuroblastoma cells down-regulates three inhibitors of endothelial cell proliferation such as Activin A, leukemia inhibitory factor (LIF) and interleukin-6 (IL-6) (98).

Taken together, this study allows us to verify the hypothesis that there is a synergistic effect between BGA002 and 13-cis RA and that it is possible to realize precision medicine achieving a selective block of cancer pathways in tumor cells only, even for the high-risk NB (MNA-NB). In addition, since MYCN amplification is not restricted to this pediatric malignancy but deregulation of MYCN occurs also in adult cancers (53), the restoration of RA treatment could be beneficial in different MNA-tumors. Therefore, the combination BGA002-RA could potentially be therapeutically relevant for a wide range of aggressive MNA-related malignancies.

6. BIBLIOGRAFY

1. EvaluatePharma ® Orphan Drug Report 2018 [Internet]. 2018. Available from: www.evaluategroup.com/OrphanDrug2018
2. Rare Diseases: Understanding this public health priority. Diseases, European Organisation for Rare Eurodis. 2005;
3. Czech M, Baran-Kooiker A, Atikeler K, Demirtshyan M, Gaitova K, Holownia-Voloskova M, et al. A Review of Rare Disease Policies and Orphan Drug Reimbursement Systems in 12 Eurasian Countries. Frontiers in Public Health. Frontiers Media S.A.; 2020.
4. Dodge JA, Chigladze T, Donadieu J, Grossman Z, Ramos F, Serlicorni A, et al. The importance of rare diseases: From the gene to Society. Archives of Disease in Childhood. 2011. page 791–2.
5. Rothenberg AB, Berdon WE, D'Angio GJ, Yamashiro DJ, Cowles RA. Neuroblastoma - Remembering the three physicians who described it a century ago: James Homer Wright, William Pepper, and Robert Hutchison. Pediatric Radiology. 2009. page 155–60.
6. Huang M, Weiss WA. Neuroblastoma and MYCN. Cold Spring Harbor Perspectives in Medicine. 2013;3.
7. Jiang M, Stanke J, Lahti JM. The Connections Between Neural Crest Development and Neuroblastoma. Current Topics in Developmental Biology. 2011.
8. Zafar A, Wang W, Liu G, Wang X, Xian W, McKeon F, et al. Molecular targeting therapies for neuroblastoma: Progress and challenges. Medicinal Research Reviews. John Wiley and Sons Inc; 2021. page 961–1021.
9. John M Maris MDHRBSLC. Neuroblastoma. Lancet. 2007;369:2106–20.
10. Maris JM. Recent advances in Neuroblastoma [Internet]. Colket Translational Research Bldg., Rm. 2010. Available from: www.ncbi.nlm.nih.gov/
11. Titilope A. Ishola, Dai H. Chung. Neuroblastoma. Surgical Oncology. 2007. page 149–56.
12. Louis CU, Shohet JM. Neuroblastoma: Molecular pathogenesis and therapy. Annual Review of Medicine. Annual Reviews Inc.; 2015;66:49–63.
13. Neuroblastoma Treatment (PDQ®) - PDQ Cancer Information Summaries - NCBI Bookshelf.
14. Sharp SE, Gelfand MJ, Shulkin BL. Pediatrics: Diagnosis of neuroblastoma. Seminars in Nuclear Medicine. 2011. page 345–53.
15. Esposito MR, Aveic S, Seydel A, Tonini GP. Neuroblastoma treatment in the post-genomic era. Journal of Biomedical Science. BioMed Central Ltd.; 2017.
16. Tomolonis JA, Agarwal S, Shohet JM. Neuroblastoma pathogenesis: deregulation of embryonic neural crest development. Cell and Tissue Research. Springer Verlag; 2018. page 245–62.
17. Jiang M, Stanke J, Lahti JM. The Connections Between Neural Crest Development and Neuroblastoma. Current Topics in Developmental Biology. 2011.
18. MacDonald BT, Tamai K, He X. Wnt/β-Catenin Signaling: Components, Mechanisms, and Diseases. Developmental Cell. 2009. page 9–26.

19. Ornitz DM, Itoh N. The fibroblast growth factor signaling pathway. Wiley Interdisciplinary Reviews: Developmental Biology. John Wiley and Sons Inc.; 2015;4:215–66.
20. Odate S, Veschi V, Yan S, Lam N, Woessner R, Thiele CJ. Inhibition of STAT3 with the generation 2.5 antisense oligonucleotide, AZD9150, decreases neuroblastoma tumorigenicity and increases chemosensitivity. Clinical Cancer Research. American Association for Cancer Research Inc.; 2017;23:1771–84.
21. Hori K, Sen A, Artavanis-Tsakonas S. Notch signaling at a glance. Journal of Cell Science. 2013;126:2135–40.
22. Chang HH, Lee H, Hu MK, Tsao PN, Juan HF, Huang MC, et al. Notch1 expression predicts an unfavorable prognosis and serves as a therapeutic target of patients with neuroblastoma. Clinical Cancer Research. 2010;16:4411–20.
23. Lamouille S, Xu J, Derynck R. Molecular mechanisms of epithelial-mesenchymal transition. Nature Reviews Molecular Cell Biology. 2014. page 178–96.
24. Jolly MK, Boareto M, Huang B, Jia D, Lu M, Onuchic JN, et al. Implications of the hybrid epithelial/mesenchymal phenotype in metastasis. Frontiers in Oncology. Frontiers Media S.A.; 2015;5.
25. Piskareva O, Harvey H, Nolan J, Conlon R, Alcock L, Buckley P, et al. The development of cisplatin resistance in neuroblastoma is accompanied by epithelial to mesenchymal transition in vitro. Cancer Letters. Elsevier Ireland Ltd; 2015;364:142–55.
26. Naftali O, Maman S, Meshel T, Sagi-Assif O, Ginat R, Witz IP. PHOX2B is a suppressor of neuroblastoma metastasis [Internet]. Available from: www.impactjournals.com/oncotarget/
27. Sokol E, Desai A. The Evolution of Risk Classification for Neuroblastoma. Children. MDPI AG; 2019;6:27.
28. Monclair T, Brodeur GM, Ambros PF, Brisse HJ, Cecchetto G, Holmes K, et al. The International Neuroblastoma Risk Group (INRG) staging system: An INRG Task Force report. Journal of Clinical Oncology. 2009;27:298–303.
29. van Arendonk K, Chung D. Neuroblastoma: Tumor Biology and Its Implications for Staging and Treatment. Children. MDPI AG; 2019;6:12.
30. Pinto NR, Applebaum MA, Volchenboum SL, Matthay KK, London WB, Ambros PF, et al. Advances in risk classification and treatment strategies for neuroblastoma. Journal of Clinical Oncology. American Society of Clinical Oncology; 2015. page 3008–17.
31. Brodeur GM. Neuroblastoma: Biological insights into a clinical enigma. Nature Reviews Cancer. 2003. page 203–16.
32. Swift CC, Eklund MJ, Kraveka JM, Alazraki AL. Updates in diagnosis, management, and treatment of neuroblastoma. Radiographics. Radiological Society of North America Inc.; 2018;38:566–80.
33. Smith V, Foster J. High-Risk Neuroblastoma Treatment Review. Children. MDPI AG; 2018;5:114.
34. Aygun N. Biological and Genetic Features of Neuroblastoma and Their Clinical Importance. Current Pediatric Reviews. Bentham Science Publishers Ltd.; 2018;14:73–90.
35. Trigg RM, Turner SD. ALK in neuroblastoma: Biological and therapeutic implications. Cancers. MDPI AG; 2018.
36. Tolbert VP, Coggins GE, Maris JM, Maris JM. Genetic susceptibility to neuroblastoma. Current Opinion in Genetics and Development. Elsevier Ltd; 2017. page 81–90.

37. Pugh TJ, Morozova O, Attiyeh EF, Asgharzadeh S, Wei JS, Auclair D, et al. The genetic landscape of high-risk neuroblastoma. Nature Genetics. 2013;45:279–84.
38. Westermark UK, Wilhelm M, Frenzel A, Henriksson MA. The MYCN oncogene and differentiation in neuroblastoma. Seminars in Cancer Biology. 2011. page 256–66.
39. Barone G, Anderson J, Pearson ADJ, Petrie K, Chesler L. New strategies in neuroblastoma: Therapeutic targeting of MYCN and ALK. Clinical Cancer Research. 2013;19:5814–21.
40. Otte J, Dyberg C, Pepich A, Johnsen JI. MYCN Function in Neuroblastoma Development. Frontiers in Oncology. Frontiers Media S.A.; 2021.
41. Rickman DS, Schulte JH, Eilers M. The expanding world of N-MYC-driven tumors. Cancer Discovery. American Association for Cancer Research Inc.; 2018. page 150–64.
42. Chromosome localization in normal human cells and neuroblastomas of a gene related to c-myc.
43. Liu R, Shi P, Wang Z, Yuan C, Cui H. Molecular Mechanisms of MYCN Dysregulation in Cancers. Frontiers in Oncology. Frontiers Media S.A.; 2021.
44. Huang M, Weiss WA. Neuroblastoma and MYCN. Cold Spring Harbor Perspectives in Medicine. 2013;3.
45. Baluapuri A, Wolf E, Eilers M. Target gene-independent functions of MYC oncoproteins. Nature Reviews Molecular Cell Biology. Nature Research; 2020. page 255–67.
46. Yoshida GJ. Beyond the Warburg Effect: N-Myc Contributes to Metabolic Reprogramming in Cancer Cells. Frontiers in Oncology. Frontiers Media S.A.; 2020.
47. Ruiz-Pérez MV, Henley AB, Arsenian-Henriksson M. The MYCN protein in health and disease. Genes. MDPI AG; 2017.
48. Eilers M, Eisenman RN. Myc's broad reach. Genes and Development. 2008. page 2755–66.
49. Song L, Ara T, Wu HW, Woo CW, Reynolds CP, Seeger RC, et al. Oncogene MYCN regulates localization of NKT cells to the site of disease in neuroblastoma. Journal of Clinical Investigation. 2007;117:2702–12.
50. Raieli S, di Renzo D, Lampis S, Amadesi C, Montemurro L, Pession A, et al. MYCN Drives a Tumor Immunosuppressive Environment Which Impacts Survival in Neuroblastoma. Frontiers in Oncology. Frontiers Media S.A.; 2021;11.
51. Fletcher JI, Ziegler DS, Trahair TN, Marshall GM, Haber M, Norris MD. Too many targets, not enough patients: Rethinking neuroblastoma clinical trials. Nature Reviews Cancer. Nature Publishing Group; 2018. page 389–400.
52. Barone G, Anderson J, Pearson ADJ, Petrie K, Chesler L. New strategies in neuroblastoma: Therapeutic targeting of MYCN and ALK. Clinical Cancer Research. 2013;19:5814–21.
53. Liu Z, Chen SS, Clarke S, Veschi V, Thiele CJ. Targeting MYCN in Pediatric and Adult Cancers. Frontiers in Oncology. Frontiers Media S.A.; 2021.
54. Beltran H. The N-myc oncogene: Maximizing its targets, regulation, and therapeutic potential. Molecular Cancer Research. American Association for Cancer Research Inc.; 2014. page 815–22.
55. Decreased expression of N-myc precedes retinoic acid-induced morphological differentiation of human neuroblastoma.
56. Reynolds CP, Matthay KK, Villablanca JG, Maurer BJ. Retinoid therapy of high-risk neuroblastoma. Cancer Letters. Elsevier Ireland Ltd; 2003. page 185–92.

57. Duffy DJ, Krstic A, Halasz M, Schwarzl T, Konietzny A, Iljin K, et al. Retinoic acid and TGF-β signalling cooperate to overcome MYCN-induced retinoid resistance. Genome Medicine. BioMed Central Ltd.; 2017;9.
58. Gupta A, Mishra A, Puri N. Peptide nucleic acids: Advanced tools for biomedical applications. Journal of Biotechnology. Elsevier B.V.; 2017. page 148–59.
59. Aboul-Fadl T. Antisense oligonucleotides: the state of the art. Current Medicinal Chemistry. 2005;44:2193–214.
60. Liang X, Liu M, Komiyama M. Recognition of target site in various forms of DNA and RNA by peptide nucleic acid (PNA): From fundamentals to practical applications. Bulletin of the Chemical Society of Japan. The Chemical Society of Japan; 2021;
61. Nielsen PE, Egholm^ M, Buchardu O. REVIEWS Peptide Nucleic Acid (PNA). A DNA Mimic with a Peptide Backbone [Internet]. Bioconjugate Chem. 1994. Available from: https://pubs.acs.org/sharingguidelines
62. Montazersaheb S, Hejazi MS, Charoudeh HN. Potential of peptide nucleic acids in future therapeutic applications. Advanced Pharmaceutical Bulletin. Tabriz University of Medical Sciences; 2018. page 551–63.
63. Nielsen PE. Targeting Double Stranded DNA with Peptide Nucleic Acid (PNA). Current Medicinal Chemistry. 2001.
64. Porcheddu A, Giacomelli G. Peptide Nucleic Acids (PNAs), A Chemical Overview. Current Medicinal Chemistry. 2005.
65. Ray A, Nordé B. Peptide nucleic acid (PNA): its medical and biotechnical applications and promise for the future.
66. Nielsen PE, Egholm M. An Introduction to Peptide Nucleic Acid. 1999.
67. U. Koppellus and P. E. Nielsen. Cellular delivery of peptide nucleic acid (PNA). Advanced Drug Delivery Reviews, 55(2), 26. 2003;
68. Quijano E, Bahal R, Ricciardi A, Saltzman WM, Glazer PM. Therapeutic Peptide Nucleic Acids: Principles, Limitations, and Opportunities. YALE JOURNAL OF BIOLOGY AND MEDICINE. 2017.
69. Paola Ringhieri et all. The influence of liposomal formulation on the incorporation and retention of PNA oligomers | Elsevie.
70. Dean DA. Peptide nucleic acids: versatile tools for gene therapy strategies. 2015.
71. Derossi D, Chassaing G, Prochiantz A. Trojan peptides: the penetratin system for intracellular delivery.
72. Sharma C, Awasthi SK. Versatility of peptide nucleic acids (PNAs): role in chemical biology, drug discovery, and origins of life. Chemical Biology and Drug Design. Blackwell Publishing Ltd; 2017. page 16–37.
73. Tonelli R, McIntyre A, Camerin C, Walters ZS, di Leo K, Selfe J, et al. Antitumor activity of sustained N-myc reduction in rhabdomyosarcomas and transcriptional block by antigene therapy. Clinical Cancer Research. 2012;18:796–807.
74. Chou TC. Theoretical basis, experimental design, and computerized simulation of synergism and antagonism in drug combination studies. Pharmacological Reviews. 2006. page 621–81.
75. Chou TC. The combination index (CI < 1) as the definition of synergism and of synergy claims. Synergy. Elsevier GmbH; 2018. page 49–50.
76. Valente AJ, Maddalena LA, Robb EL, Moradi F, Stuart JA. A simple ImageJ macro tool for analyzing mitochondrial network morphology in mammalian cell culture. Acta Histochemica. Elsevier GmbH; 2017;119:315–26.
77. Grada A, Otero-Vinas M, Prieto-Castrillo F, Obagi Z, Falanga V. Research Techniques Made Simple: Analysis of Collective Cell Migration Using the Wound Healing Assay. Journal of Investigative Dermatology. Elsevier B.V.; 2017. page e11–6.

78. Rueden CT, Schindelin J, Hiner MC, DeZonia BE, Walter AE, Arena ET, et al. ImageJ2: ImageJ for the next generation of scientific image data. BMC Bioinformatics. BioMed Central Ltd.; 2017;18.
79. Schindelin J, Arganda-Carreras I, Frise E, Kaynig V, Longair M, Pietzsch T, et al. Fiji: An open-source platform for biological-image analysis. Nature Methods. 2012. page 676–82.
80. Ruifrok AC, Katz RL, Johnston DA. Comparison of quantification of histochemical staining by hue-saturation-intensity (HSI) transformation and color-deconvolution. Applied Immunohistochemistry and Molecular Morphology. Lippincott Williams and Wilkins; 2003;11:85–91.
81. van der Walt S, Schönberger JL, Nunez-Iglesias J, Boulogne F, Warner JD, Yager N, et al. Scikit-image: Image processing in python. PeerJ. PeerJ Inc.; 2014;2014.
82. Montemurro L, Raieli S, Angelucci S, Bartolucci D, Amadesi C, Lampis S, et al. A novel MYCN-specific antigene oligonucleotide deregulates mitochondria and inhibits tumor growth in MYCN-amplified neuroblastoma. Cancer Research. American Association for Cancer Research Inc.; 2019;79:6166–77.
83. Goodman LA, Liu BCS, Thiele CJ, Schmidt M lou, Cohn SL, Yamashiro JM, et al. Modulation of N-myc expression alters the invasiveness of neuroblastoma. Clinical and Experimental Metastasis. 1997;15:130–9.
84. Gavin C, Geerts N, Cavanagh B, Haynes M, Reynolds CP, Loessner D, et al. Neuroblastoma invasion strategies are regulated by the extracellular matrix. Cancers. MDPI AG; 2021;13:1–23.
85. Saxton RA, Sabatini DM. mTOR Signaling in Growth, Metabolism, and Disease. Cell. Cell Press; 2017. page 960–76.
86. Shelake S, Eslin D, Sutphin RM, Sankpal UT, Wadwani A, Kenyon LE, et al. Combination of 13 *cis* -retinoic acid and tolfenamic acid induces apoptosis and effectively inhibits high-risk neuroblastoma cell proliferation. International Journal of Developmental Neuroscience. 2015;46:92–9.
87. Tosun M, Soysal Y, Gocmen Mas N, Karabekir HS. Comparison of the Effects Of 13-cis Retinoic Acid and Melatonin on the Viabilities of SH-SY5Y Neuroblastoma Cell Line. Journal of Korean Neurosurgical Society. Korean Neurosurgical Society; 2015;57:147–51.
88. Blanco-Luquin I, Lázcoz P, Celay J, Castresana JS, Encío IJ. In vitro assessment of the role of p53 on chemotherapy treatments in neuroblastoma cell lines. Pharmaceuticals. MDPI; 2021;14.
89. Opel D, Poremba C, Simon T, Debatin KM, Fulda S. Activation of Akt predicts poor outcome in neuroblastoma. Cancer Research. 2007;67:735–45.
90. Liu GY, Sabatini DM. mTOR at the nexus of nutrition, growth, ageing and disease. Nature Reviews Molecular Cell Biology. Nature Research; 2020. page 183–203.
91. Johnsen JI, Segerström L, Orrego A, Elfman L, Henriksson M, Kågedal B, et al. Inhibitors of mammalian target of rapamycin downregulate MYCN protein expression and inhibit neuroblastoma growth in vitro and in vivo. Oncogene. 2008;27:2910–22.
92. King D, Yeomanson D, Bryant HE. PI3King the Lock. Journal of Pediatric Hematology/Oncology. 2015;37:245–51.
93. Parzych KR, Klionsky DJ. An Overview of Autophagy: Morphology, Mechanism, and Regulation. Antioxidants & Redox Signaling. 2014;20:460–73.
94. Torii S, Honda S, Murohashi M, Yamaguchi H, Shimizu S. Autophagy involvement in oncogenesis. Cancer Science. Blackwell Publishing Ltd; 2020. page 3993–9.

95. Moosavi MA, Djavaheri-Mergny M. Autophagy: New insights into mechanisms of action and resistance of treatment in acute promyelocytic leukemia. International Journal of Molecular Sciences. MDPI AG; 2019.
96. Hixson EJ, Denine EP. Comparative subacute toxicity of all-trans- and 13-cis-retinoic acid in swiss mice. Toxicology and Applied Pharmacology. 1978;44:29–40.
97. Bayeva N, Coll E, Piskareva O. Differentiating neuroblastoma: A systematic review of the retinoic acid, its derivatives, and synergistic interactions. Journal of Personalized Medicine. MDPI AG; 2021.
98. Hatzi E, Fotsis T, Murphy C, Breit S, Schweigerer L, Zoephel A, et al. MYCN Oncogene and Angiogenesis: Down-Regulation of Endothelial Growth Inhibitors in Human Neuroblastoma Cells. Angiogenesis Advances in Experimental Medicine and Biology. 2000. page 239–48.